universität wien

DIPLOMARBEIT

Titel der Diplomarbeit

„The proteome of the peroxisomal membrane“

Verfasserin

Isabella Magyar

angestrebter akademischer Grad

Magistra der Naturwissenschaften (Mag.rer.nat.)

Wien, 2009

Studienkennzahl:	A 419
Studienrichtung:	Chemie
Betreuer:	Ao.Univ.Prof.Dr. Andreas Hartig

TABLE OF CONTENTS

1 INTRODUCTION

1.1 THE PEROXISOME

Eukaryotic cells are highly structured entities compartmentalizing their interior to allow for an efficient and manageable course of all cellular functions. The various compartments or organelles contain different proteins and provide confined spaces for certain metabolic pathways.

When peroxisomes were first isolated in 1966 by the group of de Duve, oxidases producing H_2O_2 and catalase decomposing this compound were the first enzymes found in this new organelle class, with the name "peroxisomes" reflecting the confinement of the peroxide-metabolism [1]. The size (100nm-1µm), number and protein content and hence the functions of these single-membrane bound organelles show tremendous variation depending on the organism, cell type, developmental stage and environmental condition. The metabolic functions of peroxisomes comprise biosynthetic as well as degradative pathways. For instance, yeast peroxisomes harbour parts of the lysine biosynthesis, of the degradation of amino acids and in some cases of methanol, the complete pathway resulting in β- oxidation of fatty acids, the decomposition of H_2O_2 and the glyoxylate cycle [2]. Due to their versatility, peroxisomes displaying different enzymatic contents and hence exhibiting different functions in other species like plants and trypanosomatides were named differently – "glyoxysomes" and glycosomes" respectively [3, 4]. Their appearance in the electron microscope led to the name "microbodies".

In contrast to mitochondria or chloroplasts, peroxisomes do not contain DNA and cannot synthesize their own proteins. Hence, all peroxisomal proteins are encoded by the nuclear genome and translated on free polysomes in the cytosol. Most of the proteins destined for peroxisomes carry a so-called peroxisomal targeting signal (PTS) – either a carboxy-terminal PTS1 or the less frequent amino-terminal PTS2 for translocation to the matrix or the poorly defined mPTS for integration into the membrane. It is remarkable that most of the proteins are imported in an entirely folded state – in some cases even oligomeric or with cofactors bound.

The essential role of peroxisomes is underlined by the existence of several severe inherited diseases linked to single peroxisomal enzyme deficiencies or disorders in peroxisome biogenesis which are mostly fatal [5].

1.1.1 *Saccharomyces cerevisiae* as model organism for peroxisome research

General advantages of yeasts compared to higher eukaryotes are the simple cultivation procedures (handling and media composition), the short generation times, the great variety of tools for genetic manipulation and the availability of entirely sequenced genomes. As fungi are more related to animals than to plants, results obtained in these model organisms are also relevant for human beings [6].

One of the major advantages of yeasts in peroxisome research is that peroxisome proliferation can easily be controlled by the composition of the culture medium. In *S.c.* for example, peroxisome proliferation is repressed when cells are grown on glucose, derepressed when cells are grown on glycerol or ethanol and eventually induced by growth on oleate [7]. As "the need for peroxisome function depends on the external conditions" [4], peroxisome malfunctioning does not necessarily cause lethality when yeast cells are grown in the appropriate medium. In *S.c.*, peroxisomes represent the exclusive site for β-oxidation of fatty acids and hence are essential for growth when oleic acid is provided as sole carbon source but are not required when cells are grown on glucose or ethanol [8]. In other yeast species commonly used in peroxisome research, including *Hansenula polymorpha*, *Yarrowia lipolytica* and *Pichia pastoris*, the dependence of the cells on the presence of functional peroxisomes can be controlled in a similar way applying, to some extent, other growth conditions [9, 10, 11]. This fact allowed screening for mutations leading to impaired or disrupted peroxisome biogenesis or maintenance in the different yeast species – the so called *PEX* mutations. To date, altogether 31 *PEX* genes have been found by complementation analyses; the corresponding proteins are called "peroxins". Although mostly conserved among species no organism contains all 31 *PEX* genes. In *S.c.* for instance, 26 *PEX* genes have been identified.

1.1.2 Peroxisome biogenesis and multiplication

Eukaryotic cells have to ensure that their organelles are maintained and passed on to the next generation. In case of peroxisomes the peroxins, already mentioned above, are the main actors in these events.

Regarding inheritance and biogenesis two types of organelles can be distinguished. Autonomous organelles, resulting from an endosymbiontic origin, such as mitochondria

and chloroplasts, but also the perinuclear ER multiply by "growth and division". That means they need to enlarge by taking up protein and membrane material prior to division and distribution, and once lost the cells are not able to build these organelles again. The non-autonomous organelles are thought to derive from the perinuclear ER. This group comprises amongst others ER, Golgi and lysosomes and applies a different concept of biogenesis and inheritance – continuous *de novo* biosynthesis [12]. For both groups of organelles protein and membrane acquirement is tightly coupled to the biogenesis of new organelles either by enlargement and division or by generation of new compartments. For a long time, peroxisomes could not be categorized into one of the two groups because ambiguous experimental results favoured either the one or the other concept.

At the beginning, the prevailing model was "growth and division", based on the findings that peroxisomal proteins are translated on free polysomes and imported afterwards into peroxisomes [13]. As this is a common feature of organelles of endosymbiontic origin such as mitochondria and chloroplasts, peroxisomes were also thought to belong to this group of organelles. This hypothesis was strengthened by the discovery of the peroxisomal targeting signals (PTS1 and PTS2) which allow the import of matrix proteins into peroxisomes independent from other organelles [14,15]. Greater importance was given to these findings than to previous electron microscopy studies in which peroxisomes surrounded by or almost continuous with smooth ER could be detected [16]. The appearance of glycosylated proteins – a modification proteins acquire by passage through the ER – in glyoxysomes [17] did not alter the preference for the model "growth and division of autonomous peroxisomes" either.

Later on, new results favoured the "*de novo* biogenesis" model. Especially, the observation that mutations in certain genes (*PEX3*, *PEX19*) lead to the complete loss of the peroxisome population of a cell and that their reappearance can be induced – even after several generations without peroxisomes – solely by introducing the wild type gene [18] supported the concept of *de novo* biogenesis for peroxisomes raising doubts about the growth and division model. Further support was provided by Hoepfner *et al.* who performed real-time imaging studies with *GAL* promoter controlled fluorescently labelled Pex3p and Pex19p in *pex3*Δ, *pex19*Δ and wild type cells. It was shown that Pex3p and Pex19p initially localize to spots in the ER which later dissociate from the ER. A subsequent maturation process involving matrix protein import leads to the restoration of the wild type phenotype in a

*pex3*Δ or *pex19*Δ background 5 hours after induction [19]. Rachubinsky *et al.* provided further support to this course of events using a fluorescently labelled truncated version of Pex3p only consisting of the first 46 amino acids which cannot support peroxisome biogenesis. After mating with a strain containing *PEX3* under the control of a *GAL* promoter, upon induction the truncated version of Pex3p was also moved from the ER to mature peroxisomes [20].
Consistent with these studies, large-scale phylogenetic analyses of the yeast and rat peroxisomal proteome performed by Gabaldón *et al.* [21] suggest that the majority of peroxisomal proteins comprising all peroxins are of eukaryotic origin. This was another aspect in disfavour of the assumption that peroxisomes could be of endosymbiontic origin. In addition, several of the proteins involved in peroxisome biogenesis and maintenance were found to be homologous to members of the Endoplasmic Reticulum Assisted Decay (ERAD) pathway underlining the derivation of peroxisomes from the ER [21].

Although many studies demonstrated a direct role of the ER in peroxisome biogenesis, several questions remain to be answered. To date, we do not know how the relevant peroxins traffic to the ER, how the ER resident proteins are excluded from the pre-peroxisomal compartment consequently leading to enrichment with peroxins, how the segregation process of this precompartment from the ER takes place and if there are additional fission or fusion processes after the segregation. Two models for this process are proposed – the first one assumes that a relatively large part of the ER is severed requiring several subsequent fission processes during the maturation. In the other model, small vesicles are released from the ER which are then subjected to homotypic fusion resulting in the normal sized peroxisome [22, 23]. Additionally, the interplay between the two ways of peroxisome multiplication (*de novo* formation of new peroxisomes and growth and division of already existing ones) is still not clear. The three different models presented in figure 1-1 are up for debate [24]. The first two models are based on the existence of a continuous maturation pathway starting at the ER. In contrary, the third model is rooted in the assumption that multiplication of peroxisomes follows the concept of growth and division. The role of the ER in this model is restricted to lipid membrane donation and the provision of some peroxisomal membrane proteins to allow for the growth of pre-existing peroxisomes.

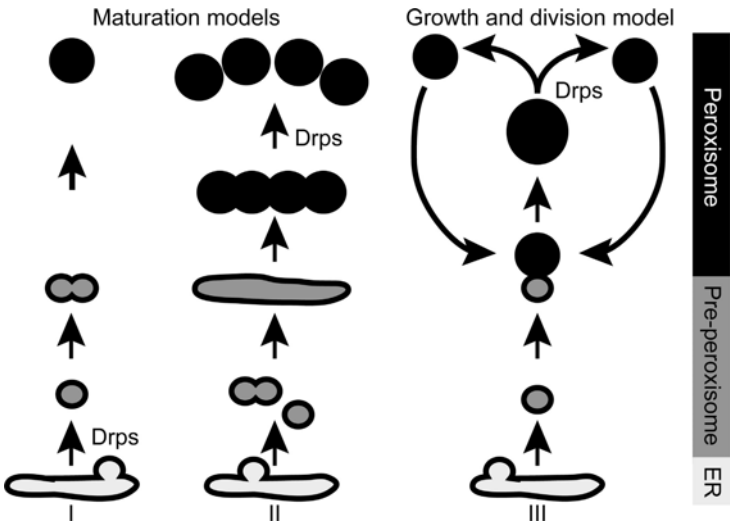

Figure 1-1: Three models for the multiplication of peroxisomes (figure taken from [24]). The first two models primarily depend on a *de novo* maturation process while the third model is based on the growth and division concept.

As the dynamin-related proteins (Drps) and dynamin (Dnm1p) – GTPases involved in budding of transport vesicles and organelle fission/fusion [25] – have been shown to be associated with peroxisomes, it is thought that these proteins may also act in peroxisome scission processes. Investigations concerning the role of the Drps Vps1p (from yeast) and the human ortholog DLP1 have shown that deletion of the corresponding genes leads to a phenotype with one or few elongated peroxisomes [26, 27] supporting the models 2 or 3 with the Drps only acting at the level of mature peroxisomes. Hettema and Motley [24] provided further support for the third model showing that GFP-PTS1 accumulating in peroxisomes is diluted out during a pulse-chase experiment indicating the continuous occurrence of fission processes of existing peroxisomes. They also showed that "all pre-existing peroxisomes obtained Pex3-GFP during pulse-chase experiments" [24]. Based on the findings that this process shows a different kinetics in WT cells than in cells lacking peroxisomes due to a segregation defect, they postulated that " although ER-derived Pex3-GFP-containing structures are able to mature into peroxisomes in WT cells, they fuse with pre-existing peroxisomes long before they mature" [24]. Although confirmed by investigations made in *Hansenula polymorpha* [28], studies in mammalian cells resulting in the conclusion that the maturation pathway from the ER accounts for the increase in peroxisome number in growing WT cells [29] are contradictory to this hypothesis. Maybe the interplay between the two ways of multiplication is species-dependant [28]. Although

experiments with Drps led to a better understanding of the multiplication of peroxisomes, the mechanism of the early segregation processes occurring at the ER remains open.

The progressive alteration of the protein composition from the peroxisomal precompartment to the mature peroxisome could shed light on some of these questions. Proteomic studies with peroxisomes and their precursors, respectively, provide a useful means to identify differences in protein composition or even novel proteins. In addition to novel peroxisomal proteins involved in these processes, new functions of already known ones would be of great interest. Peroxins may turn out to be multifunctional. Pex3p and Pex19p have been shown to be involved in very early phases of peroxisome biogenesis, but the detailed function is not yet clear. Most PMPs contain a targeting signal (mPTS) and binding sites for Pex19p [30]. Hence, "Pex19p, through its interactions with PMPs and with Pex3p, may help assemble PMPs into packageable groups for transport out of the ER" [3]. In summary, the studies by Hoepfner *et al.* and Rachubinsky *et al.* have definitely confirmed that "the ER contributes to peroxisome formation, particularly by donating lipid material for the peroxisomal membrane and thus classifying peroxisomes into the group of ER derived organelles" [19]. This knowledge, however, represents the starting point for more studies providing further details.

As of today, peroxisomes seem to use mechanisms for maintenance and inheritance from both groups of organelles, the autonomous and the non-autonomous ones. Both models, growth and division of already existing organelles and *de novo* biogenesis from the ER, seem to apply for peroxisomes.

1.2 PROTEOMIC STUDIES

1.2.1 Attractiveness of the proteome

The complete sequence of the yeast *Saccharomyces cerevisiae* genome has provided a lot of information concerning the potential protein content of the cell. However, the proteome represents a more dynamic description, reflecting the dynamic changes in protein expression, abundance, localisation, interactions and activity states in response to the external conditions of the cell [31]. Subcellular proteomics provides a possibility to identify and define the proteinaceous content of a particular part of the cell at a given time point.

Most peroxisomal matrix proteins are supposed to contain a peroxisomal targeting signal (PTS) which can be recognized by *in silico* methods and their function confirmed by experimental approaches [32]. Proteins associated permanently or transiently with the peroxisomal membrane, however, cannot be predicted by *in silico* methods and their identification at the protein level is hampered by their low amount and their intrinsic properties. Most probably, a considerable part of peroxisomal membrane proteins has not yet been identified. These proteins establish the connection between the peroxisome and the other compartments of a cell. Not only communication but also transport actions across the peroxisomal membrane have to be fulfilled by membrane proteins. So far, only very few peroxisomal transporter proteins have been identified – Pat1p, Pat2p [33], Fat1p [34] acting in long-chain fatty acid transport and Ant1p, an ADP/ATP translocator [35]. However, "considering the metabolic reactions taking place in peroxisomes and the interaction with the cytoplasm required to sustain these reactions, more transporters must exist" [3].

1.2.2 Commonly used proteomic approaches

Several methodologies are commonly used in proteomic approaches comprising *in silico* predictions, high through-put localization studies, interactome studies and mass spectrometric analyses of the protein content [31].

In silico proteomics applies computational methods resulting in predictions based on the amino acid sequence of the proteins under scrutiny. As peroxisomal proteins are transported to the peroxisomes post-translationally by the means of peroxisomal targeting signals (PTS), these signalling sequences can be used to search for yet unidentified peroxisomal proteins. Due to the poorly defined sequence of the mPTS, only the matrix targeting signals have been used. In the published studies the C-terminal PTS1 was very stringently and narrowly defined using the very last three amino acid motif of PTS1 (in most cases serine-lysine-leucine, SKL) only and an N-terminal nonamer sequence of PTS2. These studies neglected the more complex structure of PTS1 [36] most probably missing some putative peroxisomal matrix proteins and based their algorithm for PTS2 on a very small learning set. A disadvantage of these approaches is that only matrix enzymes can be detected unless the mPTS would be used. Additionally, the targeting signal can be masked due to multimer formation or protein conformation or can be inactivated by post translational modifications. Import mechanisms differing from the ones using PTS1 or PTS2 like piggy-backing with PTS containing proteins or the use of yet unidentified mechanisms are not detected either [31]. In other words, *in silico* predictions of protein localization provide an excellent hint but no proof for localization.

To date, no high through-put localization studies have been performed exclusively focusing on the peroxisomal proteome. However two genome-wide studies in *S.c.*, have led to the identification of several peroxisomally located proteins. These approaches were based on tagging all open reading frames in the genome with epitopes for indirect immunofluorescence or with GFP and on the subsequent localization analysis of the corresponding proteins by fluorescence microscopy [37, 38]. In addition, three databases filled with results from similar experiments are accessible via the SGD [39]. Two reasons account for the relatively low number of identified peroxisomal proteins. On the one hand, these globally oriented studies were usually performed under peroxisome repressing conditions (glucose presence) and on the other hand, C-terminal tags were used hence masking the PTS1 which is the most prominent targeting signal for peroxisomal matrix proteins. A repeat of these analyses under conditions that induce peroxisome proliferation combined with the use of N-terminal tags would provide a good means to upgrade the knowledge about the peroxisomal proteome – at least in terms of the matrix proteins. The identification of peroxisomal membrane proteins by this method may remain a complicated

task due to the low expression levels of membrane proteins and the resulting low fluorescence intensity.

Interactome studies aim at the elucidation of interaction partners and hence at the identification of new functions of proteins or of functional relationships between already known ones. Such studies are usually high through-put studies and have hitherto not been restricted to a set of all known peroxisomal proteins but rather aimed at the generation of interaction maps for whole *S.c.* cells. Two different methods are commonly used to perform these studies – the classical yeast two-hybrid screen and MS analysis of immune-isolated protein complexes [31].

The classical yeast two-hybrid approach is based on the idea that two domains of the GAL4-transcription factor, the DNA-binding domain and the transcription activating domain, are separately fused to a protein or a domain and upon induction between the two proteins the transcription factor becomes active consequently leading to reporter gene expression, originally the ß-galactosidase from E.coli. This way, binary interactions between all tested proteins can potentially be detected. The complex formed by the interaction between the two proteins should mimic the original GAL4 protein regarding its three-dimensional arrangement and the distance between the DNA binding site and the transcriptional activating part. Two of the largest yeast-two hybrid screens concerning the *Saccharomyces cerevisiae* interactome were performed by Uetz *et al.* and Ito *et al.* [40, 41]. Although large-scale in none of the studies the entirety of all potentially expressed proteins of a *S.c.* cell was investigated. In addition, the YTH method suffers from a high frequency of false negative and false positive results. For some proteins such an assay may not be applicable. Hydrophobic proteins, for instance, are poorly transported into the nucleus rendering the transcription-based investigation of membrane proteins a complicated task. Therefore, a modified two-hybrid assay (ubiquitin-based split-protein sensor [42]) was used in another study especially focusing on *S.c.* membrane proteins [43]. The multitude of false positive identifications may on the one hand result from protein interactions which occur in the context of the YTH assay but not *in vivo*. On the other hand, several reasons can lead to reconstitution of the transcriptional activity independent from interaction of the test proteins.

The mass spectrometry based analysis of isolated protein complexes represents the second widely used method in interactome studies. As, in contrary to the YTH approach, not only binary interactions but indeed multiple interactions within protein complexes can be identified the term “complexome” is associated with this methodology [44]. To isolate

protein complexes, cells expressing a tagged "bait" protein are generated – in case of large-scale studies this has to be done for preferably all potentially expressed proteins of the cell. After breaking the cells, the tagged protein and all its associated "prey" proteins can be isolated either by co-immunoprecipitation or tandem affinity purification. The protein members of the isolated complexes can be identified by MS. The studies by Gavin *et al.* [45] and Krogan *et al.* [46], both employing the method of tandem affinity purification, represent the most recent comprehensive investigations of the *Saccharomyces cerevisiae* interactome. However, in terms of the peroxisomal interactome these studies did not reveal extensive novel data because the cells were grown in peroxisome repressing conditions and the proteins were tagged at the C terminus.

Due to the high-throughput character of the different methods, the individual validation of each candidate interaction partner using independent experimental approaches is not realistic. Computational strategies mostly based on "a test of the correlation between the interaction data and other properties known about the proteins, protein networks, or the corresponding genes" [47] are used to increase the confidence of the data set.

In contrast to the globally oriented methods with peroxisomal proteins representing a small part of the whole genome, mass spectrometry based analyses of the whole peroxisomal protein content have to be combined with preceding subcellular fractionation techniques to enrich for peroxisomes and their proteins. A positive aspect of this strategy compared to others is that all peroxisomal proteins regardless of their import pathway can be detected. However, the predominant challenge is that by the generation of a subcellular fraction, one cannot entirely purify but only enrich for the desired organelle type. As a result, contaminations from other organelles cannot be ruled out. Additionally, expression levels varying over several orders of magnitude can be the reason that proteins of low abundance (especially membrane proteins) can be masked by high abundant ones (generally matrix proteins but also contaminating proteins). Since proteins involved in regulatory processes or being part of the membrane are present in relatively low copy number, important information may be missed. Whereas "genomic approaches have taken advantage of amplification methods such as the polymerase chain reaction, proteomics is still limited by the inability to amplify the protein content of any biological sample" [48]. To compensate this deficiency, the development of better isolation protocols including for instance immune-purification is necessary. The enormous progress in mass spectrometry in the 1990s (MALDI – "matrix assisted laser desorption ionisation" [49] and ESI – "electrospray

ionisation" [50]) made it possible to identify protein traces in complex biological samples and consequently analyse these subcellular fractions. For proteomic approaches three different setups for mass spectrometric analyses have emerged – all comprising gel electrophoresis or liquid chromatography or a combination of both methods and an enzymatic digestion of the isolated proteins generating peptides prior to the MS analysis [48]. The first setup combines a two dimensional gel electrophoresis (2DE) and the following enzymatic digestion with MALDI-MS to analyse the protein spots of the gel. However, several inconveniences are associated with 2DE, like the under-representation of membrane proteins because of their low solubility and of proteins with extreme molecular weight or isoelectric point [51]. The other two setups avoid these problems by replacing the 2DE with different separation methods. The approach performed in my study comprises one dimensional SDS-PAGE, in-gel-digestion of the separated proteins and the following analysis by liquid chromatography coupled ESI-MS. The last variant omits gel electrophoretic separation at all starting with a delipidating step (protein precipitation using a methanol-chloroform-water mixture [52]) prior to the enzymatic digestion. The separation and analysis of the resulting peptide mixture of the digested complex sample is subsequently carried out by two or more dimensional liquid chromatography-ESI-MS [53, 54].

Despite the technical advances in subcellular fractionation and MS analysis, some challenges remain. As a 100% purification of the desired organelle class – in this case peroxisomes – is not possible, the enrichment of the true organellar proteins has to be validated. This can be accomplished by demonstrating the increase of known peroxisomal proteins and the decrease or absence of known contaminating proteins from other organelles. This has to be done for all candidate proteins for a novel assignment to the peroxisomal proteome. Special methods are necessary for proteins localized to more than one compartment. In addition, the mass spectrometric analysis, especially the ionization and detection of sample peptides, depends on their physical and chemical properties rendering quantification not possible with "simple" MS strategies. As a result, MS based quantitative proteomics have been developed. The current methods have been reviewed by Aebersold and Mann in 2003 [55].

Eventually, it remains to emphasize that the proteome of an organelle (as well as the one of the whole cell) is subject to constant changes depending on the metabolic state of the cell determined by the external conditions. Consequently, one of the biggest challenges is the comprehensive investigation of the protein content of an organelle in a defined

developmental or metabolic state. The preparation of the subcellular fraction required for subsequent MS analysis necessitates time consuming isolation procedures comprising in case of *S.c.* for instance the enzymatic digestion of the cell wall and the homogenization of the resulting spheroplasts. However, as cells and their internal compartments are not static entities, they will undergo dynamic changes in response to this stress. As a result, the isolation of an organelle from cells in the desired condition seems to be currently out of reach. The development of faster isolation procedures would therefore help to overcome these problems and gain access to the proteome of organelles from cells in a clearly defined metabolic state.

1.3 FAOS – A NEW METHOD FOR ORGANELLE PURIFICATION

The principle of Fluorescence Activated Cell Sorting was developed in the 1960s with the first commercially available FACS-machines in the 1970s. Since then, progress concerning the speed of sorting and the number of measurable parameters was made although the principle of the analysis and the sorter did not change over the years [56]. In this work, the idea and major challenge is to utilize the well established method of isolating a certain cell type by sorting according to fluorescence for the purification or rather enrichment of organelles, much smaller particles than cells.

1.3.1 FACS (fluorescent activated cell sorter) – the method

In a flow cell of the BD FACSAria used in this study the sample stream is hydrodynamically focused by the surrounding stream of sheath fluid. As a result, the cells are forced to pass one or more laser interrogation points in single file. Two parameter classes are measured in this region to create morphological, structural or functional information about the cell – light scattering and fluorescence. The light scattering parameters comprise forward scatter (light scattered axial to the laser beam) and side scatter (light scattered perpendicular to the laser beam). The corresponding signals provide information about the relative size and internal complexity of the cells respectively [57]. Everything recognized by the machine via light scattering and consequently converted into an electric pulse is defined as an "event". The fluorescence emission of fluorescent dyes or fluorescently tagged molecules in or on the cells can be used to distinguish between cells differing in user defined properties. As, to date, 18 or more fluorescent channels [58] are available, several cell features can be used as sorting criteria at the same time.

After signal detection, the stream is broken into highly uniform droplets by a nozzle. The time it takes for a cell to move from the laser interception point to the droplet breakoff point is determined by the FACS. Hence, it is possible to determine which droplet will contain a cell meeting the sorting criteria and therefore representing a "positive event" (determined by light scattering and/or fluorescent properties). As soon as such a droplet detaches from the stream, electrical charge is applied to it. The charged droplet is deflected to the left or right as it passes through highly charged deflection plates. Droplets containing

either no cell or a cell not meeting the sorting criteria are not charged, therefore not affected by the electric field and collected in the waste (see figure 1-2, [57]).

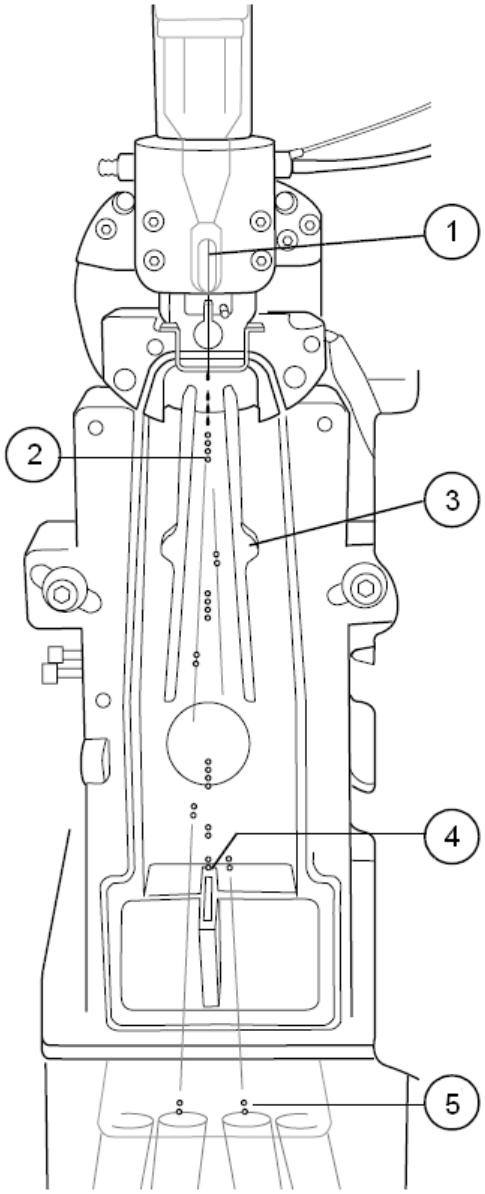

Figure 1-2: Principle setup of the BD FACSAria [57]. Sites of important events during the sorting process are indicated: (1) the sample generates light scatter and fluorescence signal in the flow cell, (2) droplets break off from the stream, (3) deflection plates attract or repel charged droplets, (4) uncharged droplets pass to waste, (5) charged droplets containing cells of interest are collected.

1.3.2 FAVS and FAOS – the further development of FACS

With the establishment of more and more fluorescent probes and protocols allowing staining for cell viability or integrity of organelle membranes, studies based on various intracellular components became possible. The first studies in this field, concentrating on

the endocytic compartment, were performed by Murphy *at al.* [59]. However, despite the labelling of endocytic vesicles, the sorting procedure was limited to the measurement of whole cells. Things changed when Allen *et al.* applied flow microfluorimetry to investigate phosphatidylcholine/cholesterol vesicles with an average diameter of 268nm [60]. They were able to analyse vesicles from unfractionated cell lysates and sort individual vesicles for further analysis. As the purification of organelles has always been a critical point in cell biology, it was obvious to combine conventional subcellular fractionation techniques with flow cytometric sorting procedures to enhance the enrichment of the desired organelles [61] – the concept of FAOS and FAVS was born. This combination is supposed to be particularly successful because subcellular fractionation techniques are usually based on physical properties, such as density, but flow cytometry exploits the biological characteristics of the desired organelles or vesicles. Hence, particles sharing the same density can be separated by an additional fluorescence activated sorting step. In this way, the two approaches perfectly complement each other. However, down-scaling the method of flow cytometry in respect to particle size also implicates a sensitivity problem because the number of fluorescent molecules bound to or associated with a defined particle is considerably smaller compared to whole cells. The right choice of the fluorescent probes (absorption coefficient and quantum efficiency) can be useful but high background signals can hamper the detection anyway. Autofluorescence, electronic noise, laser light fluctuations, room light and contaminating particles are the problems to cope with, although some improvements can be achieved by electronic compensation [62]. Two recent studies successfully exploited the method of FAVS to generate a highly pure vesicle fraction – Bananis *et al.* focused on the purification of fluorescent endocytic vesicles for subsequent biochemical analyses of the purified fraction [63] whereas Cao *et al.* combined flowcytometry based purification of fluorescent exocytic vesicles with LC/LC-MS/MS for a subsequent proteomic analysis [64].

Regarding the evolution of flow cytometry, “it has developed from an immunological scanning device for the expression of surface markers into a versatile tool for analysis of cellular functions…It facilitates subcellular fractionation and allows preparation of extremely pure organelle fractions in amounts sufficient for biochemical analysis” [62].

2 AIM OF THE THESIS

The aim of my diploma thesis was twofold – the elucidation of the proteome of mature peroxisomes from ethanol grown *Saccharomyces cerevisiae* cells and preliminary investigations of pre-peroxisomal vesicles. For both aspects, machine-based sorting methods should be implemented to further purify the subcellular fractions subjected to proteomic analysis.

As already delineated, the peroxisomal membrane proteins attracted our attention because they are involved in many peroxisomal processes not yet fully understood, such as the communication with other organelles, transport of metabolites across the peroxisomal membrane, motility of the peroxisomes, etc. Proteomic studies on peroxisomes from oleic acid grown *S.c.*yeast cells have already been performed in our laboratory. In addition to supplementing these data, my work is aimed at investigating the dynamic adaptation of the peroxisomal proteome to modified environmental conditions such as growth on different carbon sources.
No molecular details of the very early events during peroxisome biogenesis are known. It remains to be shown which peroxisomal proteins are present in the ER right from the beginning of peroxisome formation and how the proteome of the formed pre-peroxisomal vesicles changes during their maturation process. With my work, the necessary prerequisites should be established to be able to perform proteomic studies on these early stages in the future.

Our proteomic approach comprises the preparation of a highly purified peroxisomal fraction, the separation of the corresponding proteins by SDS polyacrylamide gel electrophoresis followed by an in-gel-digestion with trypsine of the whole sample lane cut into small gel pieces and the elution and analysis of the resulting peptides by nano-LC/ESI tandem MS. To generate the required highly purified peroxisomal sample, fluorescence activated organelle sorting (FAOS) should be established as a new method to further purify the peroxisomal fraction obtained by density gradient centrifugation of the post nuclear supernatant (PNS).

3 RESULTS

3.1 FLUORESCENT PEROXISOMES AND OTHER SUBCELLULAR STRUCTURES

3.1.1 Tagging of peroxisomal membrane proteins with EGFP

3.1.1.1 PCR based chromosomal EGFP tagging

To label mature peroxisomes or potential peroxisomal precursors, the peroxisomal membrane proteins (PMPs) Pex3p and Pex29p and additionally a truncated version of Pex3p only consisting of the first 46 amino acids (Pex3(1-46)p) should be C-terminally tagged with EGFP by PCR based chromosomal tagging. To generate the linear DNA fragment for homologous recombination, a PCR was performed using the plasmid pCB463 as template and the primers CB186/CB185 for *PEX3*, CB184/CB185 for *PEX3(1-46)* and CB187/CB188 for *PEX29*. The sizes of the resulting linear DNA fragments were checked and the fragments purified by agarose gel electrophoresis and subsequent extraction from the gel. A transformation was performed using the wild type *S.c.* cells (strain CB80). The *EGFP* cassette contains the *KanMX4* module leading to kanamycin resistance and the potential transformants were therefore plated on YPD G-418 and colonies resistant to G-418 (kanamycin sulphate) were selected. After 3d at 30°C, colonies of different size were visible and the big colonies were re-streaked on new selective media because they are most likely derived from single cells with stably integrated fragments due to homologous recombination.

To check if the cells of the selected colonies have properly inserted the linear fragment and to exclude colonies where it has been inserted randomly, a colony PCR for control was carried out. For *PEX3* and *PEX3(1-46)*, the control primers CB163/H796 and for *PEX29* the control primers CB163/H804 were used. CB163 binds to a region downstream of the *EGFP* and *KanMx4* ORF in the insertion cassette, whereas the primers H796 and H804 bind to a region 3' of the stop codon of the corresponding gene (539bp and 261bp respectively).

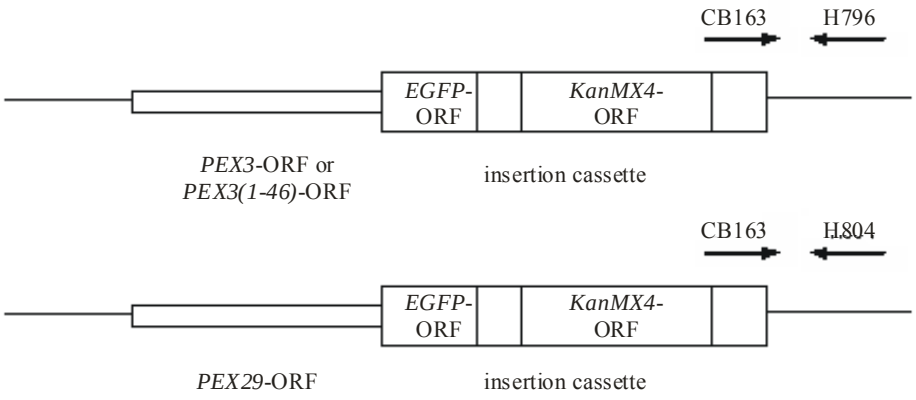

Figure 3-1: Expected chromosomal situation after correct insertion of the *EGFP*-ORF containing cassettes into the genes *PEX3* and *PEX29*. The binding regions of the control primers for the control PCR are indicated as arrows.

A PCR product can be produced only if the *EGFP*-ORF containing cassette was inserted at the right place. The expected lengths of the control PCR products were 696bp for *PEX3-EGFP* and *PEX3(1-46)-EGFP* and 416bp for *PEX29-EGFP*. Almost every selected colony gave rise to PCR fragments of expected size (see figure 3-2). In each case, colony #1 was taken for the following experiments.

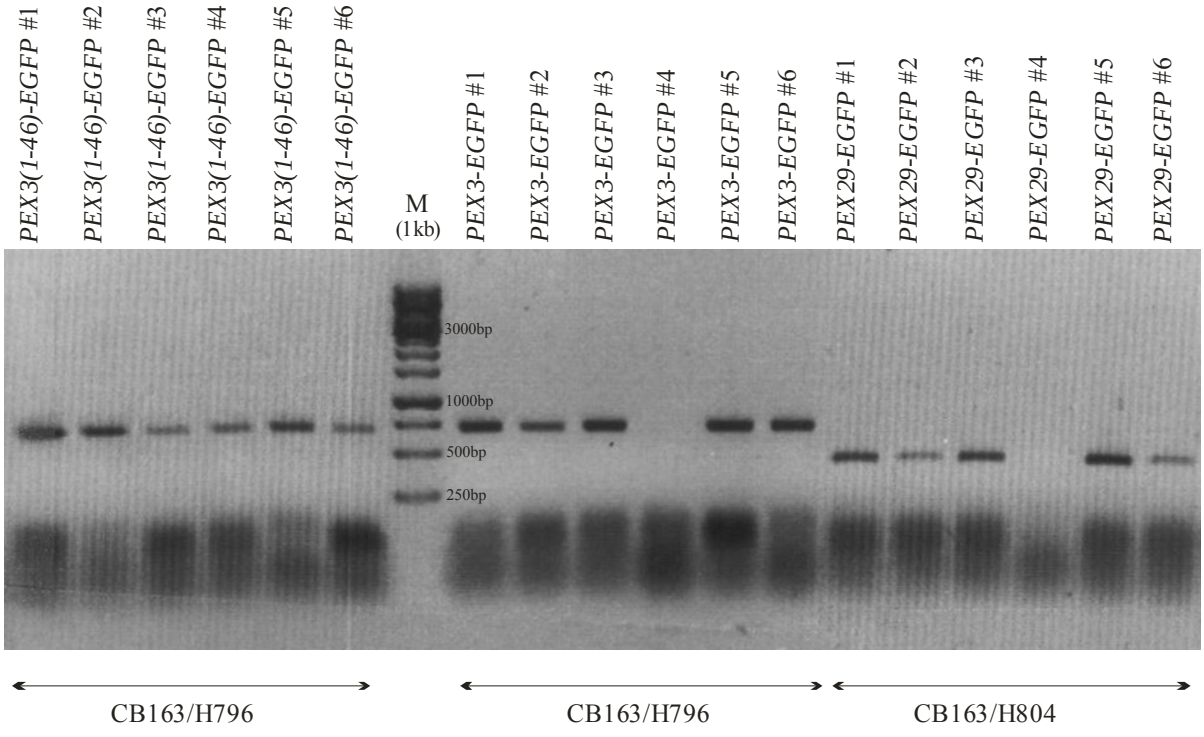

Figure 3-2: Agarose gel showing the products of the control PCRs from strains containing the denoted constructs to confirm the correct insertion of the *EGFP*-ORF containing cassette into the genes *PEX3*

and *PEX29*. As marker, a 1kb DNA ladder was used. All colonies except #4 with the potential *PEX3-EGFP* construct and #4 with the potential *PEX29-EGFP* construct contain the correctly integrated *EGFP*-cassette and were rated as positive transformants.

3.1.1.2 Fluorescence microscopy

One-step transformations with the plasmid pCB367 encoding the peroxisomal marker protein mCherry-SKL employing cells from colonies #1 containing either one of the three *EGFP* constructs were carried out in order to investigate whether the EGFP tagged proteins are able to be transported to peroxisomes.
Cells from the strains under scrutiny were grown o/n in SC –Ura with 0,5% glucose and were investigated under the fluorescence microscope without any embedding or fixation. Cells of the strains expressing the constructs *PEX3-EGFP* and *PEX29-EGFP*, transformed with mCherry-SKL, respectively, contained few small peroxisomes. The peroxisomes were doubly labelled – a bright red label resulting from the import of mCherry-SKL and a faint green label originating from the EGFP tagged PMPs. The colocalization of the labels indicates that both, Pex3p and Pex29p are EGFP tagged and that their peroxisomal localization is not disturbed. Cells of the strain with the EGFP tagged truncated version of Pex3p (Pex3(1-46)p-EGFP) also transformed with mCherry-SKL contained no detectable peroxisomes. mCherry-SKL stained the cytosol because the truncation of Pex3p impaired peroxisome biogenesis [20]. Pex3(1-46)p was expected to localize to dots in the ER but no green dots could be detected – maybe because of the small number of Pex3(1-46) proteins and the resulting faint fluorescence of EGFP.

3.1.2 *GAL* promoter controlled expression of *PEX3-EGFP* and *PEX3(1-46)-EGFP*

3.1.2.1 PCR based chromosomal insertion of the GAL promoter

To increase the fluorescence intensity of the EGFP tagged PMPs and to be able to induce peroxisome biogenesis, the expression of the EGFP tagged versions of Pex3p and Pex3(1-46)p was brought under the control of a *GAL L* or *GAL S* promoter in each case. This was accomplished by PCR based chromosomal insertion. The linear insertion constructs were generated by PCR using the plasmids pCB510 and pCB514 as template for the *GAL L* and *GAL S* promoter fragment respectively, the corresponding primers were CB206/CB207.

After purification of the linear fragments by agarose gel electrophoresis and extraction of the linear DNA fragments from the gel, cells of yeast strains expressing Pex3p-EGFP and Pex3(1-46)p-EGFP were transformed with the corresponding linear constructs. As the insertion cassette has a *natNT2* marker, the potential transformants were plated on YPD CloNAT plates to select for cells which have stably integrated the fragments by homologous recombination. After 3 days of growth at 30°C, several of the big colonies were re-streaked on new selective media.

Chromosomal DNA was isolated from the colonies of the transformants under scrutiny in order to carry out control PCRs to confirm the correct insertion of the *GAL L* or *GAL S* promoter. Three different control PCRs were carried out for the constructs *PEX3-EGFP* (*GAL L* or *GAL S* promoter controlled) and *PEX3(1-46)-EGFP* (*GAL L* or *GAL S* promoter controlled) each. Chromosomal DNA from yeast cells expressing Pex3p-EGFP was used as negative control in every case. The corresponding primers were H962/H967b, H962/CB164 and CB230/H976b. H962 binds in the *PEX3* promoter region, 540bp upstream from the start codon of *PEX3* and H967b binds to a region in the *PEX3*-ORF within the first 46 codons, 94bp downstream of the start codon. The primers CB164 and CB230 correspond to regions in the insertion cassette, whereas the other primers are *PEX3* specific. CB164 binds 305bp upstream from the *natNT2*-ORF and CB230 binds directly in the *GAL L* or *GAL S* promoter.

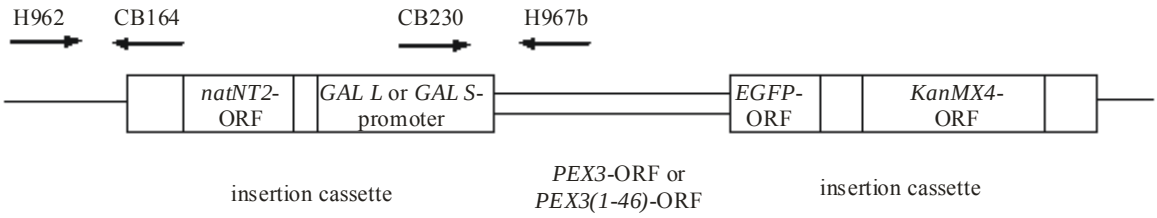

Figure 3-3: Expected chromosomal situation after correct insertion of the *GAL L* or *GAL S* promoter containing cassette to the genes *PEX3-EGFP* and *PEX3(1-46)-EGFP*. The binding regions of the control primers are indicated as arrows.

In case of insertion of the *GAL* promoter containing cassette, there will only be PCR products with the primers H962/CB164 (698bp) and CB230/H967b (466bp). PCR with the primer pair H962/H967b will give no product because the expected fragment length of 2500bp is generally too long to be synthesized by Taq polymerase. If the insertion cassette has not integrated correctly into the genome, only the PCR employing the primer pair

H962/H967b will show positive results with the fragment length being the same as in the negative control (706bp).

Only DNA isolated from the colonies containing the constructs *PEX3(1-46)-EGFP* (*GAL L* promoter controlled) #10, *PEX3(1-46)-EGFP* (*GAL S* promoter controlled) #1, #2, #6, *PEX3-EGFP* (*GAL L* promoter controlled) #1 and *PEX3-EGFP* (*GAL S* promoter controlled) #1 and #4 show the expected PCR products for a correct insertion. The other colonies show different, to some extent unexpected DNA fragment lengths and were therefore excluded from further experiments. In further experiments cells from the colonies #1 of the strain CB80 expressing Pex3p-EGFP or Pex3(1-46)p-EGFP under the control of the *GAL L* or *GAL S* promoter, respectively, were used.

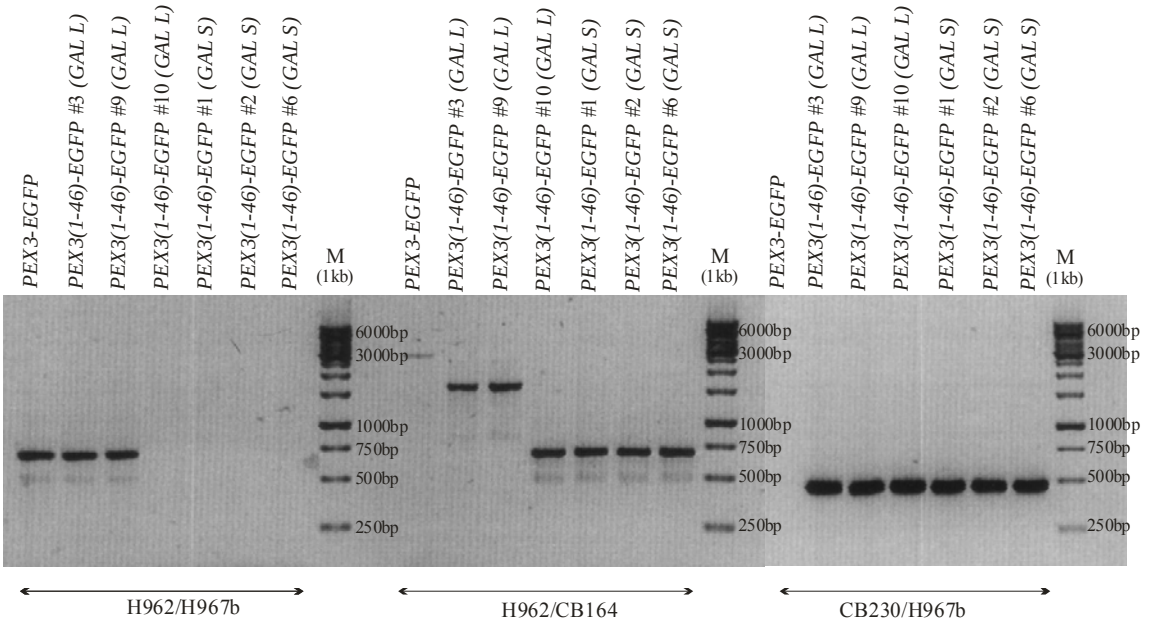

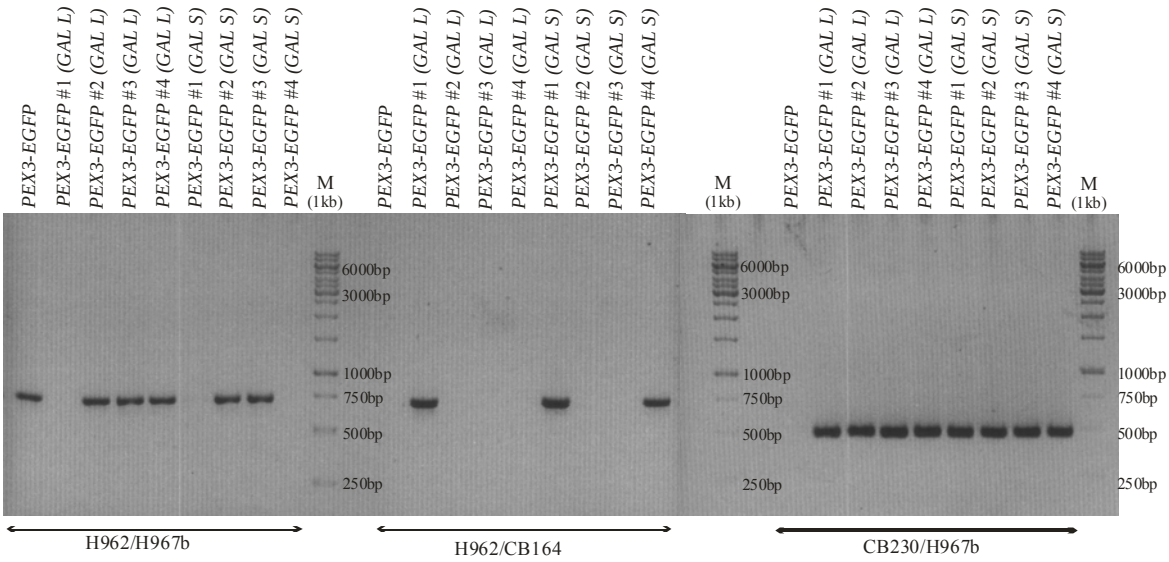

Figure 3-4: Agarose gel showing the products of the control PCRs from strains containing the denoted constructs (promoters in brackets) to confirm the correct insertion of the *GAL* promoter containing cassette to the *PEX3(1-46)-EGFP* and *PEX3-EGFP* construct, respectively. As marker, a 1kb DNA ladder was used. Only colony #10 from the strain with the *PEX3(1-46)-EGFP* construct under the potential control of the *GAL L* promoter, all three tested colonies (#1, #2, #6) from the strain with the *PEX3(1-46)-EGFP* construct under the potential control of the *GAL S* promoter, colony #1 from the strain with the *PEX3-EGFP* construct under the potential control of the *GAL L* promoter and two colonies (#1, #4) from the strain with the *PEX3-EGFP* construct under the potential control of the *GAL S* promoter showed expected results in every control PCR and are therefore judged as positive transformants.

3.1.2.2 Fluorescence microscopy

Prior to fluorescence microscopy, a one step trafo of the transformants with correctly integrated *GAL* promoter fragments employing the plasmid pCB367 encoding mCherry-SKL was carried out. To check if the *GAL* promoter correctly controls the transcription of *PEX3-EGFP* or *PEX3(1-46)-EGFP*, respectively, cells from o/n cultures of the positive transformants in SC 2% glucose and in YPG/R were investigated under the fluorescence microscope. The cells grown in glucose containing medium showed no green labelling resulting from the complete shut-down of *PEX3-EGFP* or *PEX3(1-46)-EGFP* transcription in the absence of galactose. Consequently, these cells do not have peroxisomes and mCherry-SKL was therefore localized to the cytosol. After o/n induction in galactose containing medium, however, bright green fluorescent dots were visible. In case of CB80 cells harbouring the full-length *PEX3-EGFP* under control of the *GAL L* or *GAL S* promoter, in most cases only one big green fluorescent structure per cell was visible which was also labelled with mCherry-SKL. Therefore, this structure most likely represents a peroxisome. Upon growth on galactose containing medium CB80 cells containing the construct *PEX3(1-46)-EGFP* under control of the *GAL L* or *GAL S* promoter showed one weakly green fluorescent dot per cell which was smaller and not labelled by mCherry-SKL. These dots most likely correspond to the ER regions where Pex3p-EGFP accumulates during the onset of peroxisome biogenesis. A more detailed investigation of peroxisome biogenesis by galactose induction is presented in section 3.1.5.

3.1.2.3 Halo assay

A halo assay was performed to test if the *GAL L* and *GAL S* promoters are leak-proof meaning that they really shut off transcription of the genes under their control in absence of galactose. Furthermore, the halo assay was also used to confirm the functionality of the galactose induced peroxisomes. Only CB80 cells containing the construct *PEX3-EGFP* under the control of the *GAL L* or *GAL S* promoter (in each case colony #1) were investigated in addition to cells expressing the same construct from the genuine *PEX3* promoter as positive control because the truncated version *PEX3(1-46)-EGFP* leads to a block in peroxisome biogenesis.

The *GAL L* and *GAL S* promoter should tightly shut off when the cells are grown on galactose free medium. Therefore, a halo assay was carried out with cells grown under four different growth conditions. Starting with o/n cultures in SC 2% glucose, cells were freshly diluted into the following media prior to dropping dilution series on oleic acid containing plates: SC 0,5% glucose (grown until OD_{600} ~1 or ~3), YPR (grown until OD_{600} ~1) and YPG (grown until OD_{600} ~1).

As expected, wild type cells expressing Pex3p-EGFP from the genuine promoter formed halos due to oleic acid consumption in each case. However, the two strains with the construct *PEX3-EGFP* under control of the *GAL L* or *GAL S* promoter only showed halo formation like the positive control when grown on galactose containing medium prior to spotting on oleic acid. According to this, both *GAL* promoters are leak-proof when the cells are grown on galactose free medium (SC or YPR) and the transcription of *PEX3-EGFP* and consequently peroxisome biogenesis under these conditions can be induced by presence of galactose. Since the cells were able to utilize oleic acid as sole carbon source the peroxisomes formed under these conditions must be functional. Comparing the two different *GAL* promoters, *GAL S* seems to be more suitable than *GAL L* because cells harbouring the latter produced a very weak halo around the spot with the highest concentration of cells when grown on galactose free medium. As this slight halo only appeared when the cells were spotted undiluted and as the cells did not grow on the oleic acid plate, this strain was also judged as leak-proof in absence of galactose. Growth on YPD plates was normal for each strain tested.

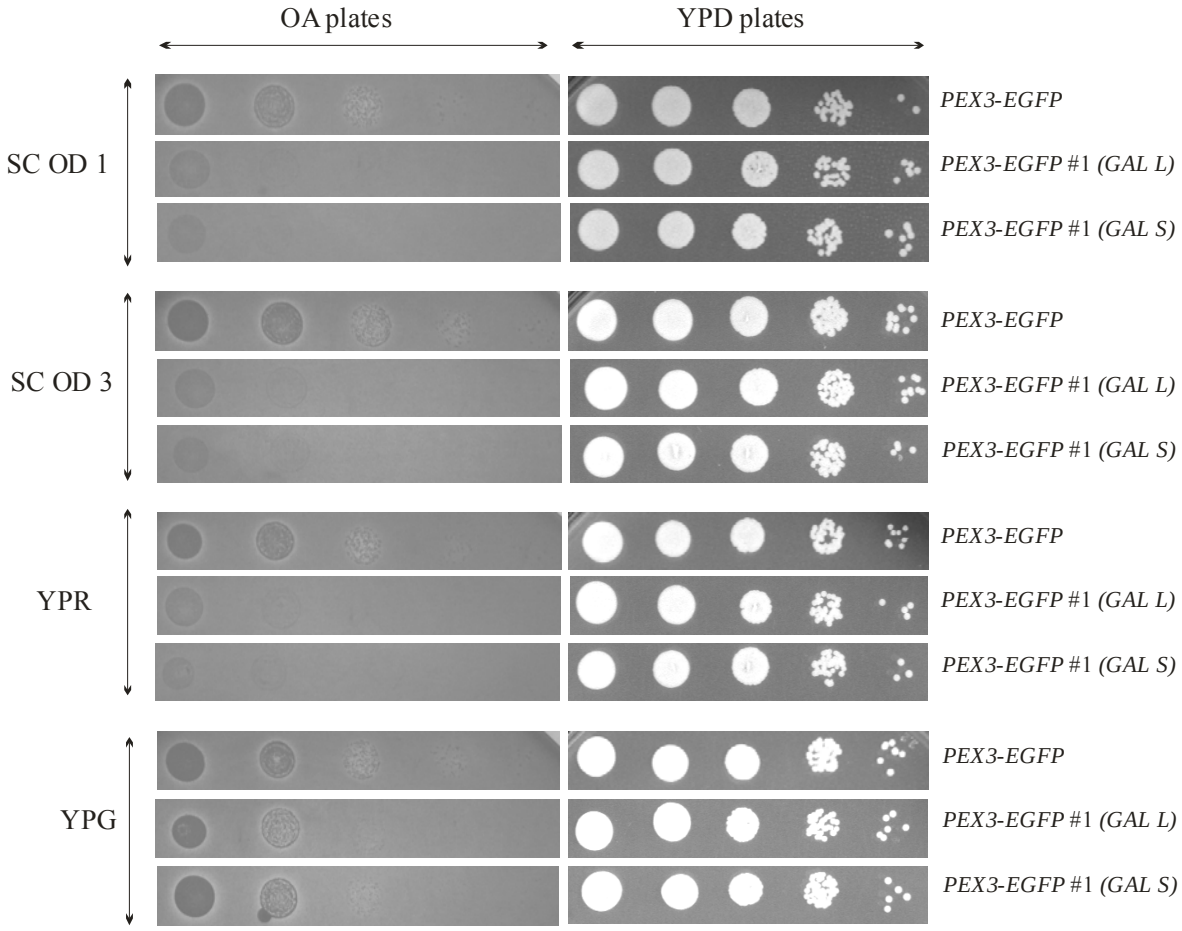

Figure 3-5: Halo assay demonstrating that cells (containing the denoted constructs) expressing Pex3p-EGFP under control of the *GAL L* or *GAL S* promoter are able to build functional peroxisomes only after induction with galactose. CB80 cells expressing Pex3p-EGFP from the genuine promoter were used as positive control. The following dilution series of the cultures was spotted onto the oleic acid plate: undiluted, 1:10, 1:100, 1:1000, 1:10 000.

3.1.3 *GAL* promoter controlled *PEX3-EGFP* in pex19Δ cells

3.1.3.1 PCR based chromosomal insertion of the deletion cassette

The attempts to label parts of the ER through *GAL* promoter controlled expression of Pex3(1-46)p-EGFP identifying these as regions of putative origin of peroxisome biogenesis lead to relatively weak fluorescent dots, possibly due to instability of the truncated fusion protein. Alternatively, the progress of peroxisome biogenesis can be inhibited by the lack of Pex19p [19], and it could be expected that full length Pex3p fused

to EGFP will accumulate in the ER in absence of Pex19p.Therefore, a PCR based chromosomal insertion was performed with a deletion cassette in order to replace *PEX19* in the genome of CB80 cells expressing Pex3p-EGFP under the control of the *GAL L* or *GAL S* promoter.

A PCR employing the plasmid pCB447 as template and CB211/CB212 as primers was carried out to generate the linear DNA construct encoding the deletion cassette. The size of the DNA fragment was checked and the fragment purified by agarose gel electrophoresis. After extraction of the DNA from the gel, cells of the yeast strain CB80 expressing *GAL* promoter controlled Pex3p-EGFP were transformed and colonies resistant to hygromycin B (*hphNT1* marker) were selected. After three days at 30°C, some of the big colonies were re-streaked on new selective medium.

To analyze whether the deletion cassette has integrated correctly into the genome, chromosomal DNA was isolated from cells of several selected colonies. Control PCRs with the primers CB225/CB257 and CB225/CB164 were carried out. CB225 binds in the *PEX19* promoter sequence, 67bp 5' of the start codon of the ORF. CB257 corresponds to a region in the *PEX19* ORF, 20bp upstream of the stop codon. As this sequence is consistent with the 3' homologous region in the deletion cassette, this primer will bind both in the wild type and in the newly generated *pex19*Δ strain. CB164 binds in the deletion cassette close to the 5' homologous region.

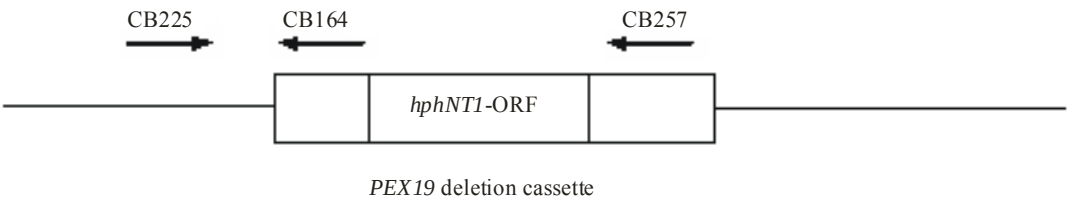

Figure 3-6: Expected chromosomal situation after correct insertion of the *PEX19* deletion cassette. The binding regions of the control primers are indicated as arrows.

The PCR employing CB225/CB257 is expected to produce a fragment of different lengths depending on whether *PEX19* has been deleted (1828bp) or not (1102bp). Using the primers CB225/CB164, only cells with a correctly integrated deletion cassette will give rise to a PCR product of 196bp. Several colonies showed consistent results in every control PCR. (The PCR products of one colony each are shown in figure 3-7).

To confirm, that all chromosomal inserts remained in place in the different strains throughout the consecutive rounds of homologous recombinations, PCRs were performed

as a final control. The strains investigated were CB80 (wt) and the already characterized and selected transformants (containing the constructs *PEX3-EGFP*, *PEX3-EGFP* under the control of the *GAL L* or *GAL S* promoter, respectively, and *pex19*Δ *PEX3-EGFP* under the control of the *GAL L* or *GAL S* promoter, respectively). The PCRs were performed with chromosomal DNA in case of the transformants but in case of the CB80 wt strain, only colony PCRs were carried out. The applied primers and the corresponding fragment lengths expected are listed in table 3-1. Except H795 which binds 67bp upstream of the stop codon of *PEX3*-ORF, all of the primers are explained in more detail in the sections 3.1.1. and 3.1.2.

	CB163/ H796	H795/ H796	H962/ CB164	H962/ H967b	CB225/ CB257	CB225/ CB164
EGFP +	696bp	(3112bp)				
EGFP -	-	631bp				
GAL L or *S* +			698bp	(2523bp or 2507bp)		
GAL L or *S* -			-	706bp		
*pex19*Δ					1828	196bp
PEX19					1102p	-

Table 3-1: Employed primers and fragment lengths expected after PCR to confirm the presence of the *EGFP* tag, the *GAL L* or *GAL S* promoter and the deletion of *PEX19*. Fragments which may be too long to be synthesized by Taq polymerase are set in brackets.

The PCR fragments produced from the chromosomal DNA isolated from the transformants investigated showed the expected length in all cases. The colony PCRs employing the CB80 wt cells did not result in expected products in two cases.

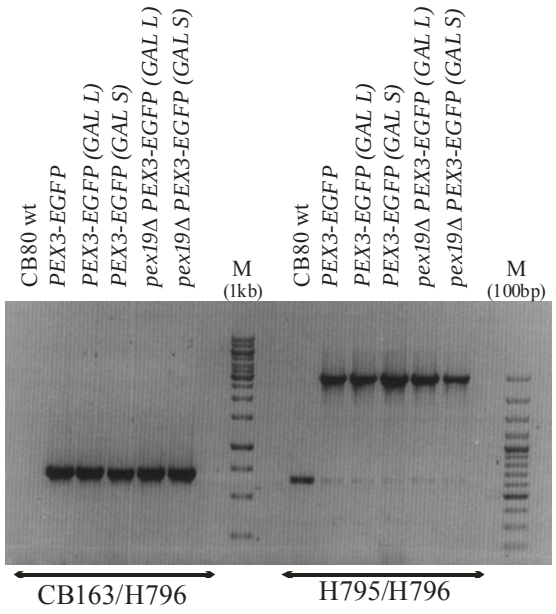
CB80 wt
PEX3-EGFP
PEX3-EGFP (GAL L)
PEX3-EGFP (GAL S)
pex19Δ PEX3-EGFP (GAL L)
pex19Δ PEX3-EGFP (GAL S)
M (1kb)
M (100bp)
CB163/H796
H795/H796

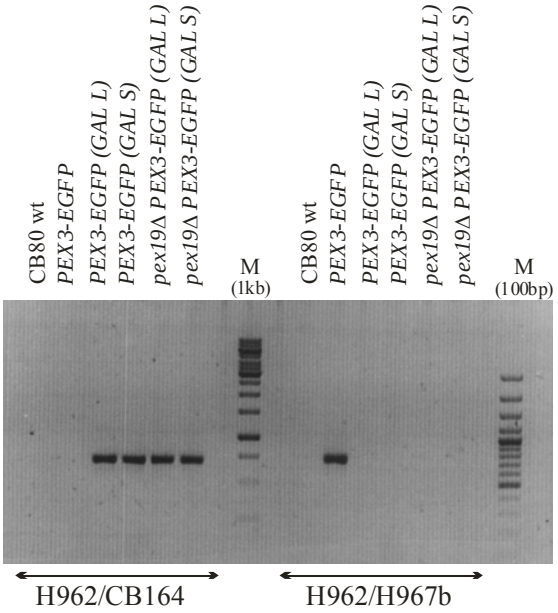
CB80 wt
PEX3-EGFP
PEX3-EGFP (GAL L)
PEX3-EGFP (GAL S)
pex19Δ PEX3-EGFP (GAL L)
pex19Δ PEX3-EGFP (GAL S)
M (1kb)
M (100bp)
H962/CB164
H962/H967b

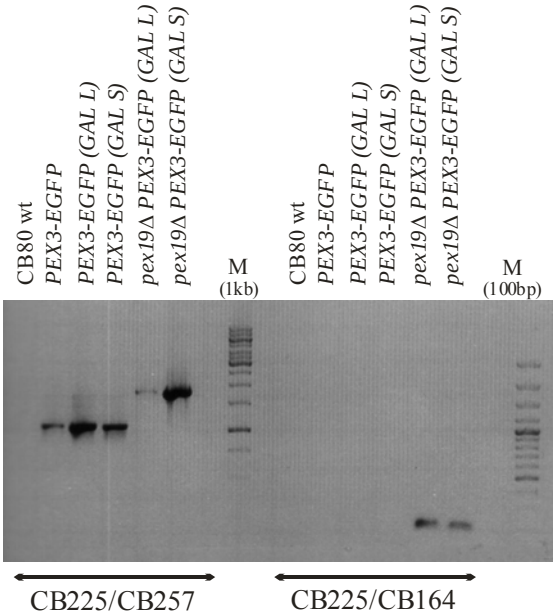
CB80 wt
PEX3-EGFP
PEX3-EGFP (GAL L)
PEX3-EGFP (GAL S)
pex19Δ PEX3-EGFP (GAL L)
pex19Δ PEX3-EGFP (GAL S)
M (1kb)
M (100bp)
CB225/CB257
CB225/CB164

Figure 3-7: Agarose gel showing the PCR products of the summarized control PCRs. All chromosomal inserts are present in the strains with the different constructs throughout the consecutive rounds of homologous recombinations. The *pex19*Δ *PEX3-EGFP* construct under the control of the *GAL L* or *GAL S* promoter could be established successfully. A 1kb and a 100bp marker were used.

3.1.3.2 Fluorescence microscopy

The plasmid pCB367 encoding mCherry-SKL was transformed into *pex19*Δ cells of the strains containing the constructs *PEX3-EGFP* under the control of the *GAL L* or *GAL* S promoter, respectively. Cells from colonies selected after transformation were grown o/n in SC-Ura 2% glucose and in YPG/R, respectively. Then, the cells were inspected under the fluorescence microscope without any embedding or fixation.

When cells where grown on galactose-free medium, mCherry-SKL was distributed throughout the cytosol due to the lack of peroxisomes and no green labelling could be detected. The cells which were grown on YPG/R, however, showed green dots resulting from the galactose induced expression of Pex3p-EGFP. As *PEX19* is deleted in the strains under scrutiny, no peroxisomes can be formed and Pex3p-EGFP localized to punctuate structures, most likely representing regions of the ER. As a result, mCherry-SKL still stained the cytosol. These results were consistent with the ones from the control PCRs and therefore underlined the correct deletion of *PEX19*.

3.1.3.3 Halo assay

Deletion of *PEX19* will inhibit biogenesis of functional peroxisomes irrespective of the expression levels of other PEX genes [19]. Therefore, the absence of functional peroxisomes in the newly produced *pex19Δ* cells was tested by a halo assay after galactose-driven induction of Pex3p-EGFP expression. Two different positive controls were included – CB80 strains expressing Pex3p-EGFP either from its native promoter or from the *GAL* S promoter, respectively.

The growth procedure started with an o/n culture in SC 2% glucose and the final medium was YPG. The cells were grown in YPG until an OD_{600} of ~1 was reached or for at least 5h to ensure sufficient galactose-driven induction of *PEX*3-*EGFP*.

Both positive controls showed the expected halo formation indicating that Pex3p-EGFP is a functional protein and its expression from the *GAL S* promoter after induction by galactose or from the native promoter is sufficient to allow peroxisome biogenesis. The

*pex19*Δ cells were unable to metabolize oleic acid and therefore formed no halos independent from the induction of Pex3p-EGFP expression.

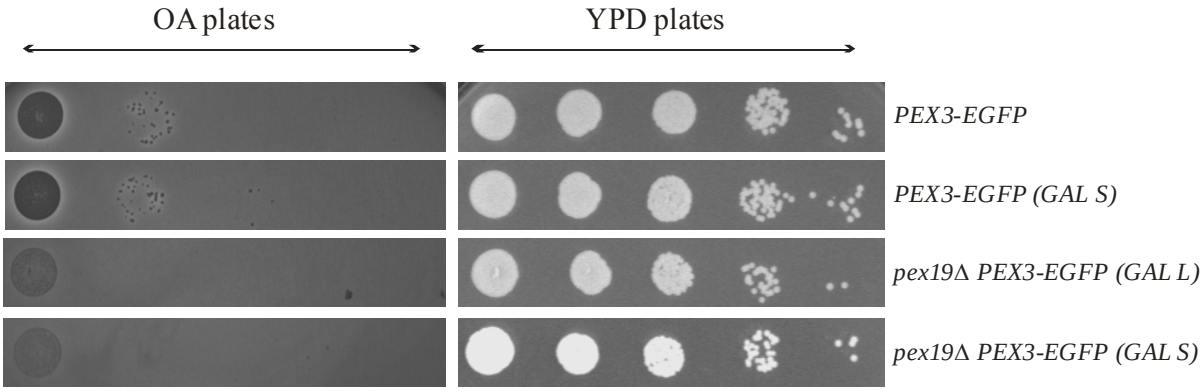

Figure 3-8: Halo formation depends on a functional *PEX19* gene. *Pex19*Δ cells and wild type cells carrying the constructs as indicated were serially diluted and spotted on oleic acid plates after growth on YPG for at least 5h. Dilution series: undiluted, 1:10, 1:100, 1:1000, 1:10 000.

3.1.4 Visualization of CTHA tagged PMPs by immunofluorescence

3.1.4.1 Immunofluorescence in whole cells employing α-HA-Alexafluor 488

S.c. cells expressing different CTHA- or HA-tagged proteins were permeabilized and incubated with the commercially available α-HA-Alexafluor 488 antibody and inspected in a fluorescence microscope. The cells expressed either one of the following CTHA or HA-tagged peroxisomal membrane proteins (PMPs):
Pxa1p-CTHA, Pxa2p-CTHA, Pex3(1-46)p-CTHA, Pex3p-CTHA, Pex11p-HA, Pex11p-CTHA, Pex13p-CTHA, Pex14p-CTHA, Pex22p-CTHA, Pex28p-CTHA, Pex29p-CTHA, Pex30p-CTHA, Pex31p-CTHA or Pex32p-CTHA. Cells from the wild type strain CB80, transformed with the plasmid pCB367 encoding mCherry-SKL were used as control for growth conditions and peroxisome appearance. The cells were grown in the oleic acid containing Rytka medium (see section 5.6.2.3.) to ensure that the cells harbour many peroxisomes. Immunofluorescence was observed as described in section 5.5.1.
Wild type CB80 cells expressing mCherry-SKL showed red punctuate structures and no green fluorescence as expected. However, green fluorescent dots were only detectable in cells from the strains expressing Pex11p-HA, Pex11p-CTHA and Pex22p-CTHA. Cells

from the first two strains showed bright fluorescence compared to the very faint fluorescence of the cells expressing Pex22p-CTHA.

The lack of visible fluorescence for most of the PMPs could result either from low expression levels, small percentage of peroxisomal localization or from a low accessibility of the antibody to these integral membrane proteins. Proteins attached to the membrane or membrane associated proteins could for instance cover parts of integral PMPs and prevent antibody interaction with the HA tag. Therefore, the experiment was repeated using an additional incubation step with 1% Triton-X-100 for 10' or 1% SDS for 5' after the partial spheroplasts had been immobilized on the microscopy slide. After this incubation, the specimen cavities were washed with PBS three times and one time with BSA-PBS. The following antibody incubation was carried out as usual.
If cells were treated with Triton-X-100, the results were exactly the same as without. If cells were treated with SDS they were washed off the microscopy slide during the following washing steps.

3.1.4.2 Visualization of α-HA-Alexafluor 488 labelled structures in organellar pellets

α-HA-Alexafluor 488 was thought to be used as fluorescent label of isolated peroxisomes to be sorted by FAOS afterwards. Therefore, I tried to incubate an organellar pellet with α-HA-Alexafluor 488. Organellar pellets were derived from cells of the strain CB80 expressing either Pxa2p-CTHA, Pex3p-CTHA, Pex11p-HA or Pex29p-CTHA and as negative control an organellar pellet was derived from cells of the strain CB80 transformed with the plasmid pCB367 encoding for mCherry-SKL. The procedure to obtain the OP is described in section 5.7. but the experiment was downscaled to a 100mL final culture. In addition, instead of PSB a BB buffer (0,6M sorbitol, 5mM MES, 1mM KCl, 0,5mM EDTA) was used for the preparation of the OP because PEG may impair antibody-epitope interactions. One half of the resulting OP was resuspended in BB buffer, the other half was resuspended in PSB buffer. The protocol for the antibody incubation is described in section 5.5.2. The samples were inspected under the fluorescence microscope without any fixation or embedding.
Consistent with the results from the immunofluorescence test employing whole cells, the organellar pellet from CB80 cells expressing mCherry-SKL showed red labelled structures,

and among many unlabelled ones only in the pellet derived from CB80 cells expressing Pex11p-HA green fluorescent structures were visible.

Besides low amounts of proteins the unsuccessful labelling of parts of the OP from cells of the strains expressing Pxa2p-CTHA, Pex3p-CTHA or Pex29p-CTHA could be due to inaccessibility of these PMPs. So, in parallel to the incubation of one half of the OP resuspension with the fluorescent antibodies, a limited proteolytic digestion was carried out with the other half of the OP resuspension prior to the labelling procedure. Thermolysin was used to carry out this limited proteolysis for 2', 10' and 20', respectively, and after careful washing the OPs were incubated with the appropriate α-HA-Alexafluor488 dilution. The results were comparable to the ones without proteolytic digestion. In the OP containing structures with Pex11p-HA green fluorescent dots were visible even after Thermolysin digestion for 20', in all other OPs not. This result showed that proteolysis had not been carried out for too long.

3.1.5 Fluorescence intensities of peroxisomal structures

To evaluate the different labelling methods for peroxisomes and the ER regions representing the putative starting points of peroxisome biogenesis, respectively, for their potential application in fluorescence activated machine-based sorting, the intensities of the visible fluorescent punctuate structures were analyzed.

strains (containing the listed constructs)	transformation
PEX3-GFP	no
PEX3-EGFP	mCherry-SKL
PEX3(1-46)-EGFP	mCherry-SKL
PEX3-EGFP (GAL S)	mCherry-SKL
PEX3(1-46)-EGFP (GAL S)	mCherry-SKL
pex19Δ PEX3-EGFP (*GAL S*)	mCherry-SKL
CB80 (wt)	GFP-SKL
PEX11-HA	no

In most cases cells were finally grown on ethanol as carbon source according to the protocol given in section 5.6.2.2. However, when the expression of the EGFP-fusion protein was controlled by a *GAL* promoter cells were grown on galactose containing medium (YPG) for the last two hours prior to being transferred to YPE.
Cells expressing Pex11p-HA were incubated with α-HA-Alexafluor488 after permeabilization, fixation and immobilization on microscope slides as described in section 5.5.1. The fixation and immobilization procedure was similar for cells expressing GFP or a GFP fusion protein. The fluorescent punctuate structures in the cells were inspected by fluorescence microscopy and pictures were taken applying exactly the same exposure times for all samples.

The intensities of the fluorescent punctuate structures visible in the cells expressing different tagged proteins were analyzed using the corresponding fluorescence microscopy pictures (see figure 3-9). EGFP labelled structures showed a slightly more intense fluorescence than GFP labelled ones. Fluorescent structures resulting from *GAL* promoter induced expression of *EGFP* constructs led to bright fluorescence but at the same time to unnatural structures as mentioned in section 3.1.2. Punctuate structures potentially representing the ER regions of putative peroxisome biogenesis showed the most intensive – although probably not sufficient – labelling in cells carrying a deletion of *PEX19* in addition to the *PEX3-EGFP* construct under the control of a *GAL* promoter. However, if the cells of this strain were grown in galactose containing medium for more than 2h and not transferred into YPE, the dots would become much brighter (data not shown). The fluorescent dots probably representing peroxisomes showed the highest intensity when Alexafluor488 or GFP-SKL was used as fluorescent label. Hence, cells expressing GFP-SKL or Pex11p-HA treated with α-HA-Alexafluor488 afterwards seem to be the most promising candidates to provide peroxisomes for the purification by fluorescence activated machine-based sorting.

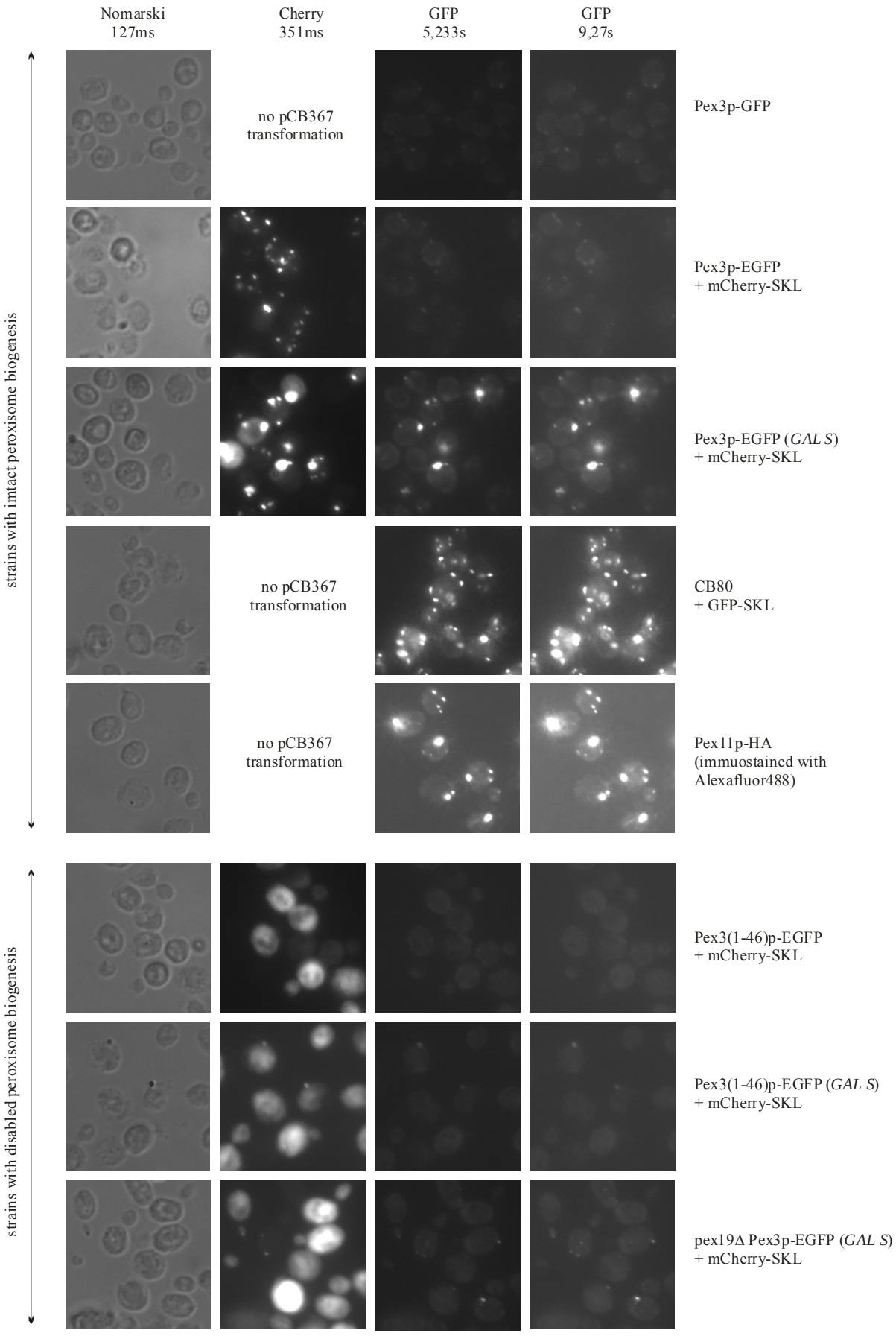
Nomarski
127ms
Cherry
351ms
GFP
5,233s
GFP
9,27s
strains with imtact peroxisome biogenesis
no pCB367
transformation
Pex3p-GFP
Pex3p-EGFP
+ mCherry-SKL
Pex3p-EGFP (GAL S)
+ mCherry-SKL
no pCB367
transformation
CB80
+ GFP-SKL
no pCB367
transformation
Pex11p-HA
(immuostained with
Alexafluor488)
strains with disabled peroxisome biogenesis
Pex3(1-46)p-EGFP
+ mCherry-SKL
Pex3(1-46)p-EGFP (GAL S)
+ mCherry-SKL
pex19Δ Pex3p-EGFP (GAL S)
+ mCherry-SKL

Figure 3-9: Fluorescence microscopy images of cells expressing different fluorescently labelled proteins. A *GAL* promoter driven expression is indicated in brackets. In cases of an additional transformation with a plasmid, the expressed protein is denoted with "+".

3.1.6 Time dependence of peroxisome biogenesis

Peroxisome biogenesis was followed in time employing cells expressing Pex3p-EGFP either from the *GAL* promoter or from the endogenous promoter. Cells from both strains had been transformed with the plasmid pCB367 encoding mCherry-SKL. They were grown and further processed according to the procedure presented in section 5.6.2.4. Fluorescence (green and red channel) was followed for many hours in cells either continuously exposed to galactose or only for 30' followed by a shift to a glucose containing medium repressing the *GAL* promoter driven expression of Pex3p-EGFP.

At the starting point of our investigation, i.e. prior to shifting the cells into galactose containing media, the cells with *GAL* promoter driven expression of Pex3p-EGFP showed diffuse red fluorescence indicating cytosolic localization of mCherry-SKL and no green fluorescence besides auto-fluorescence was detectable. In the cells from the reference strain expressing Pex3p-EGFP under the control of the endogenous promoter, doubly labelled structures were visible – weak green fluorescent dots overlapped with bright red fluorescent dots indicating that mature, import competent peroxisomes were present. The appearance of the reference strain remained unaffected by different media conditions or time points. Cells with limited *GAL* promoter driven expression of Pex3p-EGFP, however, showed the following time course of events when galactose induction was carried out. 60' after the onset of galactose induction (i.e. 30' after transfer to glucose containing media), weak green dots were visible but mCherry-SKL retained its cytosolic localization. These structures might represent ER regions or pre-peroxisomal vesicles which are not yet import competent. After 120', labelling with mCherry-SKL overlapped with the green dots. This double labelling indicated the appearance of import competent peroxisomes. Nearly complete double labelling of the punctuate structures was achieved 3-4h after the onset of galactose induction. When continuous galactose induction was carried out, the fluorescence intensity of the green dots increased steadily resulting in a much brighter fluorescence than in cells exposed to a 30' galactose pulse resembling the green fluorescence intensity achieved in the reference strain with *PEX3-EGFP* under control of the endogenous promoter. As described earlier, galactose induced expression of Pex3p-EGFP led to the formation of only one big peroxisome and sometimes some smaller ones.

In summary, the results of these experiments confirmed the previous observations [19] in our strain background.

3.2 ISOLATION AND PURIFICATION OF PEROXISOMES

3.2.1 Adjustment of the Nycodenz density gradient

In the procedure already established to isolate peroxisomes from oleic acid grown yeast cells a density gradient is applied consisting of three layers with 25%, 35% and 50% $_{w/v}$ Nycodenz, respectively. The middle layer serves to separate peroxisomes from the other organelles, mainly from mitochondria. As peroxisomes from ethanol grown *S.c.* cells were expected to be of lower density than the ones from oleic acid grown cells, the density of the middle layer had to be adjusted in order to ensure good separation from mitochondria.

Cells of the yeast strain CB80 expressing Pex22p-CTHA were grown according to the procedure described in section 5.6.2.2. After spheroplasting, homogenization and generation of the PNS, the density gradient centrifugation was carried out. In contrast to the final procedure given in "Materials and Methods", the composition of the density gradient and the duration of the ultracentrifugation were varied. The PNS was loaded onto four different gradients. The following densities were tested for the separation layer: 35%, 33,5%, 32% and 30%. The ultracentrifugation was carried out for 90' and fractions were collected. Equal volumes or equal amounts of protein from the gradient fractions and the PNS were loaded onto a SDS polyacrylamide gel. Equal volumes could be loaded in case of all gradient fractions, but from the PNS a smaller volume was used. When equal protein amounts were loaded, the peroxisomal fraction served as reference – for the fractions with a lower protein concentration, the maximum possible amount was loaded. Proteins were separated by electrophoresis and blotted onto nitrocellulose. Antibodies against Cta1p (catalase A – peroxisomal matrix protein), Por1p (porin – mitochondrial outer membrane protein) or Kar2p (ER membrane protein) were used for immune-decoration and visualized (Western blot).
Catalase A was present in the peroxisomal fraction, the mitochondrial fraction and the PNS in every case. Kar2p was detected in every fraction probably due to vesiculation during the isolation procedure. Comparing the Western blots for the different gradients, porin showed the most striking change in its distribution over the individual fractions. In the gradients containing the separation layers with 35%, 33,5% or 32% Nycodenz porin was only detectable in the mitochondrial fraction and in the overlying fractions. However, when the separation layer with 30% Nycodenz was used porin contaminated the peroxisomal

fraction. A separation layer with 32% Nycodenz seemed to be the optimal choice because on the one hand the density was high enough to prevent mitochondrial contamination in the peroxisomal fraction and on the other hand the density was low enough to not reduce the yield of peroxisomes. However, the distribution of porin within the gradient did not meet our expectations. In contrast to the results, porin should be more concentrated in the mitochondrial fraction than in the overlying ones. It might well be that the density of the 25% Nycodenz layer was too high for all mitochondria from ethanol grown yeast cells to permeate and that the duration of the ultracentrifugation was too short to ensure an equilibrium state.

The experiment was repeated employing cells from a different strain (CB80 cells expressing Pxa2p-CTHA). In this experiment, the 25% Nycodenz layer was exchanged for a 20% Nycodenz layer and the tested separation layers were 32%, 30% and 28%. In addition, the ultracentrifugation was carried out for 120'.

The results from this experiment confirmed that a separation layer with 32% Nycodenz is best suited for peroxisome isolation because porin could be detected in the peroxisomal fraction when the separation layer contained 30% or 28% Nycodenz, respectively. The lower density of the top layer and the extended time for ultracentrifugation resulted in a better enrichment of porin in the mitochondrial fraction and of catalase A in the peroxisomal fraction. In the following experiments, the time for ultracentrifugation was further increased to 150'.

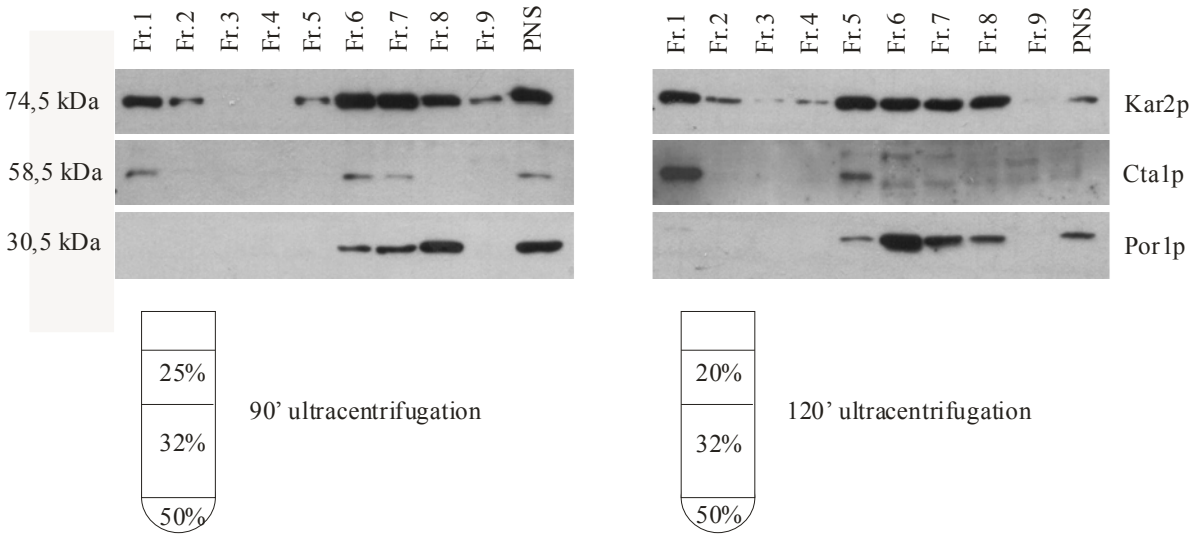

Figure 3-10: Western blots showing the fractions of the Nycodenz density gradient and the PNS. Equal amount of protein was loaded. The peroxisomal fraction was used as reference for the protein amount – in case of fractions with lower protein amount (Fr.2-5), the maximum possible amount was loaded.

The differences in the experimental setup are outlined in the sketch below. (Fr.1=peroxisomal fraction, Fr.6=mitochondrial fraction).

3.2.2 Generation of a peroxisomal pellet (PxP)

Preliminary experiments showed that the high viscosity of the Nycodenz solution disturbed the machine-based sorting procedure. Therefore, the viscosity of the peroxisomal fraction had to be reduced prior to performing FAOS, e.g. by centrifugation at ~30 000 x g similar to the centrifugation used to generate an organellar pellet. To determine the g-value and time sufficient for pelleting intact peroxisomes the following experiment was performed.

Cells of the yeast strain CB80 transformed with the plasmid pJR233 encoding GFP-SKL were grown on YPE according to the procedure described in 5.6.2.2. The peroxisomal fraction was prepared through density gradient centrifugation and diluted in PSB according to the protocol given in “Materials and Methods”. This peroxisomal fraction, isolated at the border line between the 50% and 32% Nycodenz layer, was expected to contain roughly 10% Nycodenz after the dilution step. Three equal portions of the diluted fraction (overlaid with PSB to ensure that the centrifuge tube was filled until the top) were subjected to centrifugation for 10’ at different speed (15 000 x g, 20 000 x g, 30 000 x g) and the resulting pellets were resuspended in PSB. Equal volume equivalents from the peroxisomal fraction (Fr.1 of the gradient), the diluted peroxisomal fraction, the pellets generated through high speed centrifugation, the corresponding supernatants and the overlays were mixed with SDS loading buffer, heated and loaded onto a SDS polyacrylamide gel and gel electrophoresis was carried out. Western Blots were performed using antibodies against Pex30p and Cta1p.

Catalase A was only detectable in the undiluted and diluted peroxisomal fraction of the density gradient suggesting that the centrifugation procedure was not sufficient to pellet the organelles. The distribution of Pex30p varied with the different centrifugation rates. After centrifugation at 15 000 x g, more Pex30p was detected in the supernatant than in the pellet indicating that only small fractions of the organelles were pelleted. When the centrifugation was carried out at 30 000 x g Pex30p accumulated in the peroxisomal pellet as expected although the yield was not 100%. As a result, the peroxisomal pelleting in the following experiments was carried out at 30 000 x g.

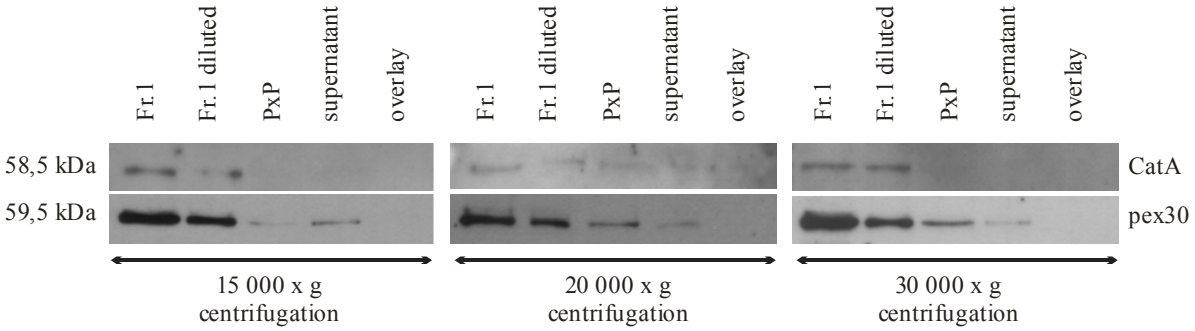

Figure 3-11: Western Blots of aliquots from the three peroxisome pelleting experiments. Equal volume equivalents were applied. The g-values from the centrifugations are indicated below. (Fr.1=peroxisomal fraction).

3.3 PROTEIN DETERMINATION AND IDENTIFICATION IN PEROXISOMAL FRACTIONS DERIVED FROM YEAST CELLS

3.3.1 Distribution of marker proteins in the gradient fractions

After each peroxisome isolation performed, all fractions of the density gradient were analysed by SDS polyacrylamide gel electrophoresis and Western blots. The applied antibodies were α-Cta1p, α-Kar2p, α-Por1p and α-Pex30p.

The distribution of catalase A, Kar2p and porin over the density gradient fractions were in all cases consistent with the results presented in section 3.2.1. Interestingly, the distribution of Pex30p did not meet our expectations. As Pex30p is supposedly an integral peroxisomal membrane protein it should be enriched in fraction 1, the peroxisomal fraction, similar to catalase A. However, Pex30p was detected in several fractions throughout the whole gradient. Either Pex30p is not exclusively localized to the peroxisomal membrane or several peroxisome families exist discriminated by their density and import ability. In the latter case the procedure used here leads to the enrichment of mature matrix protein containing peroxisomes only.

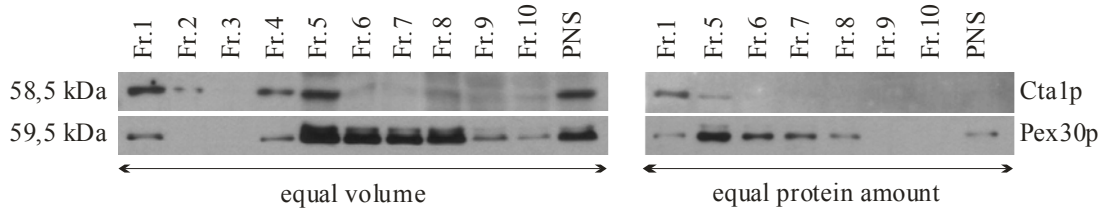

Figure 3-12: Western Blots employing the fractions of the Nycodenz gradient and the PNS. Either equal volumes (left, except for the PNS) or equal protein amounts (right) have been loaded onto the gel. (Fr.1=peroxisomal fraction, Fr.5=mitochondrial fraction).

3.3.2 Fluorescence activated organelle sorting (FAOS)

In preliminary experiments, FAOS was carried out using PNS or OP resuspensions. In later experiments the sorting procedure was applied to resuspended peroxisomal pellets (PxP).

Several fluorescently labelled peroxisome samples were monitored in the FACS in order to determine if the fluorescently labelled peroxisomal structures generate fluorescence of

sufficient intensity for a sorting process. PNS, OP resuspensions or PxP resuspensions derived from several strains expressing various fluorescent proteins were analyzed in a BD FACSAria. Pex3p-GFP, Pex14p-GFP, Pex29p-GFP, Pex3p-EGFP, Pex3(1-46)p-EGFP, Pex29p-EGFP and GFP-SKL were used as fluorescent peroxisomal marker proteins. In addition, an organellar pellet derived from cells expressing Pex11p-HA was employed in the sorting process after incubation with α-HA-Alexafluor488. The appropriate samples (PNS, OP or PxP) derived from cells of the CB80 strain expressing mCherry-SKL were used as negative control in each case.

Only the samples containing GFP-SKL or Pex11p-HA labelled with α-HA-Alexafluor488, yielded a big shift in fluorescence intensity compared to the auto fluorescence of the negative control. In the diagram forward/side scatter area, the events were distributed according to their size and internal complexity. The distribution suggests that there are different kinds of events. However, in both cases - the sample and the negative control - the distribution looked alike.

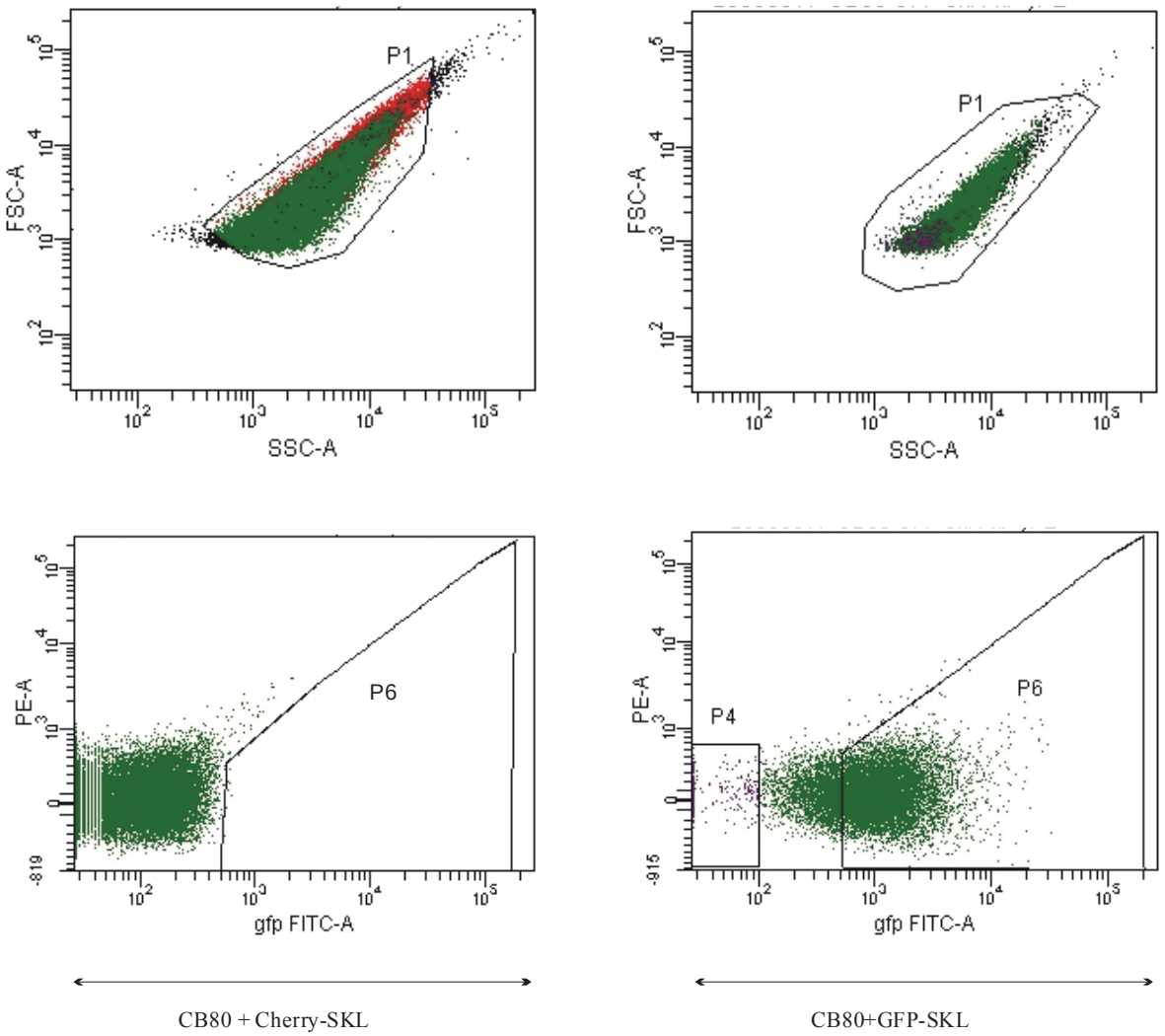

CB80 + Cherry-SKL

CB80+GFP-SKL

Figure 3-13: Diagrams showing the forward/side scatter area (top) and the intensity correlation between phycoerythrin and gfp FITC fluorescence (bottom). Gate P6 was set to exclude events of fluorescence intensities detected in a PxP containing mCherry-SKL ("negative events"). In the PxP containing GFP-SKL as fluorescent protein, 68,6% of all events appear in gate P6 ("positive events").

3.3.2.1 Sorting GFP-SKL labelled peroxisomes

Only in the PxP or the OP derived from CB80 cells expressing GFP-SKL and in the OP in which Pex11p-HA was the target for immune-decoration with α-HA-Alexafluor488 the fluorescence intensity was high enough to distinguish between positive and negative events. Since previous independent studies showed that immune affinity based separation techniques might not be the optimal method for organelle enrichment [65] we focused on GFP-SKL labelled peroxisomes.

Cells expressing GFP-SKL or mCherry-SKL, respectively, were grown on three different carbon sources – glucose, ethanol or oleic acid – and organellar pellets were produced. Sorting of the organellar pellets (~200µL) yielded diluted samples (~3mL) of positively sorted events. The sorted samples and an aliquot of the sheath fluid "FACS Flow" were subjected to TCA precipitation. The pellets were dissolved in 1x loading buffer and loaded onto a SDS polyacrylamide gel together with an aliquot of the OP derived from the ethanol grown cells. After electrophoresis, the gel was silver stained and for the OP lane also a colloidal Coomassie stain was performed.
In the sheath fluid sample, the silverstain revealed no protein bands even after very long development (data not shown). The band patterns of the three sorted samples (from glucose, ethanol and oleic acid grown cells) were very similar – only some bands in the "sort" lane from the oleic acid grown cells were different. When the pattern of protein bands visible in the lane of the OP is compared to the one in the "sort" lanes, several differences are noticeable.

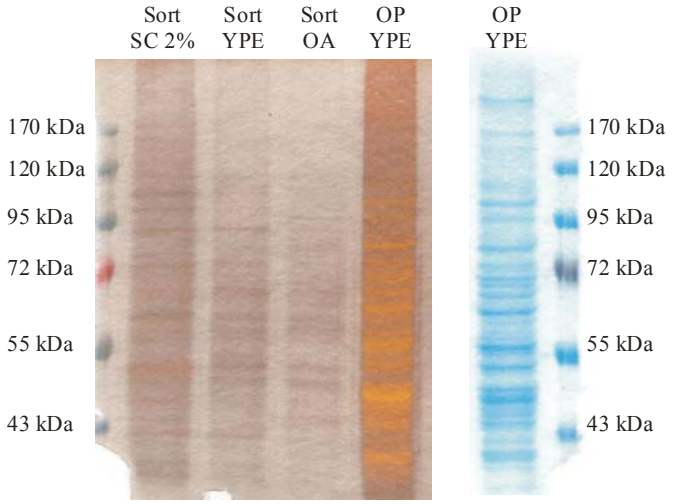

Figure 3-14: Image of a silverstained gel after separation of proteins precipitated from the positively sorted samples (from the OPs derived from glucose, ethanol or oleic acid grown cells expressing GFP-SKL) or from the OP from ethanol grown cells expressing GFP-SKL. The colloidal Coomassie stain of the OP is shown on the right side.

Following the definition that upon purification of a particular organelle the corresponding proteins should enrich with this compartment [66] genuine peroxisomal proteins should enrich in the positively sorted fraction. Identification of the proteins in both, the positively and the negatively sorted fractions by mass spectrometry should help identify novel peroxisomal proteins.

Peroxisomes were isolated and purified from ethanol grown cells expressing GFP-SKL (2L culture) yielding 200µL of the PxP. During the sorting process, two types of sorts were collected – the negative (gate P4, see figure 3-13) and the positive ones (gate P6, see figure 3-13). The events with intermediate fluorescence intensity were discarded. 1mL aliquots of the highly diluted sorted samples (several mL) from the PxP (~200µL) were again precipitated using TCA. Two pellets from each sort and an aliquot of the PxP were dissolved in 1 x loading buffer, loaded onto the gel and silverstained after gel electrophoresis.

Comparing the protein band pattern in the silverstained lanes derived from the positive and the negative sorted samples, striking similarities as well as differences are visible. As the samples were not loaded onto the gel in equal protein amounts or volume equivalents, estimations concerning enrichment of proteins in the positive sort compared to the negative sort are not possible. Although the band pattern derived from proteins of the peroxisomal pellet was almost identical in two independent experiments, the pattern of the sorted samples showed remarkable differences.

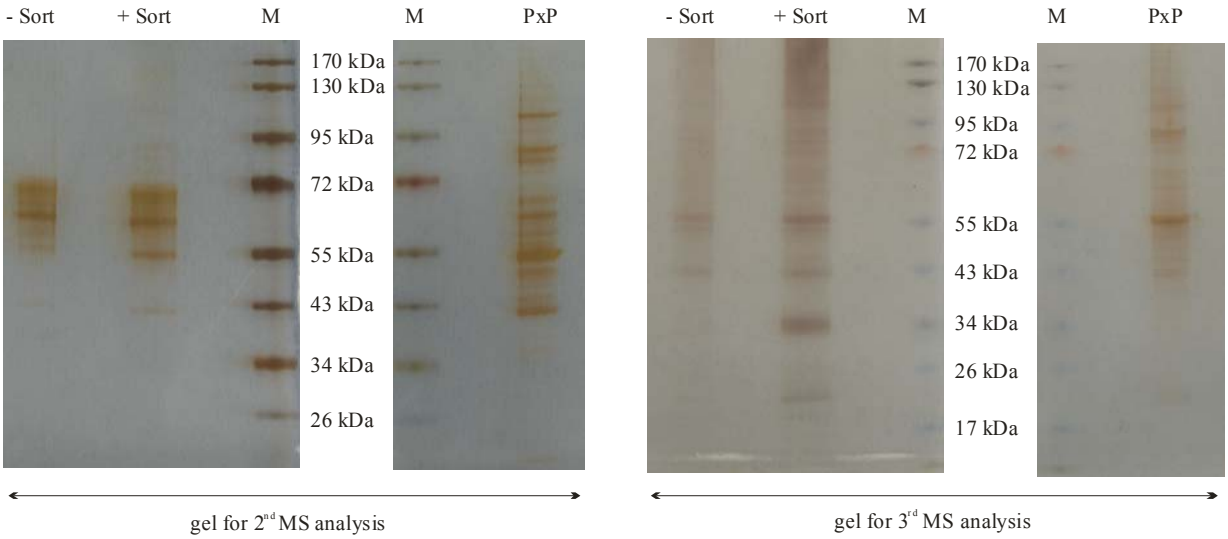

Figure 3-15: Image of silverstained gels after separation of proteins derived from the PxP or negatively or positively sorted samples from two independent experiments which were used for MS analysis afterwards.

In another experiment, droplets containing the positive sorted events (gate P6, see figure 3-13) and droplets containing all other events ("non-sorted") were collected. Protein analysis by SDS polyacrylamide gel electrophoresis applying equal volume equivalents of the PxP and the sorted samples was carried out and the distribution of Pex30p was analyzed by Western blotting.

Pex30p was detected in the PxP as well as in the positive sorted sample. The absence of Pex30p in the non-sorted fraction underlines the functionality of the sorting process. However, the amount of Pex30p present in the PxP should correspond to the amount of Pex30p present in the positive sort and the non-sort together. This is not the case suggesting that there are problems either during the sorting process or with the further processing of the sorted fractions (e.g. the TCA precipitation) rendering this experiment inconclusive.

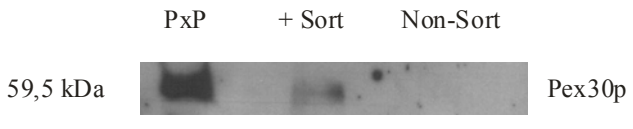

Figure 3-16: Western blot employing α-Pex30p and equal volume equivalents of PxP, the positive sorted and the non-sorted fraction.

3.3.3 MS analysis of the sorted fractions

Protein identification by mass spectrometry was performed on samples after fluorescence activated machine-based sorting. The peroxisomal pellets subjected to the sorting procedure described were derived from cells expressing GFP-SKL grown on ethanol. Positive and / or negative events were collected during the sorting (see section 3.3.2.). After TCA precipitation and separation of the proteins of these fractions by SDS polyacrylamide gel electrophoresis, the gel was silverstained and handed over to the MS facility. To identify all proteins present nano-LC tandem MS was performed on the peptides generated in each gel slice after cutting each lane in approximately 30 slices followed by in-gel trypsin digestion. The identification of the proteins was based in each experiment on a database search of the analysed peptides. The database included the proteins listed in the SGD (saccharomyces genome database) and in addition trypsin, keratins and GFP-SKL. More than 99,9% protein identification probability and not less than 2 unique peptides were required for a protein to be accepted and listed in the "raw data" table of identified proteins.

It was expected that the MS analysis – aiming at the identification of novel peroxisomal proteins – will result in a long list of proteins containing many putatively contaminating proteins from other organelles besides the true peroxisomal ones. The discrimination of true peroxisomal proteins from contaminating ones should therefore be based on the comparison between the data set of a fraction in which peroxisomal proteins are enriched (the positive sort) and the data set of a reference fraction. In the following, the results from three experiments using two different reference fractions are presented.

3.3.3.1 1st MS analysis

In the first experiment, the PxP – the original fraction subjected to the sorting process – was used as reference fraction. A comparison of the data set of the positive sort with the data set of the PxP was expected to reveal several novel peroxisomal proteins – in addition to already known ones – enriched in the sorted fraction.

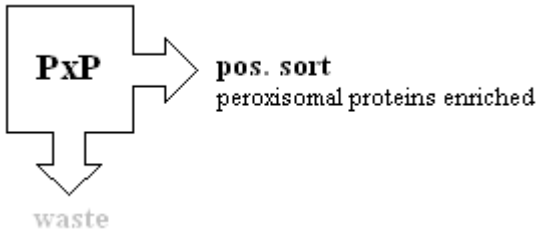

Figure 3-17: Principle setup of the 1st experiment. The positive events were sorted out from the original subcellular fraction (PxP); all other events were discarded. The fractions used for MS analysis are depicted in bold.

Using this experimental setup, the MS analysis led to the identification of 1590 proteins in the PxP and 215 proteins in the positive sort – only six of these were identified exclusively in the positive sorted sample. 5 proteins (2,3%) in the positive sort were known peroxisomal constituents according to annotations in the SGD and a list of peroxisomal proteins presented by Gabaldón *et al.* [21]. As this huge number of proteins was difficult to analyze and the number of known peroxisomal proteins was far too low, the experimental setup was changed.

3.3.3.2 2nd MS analysis

In this experiment, the idea was to compare the data sets of the positive and the negative sort (instead of the PxP). This modification should help to get a comprehensible amount of data and, in addition, it was expected that an enrichment of certain proteins in the positive sort can be pointed out more easily when the reference fraction is depleted in peroxisomal proteins facilitating the identification of novel peroxisomal proteins.

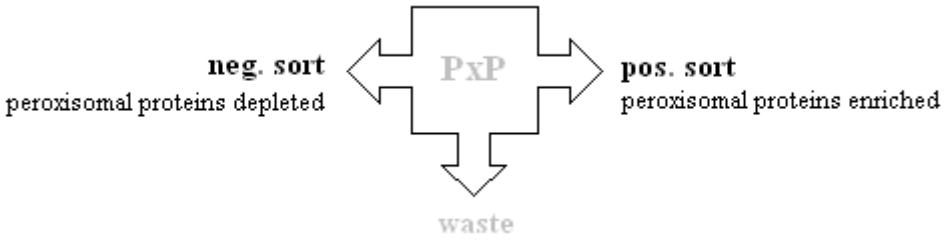

Figure 3-18: Principle setup of the 2nd experiment. The positive and negative events were sorted out separately from the original subcellular fraction (PxP); all other events were discarded. The fractions used for MS analysis are depicted in bold.

The MS analysis of the two sorted fractions resulted in a list of 296 proteins. The majority of proteins was detected in both sorted samples even though to a different extent. 11

proteins were present in only one of the two samples – 10 proteins were exclusively identified in the positive and one exclusively in the negative sort. 19 proteins (6,4%) were previously assigned to peroxisomes. Only six of these were detected exclusively in the positive sort.

Identified proteins	Systematic name
AAT2	YLR027C
ABF1	YKL112W
ABF2	YMR072W
ACC1	YNR016C
ACH1	YBL015W
ACO1	YLR304C
ACS1	YAL054C
ACS2	YLR153C
ACT1	YFL039C
ADE3	YGR204W
ADH1	YOL086C
ADH3	YMR083W
AGX1	YFL030W
ALD4	YOR374W
ARF1	YDL192W
ARO2	YGL148W
ARP4	YJL081C
ARP5	YNL059C
ARP7	YPR034W
ARP9	YMR033W
ATP1	YBL099W
ATP2	YJR121W
ATP3	YBR039W
ATP4	YPL078C
ATP5	YDR298C
ATP7	YKL016C
AYR1	YIL124W
BCY1	YIL033C
BDF1	YLR399C
BGL2	YGR282C
BMH2	YDR099W
BRE1	YDL074C
BRX1	YOL077C
CAM1	YPL048W
CAT2	YML042W
CAT8	YMR280C
CBF1	YJR060W
CBR1	YIL043C
CDC19	YAL038W
CDC31	YOR257W
CDC73	YLR418C
CIC1	YHR052W
CIT1	YNR001C
CIT2	YCR005C
CKB2	YOR039W

Identified proteins	Systematic name
LYS21	YDL131W
MDH1	YKL085W
MDH2	YOL126C
MDH3	YDL078C
MLS1	YNL117W
MMF1	YIL051C
MRT4	YKL009W
MSH6	YDR097C
NCB2	YDR397C
NCP1	YHR042W
NDC1	YML031W
NDE1	YMR145C
NGG1	YDR176W
NHP6A	YPR052C
NIC96	YFR002W
NIP7	YPL211W
NOP1	YDL014W
NOP13	YNL175C
NOP58	YOR310C
NPL3	YDR432W
NPL6	YMR091C
NUP57	YGR119C
PAF1	YBR279W
PCK1	YKR097W
PCS60	YBR222C
PDI1	YCL043C
PET9	YBL030C
PEX17	YNL214W
PGK1	YCR012W
PHB1	YGR132C
PHO88	YBR106W
PIL1	YGR086C
PKR1	YMR123W
PMA2	YPL036W
PMT2	YAL023C
PNC1	YGL037C
POB3	YML069W
POM152	YMR129W
POR1	YNL055C
POX1	YGL205W
PRE1	YER012W
PRE3	YJL001W
PRE5	YMR314W
PRE6	YOL038W
PRE7	YBL041W

Identified proteins	Systematic name
RPS25A	YGR027C
RPS5	YJR123W
RPS9B	YBR189W
RRP5	YMR229C
RSC8	YFR037C
RTF1	YGL244W
RTN1	YDR233C
RTT102	YGR275W
RVB1	YDR190C
RVB2	YPL235W
RXT3	YDL076C
SAR1	YPL218W
SCL1	YGL011C
SCS2	YER120W
SDH1	YKL148C
SDS22	YKL193C
SEC4	YFL005W
SEC61	YLR378C
SEC63	YOR254C
SEC72	YLR292C
SET1	YHR119W
SEY1	YOR165W
SHE10	YGL228W
SHM2	YLR058C
SIN3	YOL004W
SIR3	YLR442C
SIS1	YNL007C
SMC3	YJL074C
SMD2	YLR275W
SNF12	YNR023W
SNU13	YEL026W
SPC110	YDR356W
SPT16	YGL207W
SPT20	YOL148C
SRM1	YGL097W
SSA1	YAL005C
SSA2	YLL024C
SSB1	YDL229W
SSC1	YJR045C
STE23	YLR389C
STE24	YJR117W
STH1	YIL126W
STI1	YOR027W
SUB1	YMR039C
SUB2	YDL084W

CMD1	YBR109C
COR1	YBL045C
COX6	YHR051W
CPR1	YDR155C
CPR3	YML078W
CTA1	YDR256C
CTF8	YHR191C
CTR9	YOL145C
DNM1	YLL001W
EFB1	YAL003W
EFT2	YDR385W (+1)
EHT1	YBR177C
EMP24	YGL200C
ENO2	YHR174W
ERG10	YPL028W
ERG2	YMR202W
ERG6	YML008C
ERP1	YAR002C-A
ERV29	YGR284C
FAA2	YER015W
FOX2	YKR009C
FPR2	YDR519W
FPR3	YML074C
FUM1	YPL262W
GCN1	YGL195W
GCN5	YGR252W
GLR1	YPL091W
GND1	YHR183W
GPD1	YDL022W
GPM1	YKL152C
GSF2	YML048W
GSP1	YLR293C (+1)
GSY2	YLR258W
HHF1	YBR009C (+1)
HHO1	YPL127C
HIR2	YOR038C
HSP10	YOR020C
HSP104	YLL026W
HSP12	YFL014W
HSP26	YBR072W
HSP60	YLR259C
HTB1	YDR224C
HTZ1	YOL012C
IDH1	YNL037C
IDP1	YDL066W
IES5	YER092W
ILV5	YLR355C
ISW1	YBR245C
KAR2	YJL034W
LAP3	YNL239W
LPD1	YFL018C
LSC2	YGR244C
LSP1	YPL004C
LYS1	YIR034C

PRE8	YML092C
PRE9	YGR135W
PRP43	YGL120C
PRP45	YAL032C
PUP1	YOR157C
PUP2	YGR253C
QCR2	YPR191W
RAP1	YNL216W
RFC2	YJR068W
RFC3	YNL290W
RHO1	YPR165W
RIM1	YCR028C-A
RNR2	YJL026W
RNR4	YGR180C
RPA135	YPR010C
RPB11	YOL005C
RPB2	YOR151C
RPB4	YJL140W
RPB7	YDR404C
RPB8	YOR224C
RPC19	YNL113W
RPC40	YPR110C
RPL11B	YGR085C (+1)
RPL12B	YDR418W (+1)
RPL13A	YDL082W (+1)
RPL14B	YHL001W
RPL16B	YNL069C
RPL20A	YMR242C (+1)
RPL23A	YBL087C (+1)
RPL25	YOL127W
RPL26A	YLR344W
RPL27B	YDR471W (+1)
RPL30	YGL030W
RPL33B	YOR234C (+1)
RPL35B	YDL136W (+1)
RPL5	YPL131W
RPL6B	YLR448W
RPL7A	YGL076C
RPL8A	YHL033C
RPL9A	YGL147C
RPN1	YHR027C
RPN13	YLR421C
RPP2A	YOL039W
RPP2B	YDR382W
RPS12	YOR369C
RPS13	YDR064W
RPS14A	YCR031C (+1)
RPS15	YOL040C
RPS16B	YDL083C (+1)
RPS17B	YDR447C (+1)
RPS18A	YDR450W (+1)
RPS19B	YNL302C (+1)
RPS20	YHL015W
RPS24A	YER074W (+1)

SWP1	YMR149W
TAF10	YDR167W
TAF11	YML015C
TAF12	YDR145W
TAF5	YBR198C
TAF6	YGL112C
TAF9	YMR236W
TAL1	YLR354C
TDH1	YJL052W
TDH3	YGR192C
TEF2	YBR118W (+1)
TFB2	YPL122C
TFG1	YGR186W
TFP1	YDL185W
THO1	YER063W
TIF6	YPR016C
TIM9	YEL020W-A
TKL1	YPR074C
TOA2	YKL058W
TPM1	YNL079C
TPM2	YIL138C
TRA1	YHR099W
TTR1	YDR513W
TUB1	YML085C
TUB2	YFL037W
UBI4	YLL039C
UGP1	YKL035W
UTP13	YLR222C
UTP4	YDR324C
VID27	YNL212W
VMA10	YHR039C-A
WTM1	YOR230W
YBR159W	YBR159W
YDL121C	YDL121C
YDL245C-R	YDL245C-R
YEF3	YLR249W
YEL020C	YEL020C
YET1	YKL065C
YET3	YDL072C
YGL231C	YGL231C
YGR043C	YGR043C
YKL100C	YKL100C
YLL023C	YLL023C
YOR084W	YOR084W
YOR177C-R	YOR177C-R
YPR098C	YPR098C
YPT1	YFL038C
YPT32	YGL210W
YRA1	YDR381W
YRB1	YDR002W
YTM1	YOR272W
ZEO1	YOL109W
ZTA1	YBR046C

Table 3-2: All identified proteins from the 2nd experiment are listed with their standard and systematic name. Proteins which could be identified again in the 3rd experiment are depicted in bold. The selected proteins of the 2nd experiment conforming to the filter criteria are marked in grey. (known peroxisomal proteins: green, ribosomal proteins: red).

Information concerning the potential localization and the function of the approximately 300 proteins from the positive and negative sort was assembled using SGD annotations and a dataset of peroxisomal proteins described by Gabaldón *et al.* [21]. In the SGD many proteins are described as constituents of more than one compartment. When each annotation of proteins with multiple assignments was fully counted – which yields some distortion – the localization data can be summarized as follows: ~29% cytosolic, ~27% nuclear, ~21% mitochondrial, ~8% stemming from the ER, ~5% peroxisomal and the rest stemming from the vacuole, the plasma membrane, the cell wall, lipid particles or the nucleolus. The classification of the proteins according to their function (given in % of the total number of identified proteins) revealed that ~20% of the proteins play a role in metabolism, in translation and in transcription, respectively. The groups of transport proteins, heat shock proteins, proteins from the proteasome or proteins with a role in reproduction each account for ~5-6% of the proteins from the positive sort. A smaller percentage of proteins is associated with the cytoskeleton, the electron transport chain and the nuclear pore complex. 44 proteins (15%) identified in the positive sorted samples could not be assigned to a functional group. The localization as well as the functional characterisation of the proteins indicated that a considerable part of the identified proteins supposedly represents contamination from other compartments of the cell. For instance, strikingly, many nuclear proteins were present in the sorted fraction suggesting inefficient separation from nuclei during generation of the PNS (post nuclear supernatant). However, proteins cannot be excluded from being potentially novel peroxisomal proteins simply based on the current localization annotation in SGD.

Obviously, processing of the MS data was necessary to determine which proteins were enriched in the positive sorted samples. Several criteria and threshold values were applied to the dataset resulting from the MS analysis.

The parameters number of assigned spectra, number of unique spectra, number of unique peptides, percentage of sequence coverage, percentage of total spectra and protein identification probability provided the basis for the calculation of several enrichment values which are explained in the following. The first criterion is based on the number of

assigned and unique spectra, respectively. The proportion from the unique spectra of the assigned spectra gives information about the amount of the protein since in the situation of a high protein concentration a certain unique spectrum can be encountered several times. This increases the number of assigned spectra, but the number of unique spectra stays the same or shows only a small increase resulting in a small proportion. To demonstrate how this proportion changes in the positive sort compared to the negative sort, the quotient between the associated proportions is calculated. Proteins with a quotient smaller than 0,8 were judged positive under this criterion. The next three criteria were the relative change in the number of unique peptides, the percentage of sequence coverage and the percentage of total spectra, respectively, in the positive sort compared to the negative sort. All proteins which had a quotient bigger than 1,5 were judged as positive according to these three criteria.

The list of proteins in the positive sort was shortened consecutively applying the filters listed in table 3-3. The selected proteins of the positive sort had to have at least 99,9% protein identification probability, more than 3% sequence coverage and at least 2 unique peptides in the positive sort. In addition, one of the above described criteria had to be fulfilled and the values of all the criteria had to direct towards enrichment. Those proteins, which could only be detected in the positive sort, escaping the above mentioned criteria, had to be represented by at least one unique peptide per 20 kDa except for those with transmembrane domains. However, proteins which were represented by more than 15 assigned spectra could not be neglected and were kept in the list despite of the filters.

Applying the consecutive filter steps, the number of proteins found in the positive sort could be reduced from 296 to 140. The step wise alteration of peroxisomal proteins in comparison to representative contaminating proteins (given in percentage of the total protein number) was expected to demonstrate the enrichment of peroxisomal proteins under the imposed constraints. Ribosomal proteins were chosen as prime example for contaminating proteins from other subcellular compartments as to date no connection between peroxisomes and ribosomes has been shown. Interestingly, the percentage of known peroxisomal proteins increased steadily whereas the percentage of ribosomal proteins did not show a clear trend indicating that contaminations can be decreased. Consequently, the selected proteins represent a pool of new candidates for peroxisomal proteins, but true peroxisomal localization has to be demonstrated by fluorescence

microscopy for instance. The selected proteins, conforming to the filter criteria, are marked in table 3-2.

filter steps	filter properties	peroxisomal proteins (% of total)	ribosomal proteins (% of total)	total number of proteins
filter 0	- no filter applied	6,4	11,2	296
filter 1	- more than 99,9% protein identification probability in the pos. sort	7,2	9,5	263
filter 2	- percentage of sequence coverage ≥ 3% in the pos. sort - unique peptides ≥ 2 in the pos. sort - at least one criterion (see text) fulfilled	10,2	9,1	176
filter 3	- proteins which are only present in the pos. sort must have at least 1 unique peptide / 20 kDa	11,1	10,5	153
filter 4	- all criteria (see text) have to direct towards enrichment	12,1	10,7	140

Table 3-3: Filters used to shorten the MS data set for the positive and negative sort in order to screen for enrichment of candidate proteins for peroxisomal localization. The associated alteration of the total number of proteins and the percentages of peroxisomal and ribosomal proteins in relation to the total protein number are listed.

3.3.3.3 3rd MS experiment

The third MS experiment represented a repeat of the 2nd experiment. In the positive and negative sort 182 proteins were identified, whereas 135 proteins (i.e. 74%) were consistent with the results from the 2nd experiment (see table 3-2). A remarkable large number of proteins (134) was only detectable in the positive sort whereas 4 proteins were exclusively present in the negative sort. The difference compared to the 2nd experiment was also

reflected in the silverstains of the two experiments presented in section 3.3.2.1. Known peroxisomal proteins accounted for 4,4% of all identified proteins but this percentage could not be increased significantly applying the above described filter steps. The number of proteins was step wise reduced to 147, whereas 57 proteins (i.e. 39%) were consistent with the selected proteins from the 2nd MS experiment.

4 DISCUSSION

For the identification of all proteins being part of a specific subcellular fraction, in other words for the establishment of a subcellular proteome, the purity of the material to be analyzed is of utmost importance [67]. Therefore, the challenge for this thesis was to develop machine-based purification or enrichment procedures to increase the purity of the fraction in addition to the established density gradient procedure for peroxisome isolation [65] or to the method for ER enrichment [68]. As fluorescence-based flow cytometry was the method of choice for this further purification, peroxisomes or ER microsomes had to be fluorescently labelled.

There are different possibilities to label organelles or particles for fluorescence activated sorting in a FACS machine. Either the purified organelles are labelled with fluorescent antibodies employing the widely-used method of immune affinity labelling or, alternatively, highly fluorescent proteins are localized specifically to the subcellular entity during growth (*in vivo* labelling) giving rise in our case to fluorescent peroxisomes or particles representing peroxisomal precursors. In previous studies from our laboratory [65] application of antibodies recognizing tagged peroxisomal membrane proteins (PMPs) was shown not to be the best choice for further specific enrichment of density gradient purified peroxisomes. Therefore, we decided to express fluorescent proteins and label subcellular structures *in vivo* rendering the fluorescence an inherent property of the membraneous compartment. As a first step, yeast cells producing green fluorescent peroxisomal proteins should be generated. For *in vivo* staining of mature peroxisomes, the expression of GFP extended by a peroxisomal targeting signal (GFP-SKL) was used. Despite previous difficulties with immune affinity purification a fluorescently labelled antibody was applied, too, in combination with peroxisomes purified from cells expressing various HA-epitope tagged peroxisomal membrane proteins (PMPs). A commercial α-HA-Alexafluor488 antibody was used to interact with HA tagged PMPs. Among the different PMPs tagged (Pxa1p-CTHA, Pxa2p-CTHA, Pex3(1-46)p-CTHA, Pex3p-CTHA, Pex11p-HA, Pex11p-CTHA, Pex13p-CTHA, Pex14p-CTHA, Pex22p-CTHA, Pex28p-CTHA, Pex29p-CTHA, Pex30p-CTHA, Pex31p-CTHA or Pex32p-CTHA) only peroxisomes containing Pex11p-HA or Pex11p-CTHA were sufficiently labelled with the fluorescent antibodies. Attempts to improve the accessibility of the antibody to other HA tagged PMPs by limited

proteolysis or by application of detergents prior to antibody incubation remained unsuccessful. Both strategies, *in vivo* and *a posteriori*, led to bright fluorescent peroxisomes which could be sorted by FAOS.

In contrast, peroxisomal precursors are not yet import competent and labelling with peroxisomal matrix proteins would not represent a successful strategy for the isolation of precursor structures. Membrane proteins supposed to be part of peroxisomal precursors and thought to be also present in regions of the ER which represent the starting points of peroxisome formation were fused to fluorescent proteins. As GFP tagged versions of the relevant PMPs showed only very faint fluorescence, EGFP constructs were generated and the fluorescence intensity could further be amplified by increasing the expression levels through the introduction of a *GAL* promoter and applying the corresponding growth conditions. Our studies focused on labelling Pex3p found to be present at very early stages of peroxisome formation until the mature stage. Utilizing the *GAL* promoter as instrument to control this pathway through growth conditions, the kinetics of the associated events can be investigated. According to Hoepfner *et al.* [19], Pex3p first localizes to subregions of the ER and loses its association with the ER in a Pex19p-dependant manner afterwards. Newly formed structures containing fluorescently labelled Pex3p develop the capacity to import peroxisomal matrix proteins 120 minutes after turning on the expression of Pex3p presumably converting them into mature peroxisomes. Our experimental setup revealed similar results. However, as these peroxisomal precursors are only present in a short time window a time consuming isolation procedure cannot be applied. Therefore, in addition to a strain expressing Pex3p-EGFP under the control of a *GAL* promoter, we established strains with a *GAL* promoter controlled expression of fluorescently labelled proteins which accumulate in the described ER regions consequently inhibiting peroxisome formation. Hence, the constructs *PEX3(1-46)-EGFP* (*GAL L* or *GAL S* promoter controlled) in wt background and *PEX3-EGFP* (*GAL L* or *GAL S* promoter controlled) in a *pex19Δ* background were generated. Brighter fluorescence was seen in cells expressing the truncated Pex3p protein fusion from the shorter promoter. These structures have not been used for fluorescence based sorting (FAVS) but the basis is set for future studies. The first step will be the establishment of an isolation procedure for ER-derived microsomes followed by adaptation of the sorting process to these fluorescently labelled microsomes. A mass spectrometric identification of the proteins in the sorted fraction of the microsomes could reveal the proteins participating in the onset of peroxisome formation.

To elucidate the proteome of mature peroxisomes from ethanol grown *S.c.*yeast cells, a crucial point is the generation of a highly purified peroxisomal fraction whose protein content can be analysed afterwards by MS. Due to previous studies in our laboratory, an isolation procedure has already been established. However, two aspects required adaptation or changes of the procedure. On the one hand, the previous studies were established for the isolation of peroxisomes from oleic acid grown *S.c.* cells which have properties different from the ones isolated from ethanol grown *S.c.* cells. As the density of the peroxisomes varies depending on the growth conditions, the density gradient composition had to be adjusted. The density of the separation layer and the top layer of the Nycodenz gradient had to be decreased to ensure a good separation of peroxisomes from mitochondria (from 35% and 25% to 32% and 20%, respectively). In addition, the duration of the centrifugation was extended from 60 to 150 minutes. On the other hand, FAOS should be established as a new method for further purification of the peroxisomal fraction. To avoid turbulences during the sorting procedure in the FACS instrument, no samples with high density should be used and therefore Nycodenz had to be removed from the peroxisomal fraction. This was accomplished by an additional centrifugation step after diluting the peroxisomal fraction yielding the peroxisomal pellet PxP. The PxP resuspension in the buffer used for spheroplasts homogenization (PSB) was employed for the sorting process. Clearly, centrifugation may result in tiny little aggregates that cannot be resolved completely by resuspension.

Examination of the density gradient based purification procedure using Western blot analysis of all gradient fractions confirmed that there was no detectable mitochondrial contamination in the peroxisomal fraction whereas catalase A, a prominent peroxisomal matrix enzyme, was most enriched in the peroxisomal fraction. The ER marker enzyme Kar2p was detected in almost every fraction possibly because of formation of vesicles with varying densities. Interestingly, the distribution of Pex30p – according to the database SGD a PMP – did not match the distribution of catalase A pointing at the presence of different families of peroxisomes. Actually, there are “observations of heterogeneous populations of peroxisomes that differ in size, buoyant density, protein composition, and import capacity” [68]. Therefore, the established isolation procedure results in the enrichment of a subset of peroxisomes only – among them the import competent mature peroxisomes. Other subgroups might be missed because a further reduction of the density of the separation layer would lead to mitochondrial contamination.

The important innovation in the novel isolation procedure should be a further enrichment employing the method of FAOS (Fluorescence Activated Organelle Sorting). There have already been made successful attempts to sort vesicles by flow cytrometry – termed FAVS (Fluorescence Activated Vesicle Sorting) – concluding that "FAVS may be a useful tool for isolation of cellular organelles for comprehensive LC/LC-MS/MS analysis" [64]. As mentioned earlier, only peroxisomes from cells expressing GFP-SKL or peroxisomes labelled with α-HA-Alexafluor488 via Pex11p-HA exhibited sufficiently intense fluorescence to be monitored by the flow cytometer. A GFP or EGFP tag on membrane proteins (PMPs) did not lead to FAOS detectable structures. Organelles from wild type cells expressing the fluorescent proteins GFP or mCherry extended by a peroxisomal targeting signal PTS1 (ELSKL) were used for the sorting procedure to provide highly enriched peroxisome fractions to the mass spectrometry based proteomic analysis. Peroxisomes from CB80 cells expressing mCherry-SKL were used as negative control since the laser of the flow cytometer does not recognize red fluorescence but growth conditions and purification procedures were identical. Employing the peroxisome fraction from this strain gates were set in different dot plot representations to define the "negative" events not to be positively sorted using the strain expressing GFP-SKL. Events of higher green fluorescence intensity were regarded as "positive" when peroxisomes containing GFP-SKL were subjected to the sorting process. The proteins from the sorted events (negative and positive) were identified by mass spectrometry after separation by SDS-PAGE followed by silverstaining. The staining already revealed a dramatic decrease in the amount of protein in both, the positive and negative sorted fraction compared to the peroxisomal pellet. Western blot analysis using α-Pex30p showed that a protein regarded as peroxisomal according to the SGD is only detectable in the "positive" sort but not in the "non-sort" fraction (including all events which are not present in the "positive" sort) suggesting that the sorting procedure leads to further enrichment of peroxisomes. The loss of protein amount just mentioned points to methodical problems during the sorting procedure or in the further processing of the sorted fractions. Starting with 200µL PxP resuspension (protein concentration 0,1-1mg/mL), the sorting process yielded ~5-20mL positive and negative sorted fractions each. The extreme dilution of the samples could lead to adhesion of hydrophobic proteins to plastic tube walls preventing quantitative precipitation by TCA. The fact, that the sheath fluid "FACS Flow", similar to PBS buffer, does not osmotically stabilize organelles even deteriorates this situation. Although peroxisomes may persevere an osmotic shock for the duration of the sorting process which

is only a few milliseconds from mixing to droplet formation, peroxisomes are certainly disintegrated in the collected samples. The addition of osmotically stabilizing agents to the sheath fluid may help to receive intact peroxisomes after the sort and may therefore reduce adhesion problems. Another possibility for the loss of protein amount could be an incomplete TCA precipitation. This could be overcome by adding a highly pure but "inert" protein which can be mostly separated by SDS-PAGE afterwards.

General criticism on the method of FACS being adapted to subcellular structures can be raised. In the FACS machine, the size of the drops being sorted accommodates whole cells and the settings allow one cell per drop. Peroxisomes, usually 200-500nm in diameter, are much smaller than mammalian cells (20-50µm) and a dilution resulting in one organelle per drop seems not realistic. The dot plot representation forward scatter width versus forward scatter area can be used to estimate if single events can be registered and consequently separated. If single events are detected individually, they will have approximately the same width of the forward scatter signal as they pass through the laser beam with the same velocity. However, if the distance between successive events becomes too short or if particle aggregates pass through the laser beam, the signals will melt and the corresponding width will increase. So, in the ideal situation of a single-event-separation, diverse events (differing for instance in forward scatter area) should have approximately the same forward scatter width consequently being represented by a straight horizontal line in the diagram FSC-W/FSC-A. In our case, however, this ideal situation was not achieved and the gated events were still spread over a wide range of forward scatter widths (see figure 4-1) indicating that sorting of one organelle at a time is not possible.

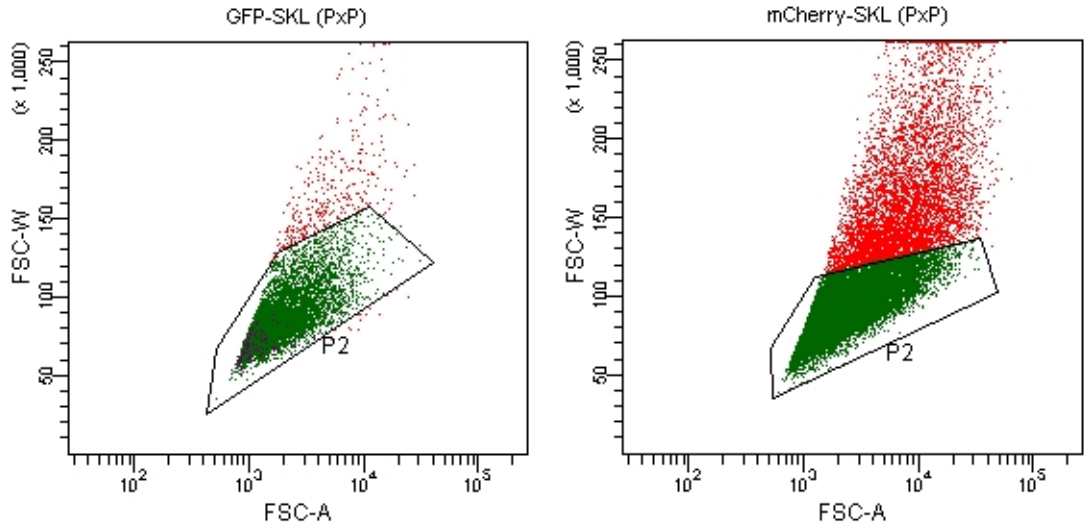

Figure 4-1: Diagrams showing the forward scatter width versus the forward scatter area. The monitored events are spread over a wide range of forward scatter widths indicating that single-event-separation is not possible.

Probably, in this case the sorting process should be seen as an enrichment procedure in which drops with several events are sorted. Of course, contaminations in the drop cannot be avoided but in future experiments the gates in the FSC-W/FSC-A diagram should be set more stringent. For even smaller particles such as vesicles thought to not require osmotic stabilization in addition repetitive rounds of fluorescence activated sorting could be used to stepwise decrease these contaminations.

Previous studies aiming at the elucidation of the yeast peroxisomal proteome employed oleate grown yeast cells, and one of the goals of my work was to identifiy differences when cells were grown on other carbon sources. Although MS is an excellent method for protein identification in a complex sample, quantification and designation of contaminating proteins from other organelles is a big challenge. Marelli *et al.* saw the reasons for that in "the polydispersity within organelle classes resulting from biological diversity and the limited resolving power of subfractionation techniques" [66]. To deal with this problem one can refer to de Duve's (1992) definition that the components of a subcellular fraction are not necessarily the ones present in the fraction but in fact the proteins which specifically enrich there [66].
Therefore, in our analyses we compared the protein content in the PxP, the "positive" and the "negative" sort. The comparison of the protein content of the latter two is best suited to identify a distinct enrichment. Clearly, such an experiment has to be performed independently more than once. To elaborate the enrichment in the "positive" sort compared to the "negative" sort certain criteria for enrichment and threshold values needed to be defined on the basis of the MS data set. As an example for enrichment of one group of proteins versus various contaminating proteins the percentage of known peroxisomal proteins (which were thought to be enriched in the positive sort) and ribosomal proteins (chosen as prime example for contaminating proteins) was examined applying consecutively the various criteria set. As the percentage of known peroxisomal proteins increased with every criterion applied in contrast to the percentage of ribosomal proteins, the "enrichment criteria" seem to be characteristic for peroxisomal proteins. Hence, the established criteria should be a good tool to search for proteins which specifically enrich with known peroxisomal proteins representing candidates for a novel peroxisomal

localization. Under these constraints, the list of ~300 proteins in the "positive" sort was reduced to 140 proteins which fulfil all criteria set to be regarded as truly peroxisomal proteins in yeast cells grown on ethanol as sole carbon source.

According to the criteria, two peroxisomal matrix proteins (malate synthase 1; Mls1p and fatty acyl CoA synthetase 2; Faa2p) had to be deleted from the list. In the case of Faa2p, the protein was detectable in the positive and not in the negative sort but it was not represented by at least one unique peptide/20kDa. As Faa2p participates in the conversion of free fatty acids into CoA-derivatives, substrates for the ß-oxidation of fatty acids, a low amount of this protein in peroxisomes of ethanol grown cells could be expected. However, ß-oxidation enzymes are detectable in larger, not negligible amounts. It may well be that under-representation of this protein is due to its amino acid composition leading to an insufficient identification by MS. Concerning Mls1p, every criterion pointed towards enrichment only the threshold values were not reached. Mls1p is an enzyme essential for growth on ethanol being part of the glyoxylate cycle – it catalyzes the condensation of glyoxylate with acetyl-CoA into malate. The low amount may be due to the cytosolic localization of Mls1p. Although during growth on oleic acid part of the glyoxylate cycle and the production of acetyl-CoA occurs in the peroxisome, "when yeast cells utilise ethanol as sole carbon source, acetyl-CoA is provided in the cytosol and under these conditions malate synthase is predominantly found in the cytosol despite a functional PTS1." [69]. The detected Mls1p may therefore represent residual amounts due to partial import or may result from the cytosolic pool either due to insufficient separation or external association with peroxisomes.

In conclusion, the results from the MS analysis indicated that peroxisomal proteins could be enriched in the "positive" sort compared to the "negative" sort and the peroxisomal pellet. However, the overall percentage of known peroxisomal proteins was relatively low suggesting that a major part of the proteins identified here are either novel components of the peroxisome because of dual localization or represent contaminations from other subcellular compartments. In any case, the localization of proteins detected for the first time in peroxisomes need to be verified by different methods, too. In addition, our experiments aimed at the elucidation of the peroxisomal proteome comprising matrix and membrane proteins but only two known membrane proteins (Emp24p and Pex17p) were detected. As mentioned before, this shortcoming might originate from the high dilution of the sorted samples and the potential association particularly of hydrophobic proteins to plastic tube walls. In summary, this work does not represent a conclusive proteomic study

about peroxisomes, but provides an excellent starting point for further investigations on proteins possibly associated with peroxisomes. In future experiments more complex sorting procedures resulting in even further enrichment of peroxisomal proteins by "iterative" sorts may be carried out. Generation of *S.c.* strains in which proteins involved in the very early steps of peroxisome biogenesis at the ER are labelled with fluorescence of sufficient intensity may provide further insight in the proteins required for the formation of pre-peroxisomal vesicles using sorting procedures like the ones described in this work. This may pave the way for a better understanding of the individual steps in peroxisome biogenesis.

5 MATERIALS AND METHODS

5.1 STRAINS, PLASMIDS, OLIGONUCLEOTIDES AND ANTIBODIES

5.1.1 *Saccharomyces cerevisiae* strains

All strains except for the strains containing an *EGFP* or a *GAL* promoter construct (established during the diploma thesis) were taken from the strain collection of Andreas Hartig's and Cécile Brocard's laboratory (collection VW and collection CB).

	name	**features**
wild type:	CB80	his3-20, leu2–1, , trp-1-63, ura3-52
HA tags:	CB182	CB80 ***PEX28-6HA***::KanMX4
	CB183	CB80 ***PXA1-6HA***::HIS
	CB184	CB80 ***PXA2-6HA***::HIS
	CB502	CB80 ***PEX11-3HA***::KanMX4
CTHA tags:	CB175	CB80 ***PEX29-CTHA***::KanMX4 colony #7
	CB177	CB80 ***PEX14-CTHA***::KanMX4#4
	CB218	CB80 ***PEX30-CTHA***::KanMX4
	CB220	CB80 ***PEX11-CTHA***::KanMX4
	CB221	CB80 ***PEX13-CTHA***::KanMX4
	CB222	CB80 ***PEX22-CTHA***::KanMX4
	CB228	CB80 ***PEX31-CTHA***::KanMX4#4
	CB229	CB80 ***PEX32-CTHA***::KanMX4#4
	CB230	CB80 ***PEX3-CTHA***::KanMX4#4
	VW147	CB80 ***PEX3(1-46) -CTHA***::KanMX4
GFP tags:	CB204	BY4741 ***PEX25-GFP***::HISMX6
	CB208	BY4741 ***PEX29-GFP***::HISMX6
	CB447	BY4741 ***PEX3-GFP***::HISMX6

	CB453	BY4741 ***PEX14-GFP***::HISMX6
	CB455	BY4741 ***PEX17-GFP***::HISMX6
EGFP tags:	CB442	CB80 ***PEX3(1-46)-EGFP***::KanMX4
	CB443	CB80 ***PEX3-EGFP***::KanMX4
	CB444	CB80 ***PEX29-EGFP***::KanMX4
GAL promoter:	CB482	CB80 ***PEX3(1-46)-EGFP***::KanMX4 (***GAL L***::CloNAT)
	CB483	CB80 ***PEX3(1-46)-EGFP***::KanMX4 (***GAL S***::CloNAT)
	CB484	CB80 ***PEX3-EGFP***::KanMX4 (***GAL L***::CloNAT)
	CB485	CB80 ***PEX3-EGFP***::KanMX4 (***GAL S***::CloNAT)
	CB486	CB80 ***PEX3-EGFP***::KanMX4, ***pex19Δ***::hphNT1 (***GAL L***::CloNAT)
	CB487	CB80 ***PEX3-EGFP***::KanMX4, ***pex19Δ***::hphNT1 (***GAL S***::CloNAT)

5.1.2 Plasmids

All plasmids were taken from the plasmid collection of Andreas Hartig's and Cécile Brocard's laboratories.

5.1.2.1 Plasmids for 1-step-trafo

name	**encoded protein**	**promoter**	**mutation complemented**
pCB367	mCherry-SKL	MLS1	*ura3*
pCB441 = pJR233	GFP 2-SKL	MLS1	*ura3*

5.1.2.2 Plasmids for generating linear constructs for homologous recombination

name	**encoded tag/deletion cassette**	**resistance**
pCB447	*PEX19* deletion cassette	*hphNT1*
pCB463	C terminal *EGFP* tag	*KanMx4*
pCB510	*GAL L* promoter	*natNT2*
pCB514	*GAL S* promoter	*natNT2*

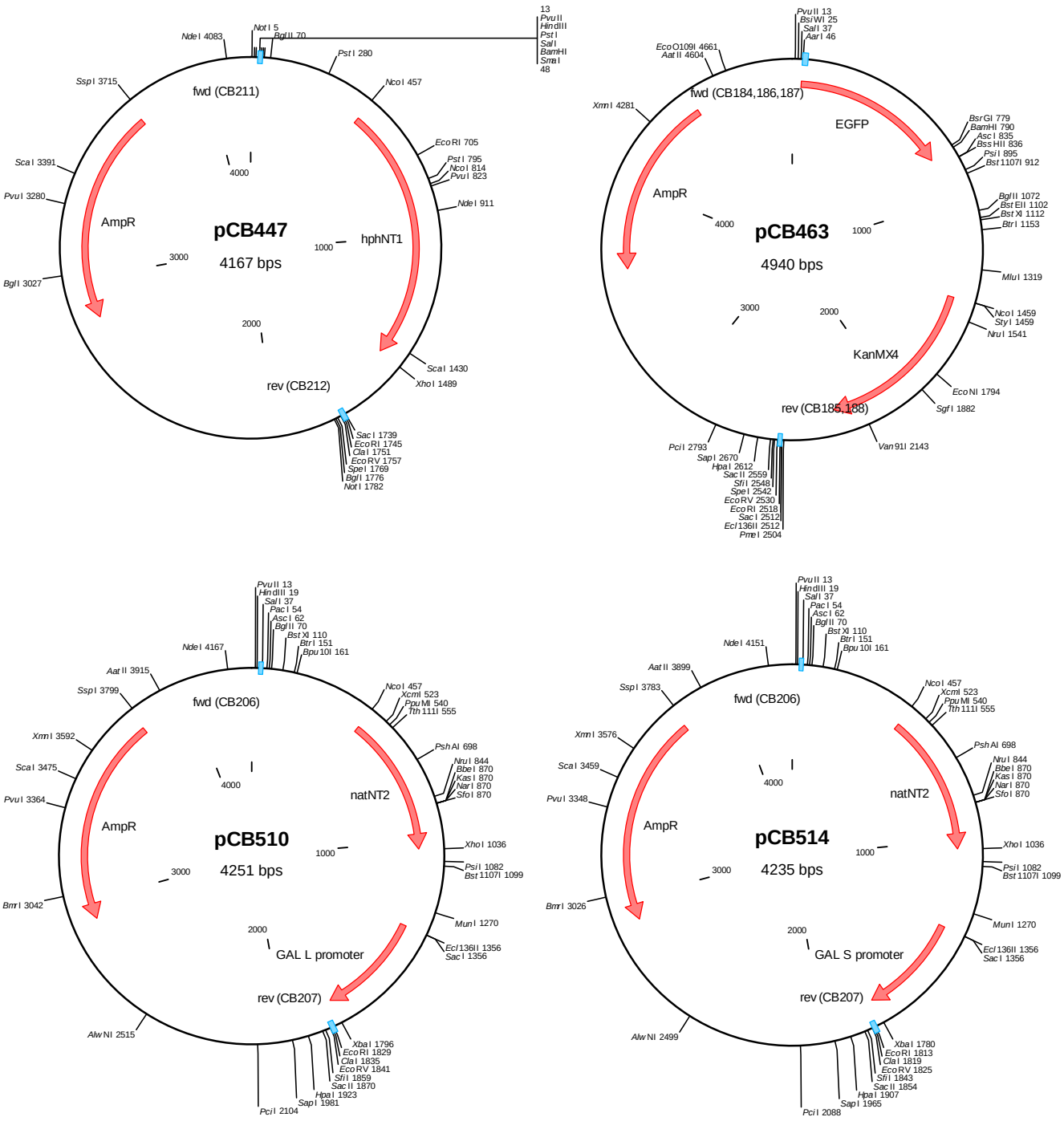

Figure 5-1: Plasmid maps for the plasmids used as templates for the construction of the linear DNA fragment for homologous recombination. The resistance genes and the insertion or deletion cassettes are indicated as arrows. The regions representing the binding sites for the forward and reverse primers during the generation of the linear construct for homologous recombination are marked as blue boxes.

5.1.3 Oligonucleotides

5.1.3.1 Primers for generating linear constructs for homologous recombination

name	sequence	gene	application	details
CB184	CGGTGGTAGTGTTTTTCGTGAAGAGATGG TTGTATAAACAG**GGAGCAGGTGCTGGTG CTGGTGCT**	*PEX3*	C terminal *EGFP* tagging of *PEX3(1-46)*	fwd
CB185	ACGCTATATATATATATATTCTGGTGTGA GTGTCAGTACTTATTCAG**ATCGATGAATT CGAGCTCG**	*PEX3*	C terminal *EGFP* tagging	rev
CB186	CGTATACAGCAACTTTGGCGTCTCCAGCT CGTTTTCCTTCAAGCCT**GGAGCAGGTGCT GGTGCTGGTGCT**	*PEX3*	C terminal *EGFP* tagging	fwd
CB187	CGTCAATCGAAGAGCTAACAGACACTCTC AATTCAACTATA**GGAGCAGGTGCTGGTG CTGGTGCT**	*PEX29*	C terminal *EGFP* tagging	fwd
CB188	GTTGACTGTATCATCAGTGAACATATAGT ATAACAAATC**ATCGATGAATTCGAGCTC G**	*PEX29*	C terminal *EGFP* tagging	rev
CB206	TACTAGTCATCGTAAAAGCAGAAGCACGA AACAAGGAGGCAAACCACTAAAAGGATG **CGTACGCTGCAGGTCG**	*PEX3*	N terminal insertion of *GAL* promoter	fwd
CB207	ATGAGTACCTTTCCTCGATGTCTCTGCAG AAGCGAACGTGATCTTTGATTTGGGGC**CA TCGATGAATTCTCTGTCG**	*PEX3*	N terminal insertion of *GAL* promoter	rev
CB211	CCGAAGTATTGACGGAAAGAAGAAATGC CAAACATACAACACGAAGTA**CGTACGCT GCAGGTCGAC**	*PEX19*	insertion of deletion cassette	fwd
CB212	CTGTTATCATAAATATATATACCTTATTGT TGTTTGCAACCGTCGG**ATCGATGAATTC GAGCTCG**	*PEX19*	insertion of deletion cassette	rev

5.1.3.2 Primers for control PCR

name	sequence	gene	Application	details
CB163	CATCATCTGCCCAGATGCGAAG	*KanMx4*	control for insertion	fwd
CB164	GTCAAGACTGTCAAGGAGGG	*KanMx4*	control for insertion	rev
CB165	CCACTCTTGACGACACGGC	*natNT2*	control for insertion	fwd
CB225	GAATTACAAATTGTGGGAACCG	*PEX19*	control for pex19	fwd
CB230	CAGTAACCTGGCCCCACAAAC	*GAL L/S* promoter	control for insertion	fwd
CB257	GCCGCTAGCTTGTTGTTTGCAACCGTCGG	*PEX19*	control for pex19	rev
H795	GCTCGATGATCTGAGCGCCAG	*PEX3*	control for C-terminal tagging	fwd
H796	CAGGGAAGTTAGAGTCTCTGTG	*PEX3*	control for C-terminal tagging	rev
H803	GAGGGAAGAAACATATAGGCAAG	*PEX29*	control for C-terminal tagging	fwd
H804	ATCTGAGTTCGTTGTTCCAAC	*PEX29*	control for C-terminal tagging	rev
H962	GGTGGCCTGACATAATCTTGGTCAGG	*PEX3*	control for N-terminal insertion	fwd
H967b	CAGAGCTCTTACCTAGGCTGTTTATACAA CCATCTCTTCACGAAAAACACTACCACCG	*PEX3*	control for N-terminal insertion	rev

5.1.4 Antibodies

5.1.4.1 Primary antibodies

1° antibody	recognized protein	features	dilution in TBST (Western Blot)	source
α-Cta1p	Catalase A (px)	goat, polyclonal	1 : 20 000	A. Hartig, MFPL

α-HA	HA tag	mouse, polyclonal	1 : 2000	G. Schaffner, IMP
α-Por1p	Porin (mito)	mouse, polyclonal	1 : 15 000	commercial, Molecular Probes
α-Cox4p	Cytochrome c oxidase subunit IV	rabbit, polyclonal	1 : 10 000, 1 : 2000	kind gift from G. Schatz, Basel
α-Kar2p	ER membrane protein	rabbit, polyclonal	1 : 20 000	kind gift from B.Distel, Amsterdam
α-Mls1p	Malate Synthase	rabbit, polyclonal	1 : 20 000	MFPL, [70]
α-Pex30p	Peroxin 30	rabbit, polyclonal	1 : 20 000	C. Brocard, MFPL
α-Fox3p	Thiolase	rabbit, polyclonal	1 : 10 000	kind gift from W. Kunau, Bochum
α-GFP	EGFP tagged proteins	rabbit, polyclonal	1 : 5000	kind gift from M. Rout [71], New York

1° antibody	**recognized protein**	**features**	**dilution in BSA-PBS (IF test)**	**source**
α-HA-Alexafluor488	HA tag	mouse, monoclonal	1 : 10	Cell Signalling Technology

5.1.4.2 Secondary antibodies

2° antibody	**features**	**dilution in TBST**	**manufacturer and order number**
α-goat-IgG-HRP	rabbit, monoclonal	1 : 10 000	ZYMED, 81-1620
α-mouse-IgG-HRP	sheep, monoclonal	1 : 10 000	GE Healthcare, NA931V
α-rabbit-IgG-HRP	donkey, monoclonal	1 : 10 000	GE Healthcare, NA934V

5.2 MICROBIOLOGICAL METHODS

5.2.1 Isolation of DNA

5.2.1.1 Isolation of chromosomal DNA from S.c.:

chromosomal DNA buffer:	1xTE:
50mM Tris/HCl pH 7,5 20mM EDTA 1% SDS	10mM Tris/HCl pH 8,0 1mM EDTA

S.c. cells grown in 100mL selective media over night at 30°C were pelleted for 5' at 1500 x g. The supernatant was discarded and the pellet resuspended in 0,5mL dH_2O. The resuspension was transferred to a microcentrifuge tube with a screw cap and pelleted again for 10'' at full speed. The supernatant was discarded and the pellet was resuspended in 0,5mL chromosomal DNA buffer. After adding 0,5mL glass beads and brief vortexing, the cells were broken in the FastPrep120 from Thermo Savant (3 times à 20'', level 6). Between the three FastPrep steps, the sample was cooled on ice for 1'-2' to avoid heating. Using a heated needle, a hole was made in the bottom of the microcentrifuge tube and the suspension was transferred to a 1,5mL microcentrifuge tube by short centrifugation. After incubation at 70°C for 10' without shaking, 200µL 5M KOAc (without pH adjustment) and 150µL 5M NaCl were added and mixed by vortexing. The sample was incubated on ice for 20' and spun in an Eppendorf-centrifuge afterwards for 15' at full speed (4°C). 750µL of the supernatant were transferred to a new 1,5mL microcentrifuge tube, 250µL of 30% PEG_{6000} were added and mixed by gently inverting. After incubation on ice for 20' another 15' centrifugation step at full speed (4°C) yielded the chromosomal DNA pellet. The supernatant was discarded and the pellet was washed with ice-cold 70% EtOH (the pellet was often not completely resuspended). After centrifugation for 2' at full speed (4°C) the ethanol could be discarded. The pellet was dried in the open microcentrifuge tube either at room temperature or in the SpeedVac. To resuspend the dried chromosomal DNA pellet, 100µL 1xTE buffer were added and the microcentrifuge tube was shaken at room temperature until the whole pellet was resuspended. The amount of isolated chromosomal DNA was determined by the Qubit Fluorometer.

5.2.1.2 Isolation of chromosomal DNA from S.c. (for colony PCR)

Cells from a plate were resuspended in 50µL 20mM NaOH by vortexing. After incubation at 95°C for 15', the sample was chilled on ice for 3'. The suspension was spun in an Eppendorf-centrifuge for 10' at full speed (4°C). 40µL of the supernatant were transferred to a new microcentrifuge tube and neutralized by the addition of 2µL of 1M Tris/HCl pH 7,4.

5.2.1.3 Isolation of plasmid DNA from E.coli (MiniPrep)

MiniPrep:

10x TE:	10x stop solution:
100mM Tris/HC pH 8,0 10mM EDTA pH 8,0	4M Urea 50% Saccharose 50mM EDTA pH 8 0,1% Bromphenolblau

The MiniPrep was carried out as described in the protocol of the kit "Wizard Plus SV Miniprep; DNA purification system" (Promega). The isolated plasmid was eventually dissolved in 100µL nuclease free H_2O. Afterwards 10µL of 10xTE buffer was added in order to store the plasmid at 4°C.

Digestion with restriction enzymes:

To test if the isolated plasmid was the correct one and to estimate the amount of isolated plasmid a digestion with restriction enzymes was performed. Usually, a restriction enzyme is chosen which cuts two times and therefore produces two DNA fragments of different length. To 2µL of the isolated plasmid 6,5µL of dH_2O, 1µL of the corresponding restriction enzyme buffer and 0,5µL of the restriction enzyme were added so that the sample volume was 10µL. The mixture was incubated at 37°C for 2-3h to ensure complete digestion of the plasmid. Afterwards the sample was mixed with 10x stop solution which also serves as loading buffer and loaded into the slots of a 1% agarose gel. Additionally 3µL of a marker (1kb DNA ladder or 100bp DNA ladder plus from Fermentas depending on the expected fragment length) was loaded onto the gel. The gel was prepared as described in "Seperating PCR fragments on agarose gels" (section 5.2.3.4.). The length of

the DNA fragments was determined and by comparison of the intensity of the bands with the intensity of the marker bands the amount of the isolated plasmid was estimated.

5.2.2 Transformation of yeast cells

5.2.2.1 One-step-trafo

one-step-mix:	1xTE:
40% PEG_{4000} 200mM LiOAc 100mM DTT	10mM Tris/HCl pH 8,0 1mM EDTA

150µL of the one-step-mix were mixed with 2µL of plasmid DNA and 2µL of hering sperm (HS)-DNA (10mg/mL) which has previously been denatured at 95°C. Yeast cells from a plate were resuspended in this mixture by vortexing. After incubation at 45°C for 45' without shaking, the suspension was spun in an Eppendorf-centrifuge for 4' at 1500 x g. The cell pellet was resuspended in 100µL 1xTE buffer, plated on selective medium and the plate was incubated at 30°C.

5.2.2.2 Transformation using homologous recombination

The protocol for the transformations was adapted according to [72, 73].

Preparation of chemically competent *S.c.*:

TE/LiOAc:
10mM Tris/HCl pH 8 1mM EDTA/NaOH pH 8 100mM LiOAc pH 7,5

An o/n culture of *S.c.* grown on YPD (1,5mL/transformation) was diluted into 25mL to an OD_{600} = 0,2. The culture was incubated at 30°C until an OD_{600} of 0,4-0,6. Afterwards, the cells were pelleted by centrifugation for 5' at 1000 x g and washed once in dH_2O. The cell pellet was resuspended in 100µL freshly prepared, cold TE/LiOAc per transformation. The chemically competent *S.c.* can either be used immediately or can be stored at 4°C for a few days prior to transformation.

Transformation with linear pieces of DNA (integration by homologous recombination):

PEG/LiOAc:	1xTE:
40% PEG_{4000} 10mM Tris/HCl pH 8 1mM EDTA/NaOH pH 8 100mM LiOAc pH 7,5	10mM Tris pH 8,0 1mM EDTA

HS-DNA (10mg/mL) was denatured at 95°C for 1' and put on ice afterwards. 0,5-1µg PCR-DNA was mixed with 0,1mg HS-DNA and 100µL of chemically competent *S.c.* by vortexing. For the negative control no PCR-DNA was added. After addition of 600µL PEG/LiOAc, the mixture was vortexed and put at 30°C for 30' with vigorous shaking. Then, 70µL 100% DMSO were added and mixed by gently inverting the tube. After a heat shock at 42°C for 15' without shaking, the cells were put on ice for 1-2'. Centrifugation for 1' at 4500 x g yielded a cell pellet which was carefully resuspended in 1mL YPD, transferred to a glass tube and incubated at 30°C with shaking for 3h. Afterwards, the cells were pelleted (1' at 4500 x g), resuspended in 100µL 1xTE, plated on selective medium and the plate was incubated at 30°C.

5.2.2.3 Selection of transformants:

In one-step-trafos only auxotrophy markers were used to select for cells containing the plasmid. Both commonly used plasmids (pCB367 and pJR233) contain an *ura3* marker, so the selective medium was a synthetic complete medium with 2% glucose lacking uracil. For integrative transformations only resistance markers were used to select for the cells in whose genome the DNA fragment was integrated. Three different resistance markers were used: *kanMX4* (in case of *EGFP* constructs), *natNT2* (in case of *GAL* constructs) and *hphNT1* (for deletion of *PEX19*). The cells were therefore plated on YPD plates containing G-418, nourseothricin (CloNAT) or hygromycin B, respectively. After three days at 30°C the colonies were re-streaked on new selective medium.

5.2.3 Amplification of DNA fragments by PCR

5.2.3.1 PCR using puReTaq Ready-To-Go PCR-beads (GE Healthcare)

For one bead the sample volume was 25µL but in some cases twice the volume was necessary (50µL/2 beads). For 25µL sample volume 20pmol of each primer (i.e. 2µL of a 1:10 dilution of the 100µM stock solutions) and 50pg of plasmid DNA or 50ng of genomic DNA were added to a tube containing one PCR-bead. The rest of the volume was filled up with ddH_2O. To mix the components the tube was vortexed gently and spun afterwards for a few seconds. The mixture was covered by a few drops of mineral oil and if the PCR machine was not ready at that time the sample was stored on ice or in the cold block of the PCR machine until cycling started.

5.2.3.2 PCR using home made Taq

10xPCR buffer:
200mM Tris/HCl pH8,8 100mM $(NH_4)_2SO_4$ 100mM KCl 20mM $MgSO_4$

The sample volume of 25µL contained 50pg of plasmid DNA or 50ng of complex genomic DNA, 2,5µL 10xPCR buffer, 1µL Taq, 0,5µL dNTPs (10mM stock solution), 2µL of each primer (1:10 dilution of 100mM stock solution) and ddH_2O. For the amplification of very long DNA fragments (i.e. more than 1000bp) 0,5µL of Pfu polymerase was added to ensure that the whole fragment could be amplified.

5.2.3.3 PCR program on Robocycler 40 (Stratagene)

The PCR program (melting temperature and time, annealing temperature and time, elongation time and cycle number) was set according to the length and sequence of the primers and the length of the expected fragments.

5.2.3.4 Separating PCR fragments on agarose gels

1xTBE:
90mM Tris 3mM EDTA 90mM Borsäure

1% agarose gels were used to separate PCR fragments from contaminants (e.g. primers). 1g of agarose was added to 100mL of 1xTBE buffer and heated until its complete dissolution. After cooling to approximately 50°C, 5µL of ethidium bromide (5mg/mL stock solution) was added and mixed by gently swaying the flask. Then the gel was poured. The samples were mixed with 10x loading buffer and loaded into the slots of the gel. Electrophoresis was carried out at 120V.

5.2.3.5 Extraction of PCR fragments from agarose gels:

The isolation of purified PCR fragments from the gel was done as described in the protocol of the isolation kit "Wizard SV gel and PCR clean up system".

5.2.4 Halo assay

1xTE:
10mM Tris pH 8,0 1mM EDTA

Halo assays were performed essentially according to [74] to test if the *S.c.* strains under scrutiny can metabolize oleic acid when provided as sole carbon source. o/n cultures of the *S.c.* strains grown on selective medium were diluted to OD_{600} = 0,2-0,3 in selective medium. The cultures were again grown on 30°C until an OD_{600} of approximately 1was reached. A dilution series of the cultures consisting of the dilutions 1:10, 1:100, 1:1000 and 1:10 000 in 1xTE was prepared. 2,5µL of the undiluted culture and of each dilution were spotted onto an oleic acid plate and a YPD plate as positive control according to the scheme shown in figure 5-2. The plates were incubated at 30°C. In contrast to YPD plates oleic acid plates should be nearly closed with parafilm (one quarter of the plate open to ensure enough supply of oxygen). Additionally, they have to be stored in a box equipped

with a glass of dH_2O in order to prevent the drying-out of the thin oleic acid plates. After 2d of incubation at 30°C growth on the YPD plates was recorded. Halo formation and growth of the cells on oleic acid was determined after 5-10d of incubation at 30°C.

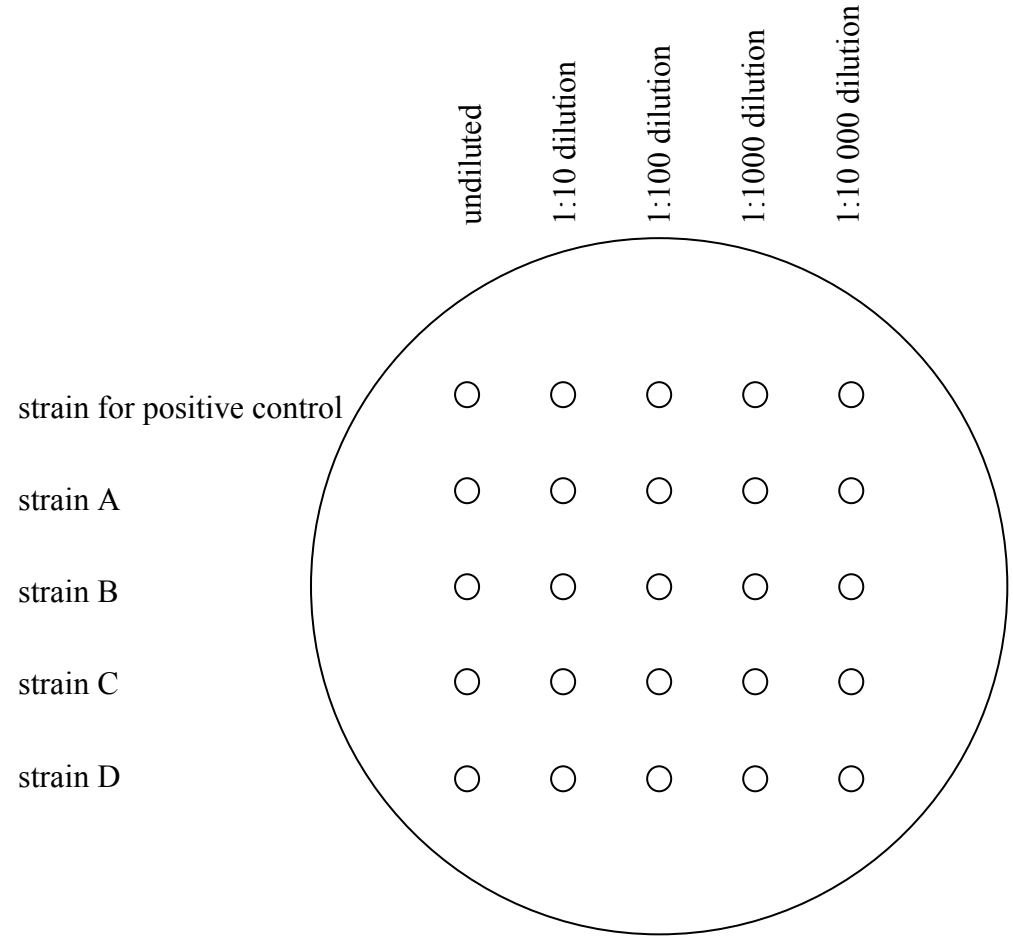

Figure 5-2: Scheme for spotting the dilution series of the cell cultures under scrutiny onto oleic acid and YPD plates, respectively.

5.3 ANALYTICAL METHODS

5.3.1 Bradford Assay for protein quantification

The assay was essentially performed according to [75]. The BIO-RAD Protein Assay solution was diluted 1:5 in dH_2O. 1mL of this solution was added to 1µL of the sample respectively to 1µL of BSA standard solutions (0-20mg/mL H_2O). These mixtures were incubated at 30°C for 10'. Afterwards, the absorbance at 595nm was measured and compared to the BSA standard calibration line.

5.3.2 Qubit Fluorometer for DNA quantification

The quantification of dsDNA using the Qubit Fluorometer from Invitrogen was performed as described in the enclosed instruction manual.

5.4 PROTEIN METHODS

5.4.1 Protein precipitation with TCA

Essentially according to [64], 16,5µL of 2% desoxycholate (DOC) were added to 1mL of sample and mixed by gentle vortexing. After incubation on ice for 10', $72\%_{w/v}$ TCA solution was added to a final TCA concentration of either 7% (100µl 72% TCA/1 mL sample) or 20% (385 µL 72% TCA/1 mL sample). The mixture was put on 4°C o/n to obtain a high degree of precipitation. To get a protein pellet, the sample was spun down in a centrifuge at 18 000 x g for 10' at 4°C. Afterwards, the pellet was resuspended in -20°C cold acetone and spun again at 18 000 x g for 5' at 4°C. The obtained pellet was dried at 37°C and stored at -80°C.

5.4.2 SDS page

5.4.2.1 For normal purposes

SDS polycrylamide gel electrophoresis was adapted according to [76].

pouring the gel:

Separation Gel:	15%	10%
1,5M Tris/HCl pH 8,8	2,5mL	2,5mL
30% Acrylamide (0,8%bis)	5,0mL	3,3mL
dH_2O	2,4mL	4,1mL
10% SDS	100µL	100µL
20% APS	15µL	15µL
TEMED	15µL	15µL

Stacking Gel:	5%
1M Tris/HCl pH 6,8	1,25mL
30% Acrylamide (0,8%bis)	0,8mL
dH_2O	2,9mL
10% SDS	50µL
20% APS	15µL
TEMED	7,5µL

15% separation gels were used when the protein of interest had a low molecular weight (30kDa or below) whereas 10% separation gels were used to separate proteins with middle or high molecular weight. The stacking gel remained the same in either case. For pouring

the gel a BIO-RAD gadget was used. 1,5mm thick gels were used for subsequent Western blot analysis and 0,75mm thick gels were used for the silverstaining procedures. First, the components of the separation gel were mixed except for 20% APS and TEMED which were added separately and mixed thoroughly shortly before pouring the gel. The separation gel was covered with a layer of isopropanol during the polymerization process. After polymerization the isopropanol was removed and the gadget was rinsed with dH_2O three times and dried using filter paper. Then, the components of the stacking gel were mixed (20%APS and TEMED added shortly before pouring), the stacking gel was poured onto the already polymerized separation gel and a comb was inserted. After polymerisation, the gel was either used immediately or stored at 4°C for about one week covered with wet papers and enclosed in a plastic bag.

Sample preparation:

2xSB:
125mM Tris/HCl pH 6,8 4% SDS 1,4M ß-Mercaptoethanol 20% Glycerol 0,01% Bromphenolblue

Liquid samples were mixed with the hot (95°C) 2xSB. Pellets were dissolved in hot 1xSB. Prior to loading, samples were incubated at 95°C for 2' and then filled into the slots of the gel. As marker, a pre-stained protein ladder from Fermentas was used. 5µL were applied when Western blot analysis was carried out and 1µL was loaded if the gel was silverstained afterwards.

Electrophoretic separation:

10xSDS buffer:
250mM Tris 2M Glycin 1% SDS no adjustment of pH

The gel was immersed in 1xSDS buffer and a constant current of 30mA/gel was applied. The voltage limit was set at 170V. Electrophoresis was stopped when the bromphenolblue front has reached the end of the gel.

5.4.2.2 For MS analysis

For MS analysis a commercially available gradient gel NuPAGE Novex Bis-Tris Mini Gel 4-12% (Invitrogen) was used. The sample preparation was the same as described in "SDS PAGE for normal purposes". Electrophoresis was carried out with a 1xMOPS buffer diluted from a commercially available 20xMOPS buffer (Invitrogen). The NuPAGE gadget was rinsed with ddH_2O before it was equipped with the gel and the running buffer. Electrophoresis was carried out at 200V (constant) with a current limit of 300mA for 50'.

5.4.3 Western Blot

5.4.3.1 Semidry Blot

1xTransfer buffer:
25mM Tris 200mM Glycin no adjustment of pH

The semi-dry blotting procedure was performed essentially according to [77]. The SDS polyacrylamide gel, a nitrocellulose membrane (Whatman) and filter papers were soaked in the 1x transfer buffer. Afterwards, a blot sandwich was arranged as follows: 2 filter papers, the nitrocellulose membrane, the gel and 2 filter papers. The transfer was performed in a semidry blotting chamber with 60mA/blot (constant) and a voltage limit of 25V for 1,5h.

5.4.3.2 Ponceau S staining

Ponceau S solution:
0,2% $_{w/v}$ ponceau S 3% $_{w/v}$ TCA

As a pre-stained marker was used in every SDS PAGE, Ponceau S staining was performed only to control if the same amount of protein was loaded and whether the blotting procedure worked well. The blot was put into the Ponceau S solution and was swayed in

this solution for 30''-5'. Then, the blot was washed with dH_2O to diminish the background staining. The Ponceau S solution can be used again.

5.4.3.3 Blocking step

1xTBST:
150mM NaCl 50mM Tris adjust to pH 7,5 /w HCl 0,05% Tween20

A 4% $_{w/v}$ skim milk powder solution in 1xTBST was prepared (25mL/blot) and the blot was swayed in this solution either for 1h at room temperature or o/n at 4°C.

5.4.3.4 Incubation with antibodies

After the blocking step, the blot was rinsed with 1xTBST two times. Afterwards, the blot was incubated by gentle moving in a dilution of the primary antibody in TBST (dilutions for the specific antibodies listed in section 5.1.4.) for 1h at room temperature. Following 3x10' washing steps with 1xTBST, the incubation with the secondary antibody dilution (dilutions for the specific antibodies listed in section 5.1.4.) was carried out for 1h at room temperature. Finally, the blot was washed again 3x10' in TBST.

5.4.3.5 Chemiluminescent detection

The signal of the protein band identified by the primary antibody was visualized using a chemiluminescent kit. Usually, the Super Signal West Pico Chemiluminescent Substrate (Thermo Scientific) was used, whereas the Immune-Star Western C Kit (BioRad) was applied when only weak signals were expected or a higher sensitivity was needed. In both cases, the chemiluminescent substrate and the enhancer solution were mixed 1:1 and the blot was incubated with this mixture for about 30''-1'. The blot was taken out and the superfluous solution was removed. The blot was put into a dark box and in the photo lab films were exposed successively to the blot for increasing time periods ranging from 10'' to 30' or even o/n according to the signal strength.

5.4.3.6 Stripping the blot

sripping solution:
2M $MgCl_2.6H_2O$ 100mM Acetic Acid pH not adjusted

To remove the bound antibodies from the blot in order to reuse the Western blot with different antibodies, the blot was gently moved in the stripping solution (25mL/blot) at room temperature for 10'. After washing 3x20' in TBST the blot was ready for reuse starting the procedure with the blocking step.

5.4.4 Colloidal Coomassie staining

incubation solution:
34% Methanol 2% Phosphoric Acid 17% Ammoniumsulfate

fixing solution:
50% Methanol 2% Phosphoric Acid

The colloidal Coomassie staining was carried out at room temperature, essentially according to [78]. The SDS polyacrylamide gel was fixed for 1h to o/n in the fixing solution. Following 3x30' washing steps in dH_2O, the gel was incubated with the incubation solution for 1h. Then, spatula tips of Coomassie were added stepwise to the incubation solution. The staining took place for 1-3d and then the gel was destained with dH_2O to reduce the background.

5.4.5 Silver staining

fixing solution:
50% Methanol 5% Acetic acid

sensitizing solution:
1,2mM $Na_2S_2O_3.5H_2O$

developing solution:
70mM $Na_2CO_3.10H_2O$ 0,014% Formaldehyd

washing solution:
50% Methanol

silver solution:
6 mM $AgNO_3$

stop solution:
5% Acetic Acid

The protocol for the silver staining procedure was adapted according to [79]. Usually, the solutions were prepared with dH_2O. If the separated proteins should be analysed by MS, ddH_2O was used for the preparation of the solutions and for the washing steps. The sensitizing, silver and developing solutions had to be prepared freshly; all other solutions were stored at room temperature. The gel was fixed swaying in the fixing solution for 20'. After 10' incubation in the washing solution, the gel was washed further with dH_2O for 2h at minimum but preferentially o/n. Afterwards, the gel was incubated in the sensitizing solution for 1'. After two washing steps with dH_2O for 1' each, the gel was swayed in the silver solution for 20' at 4°C, washed again two times with dH_2O for 1' and incubated with the developing solution until bands appeared and the marker bands were also stained. Then, the development was terminated by treatment with the stop solution three times for 1'.

5.5 MICROSCOPY METHODS

The specimens were investigated with a fluorescence microscope (Axioplan2, Zeiss) using a 63x oil immersion objective.

5.5.1 Indirect or direct immunofluorescence test

Immunofluorescence tests were performed essentially according to [80].

5.5.1.1 Fixation and spheroplasting

SP buffer: 1,2M Sorbit 20mM K_2HPO_4/KH_2PO_4 pH 7,4

The cells were grown in the appropriate medium (culture volume 20mL) to the desired OD_{600} (in most cases OD_{600} = 2). 2mL 37% formaldehyde solution and 2mL 1M K_2HPO_4/KH_2PO_4 pH 6,5 were added and the culture was allowed to shake another 30' at 30°C. Afterwards, the cells were pelleted by centrifugation at 1000 x g for 2'. The cell pellet was resuspended in 20mL 3,7% formaldehyde, 0,1M K_2HPO_4/KH_2PO_4 pH 6,5 and shaken at RT for 45'. 10mL of the suspension were again pelleted by centrifugation at 1000 x g for 2' and resuspended in 5mL 0,1M K_2HPO_4/KH_2PO_4 pH 7,5. (The fixed cells could be stored at 4°C o/n.)

The fixed cells were pelleted and washed in 3mL SP buffer by centrifugation at 1000 x g for 2'. The pellet was resuspended in 1mL SP buffer, and 2µL ß-Mercaptoethanol and 20µL Zymolyase 20T (10mg/mL solution, Seikagaku Biobusiness) were added. The resuspension was transferred to a 1,5mL microcentrifuge tube. Spheroplasting was carried out at 30°C for 45'. The suspension was mixed from time to time by inverting the microcentrifuge tube. The spheroplasts were pelleted by centrifugation at 1500 x g for 30'', gently resuspended in 0,5mL SP buffer with 0,1% TritonX100 and the mixture was allowed to stand at RT for 10'. Afterwards, the spheroplasts were washed twice in SP buffer and the pellet was finally resuspended in 300µL SP buffer. The fixed spheroplasts can be stored at RT until everything is set up for the antibody incubation.

5.5.1.2 Preparation of the microscope slide and antibody incubation

BSA-PBS:

1% BSA
40mM K_2HPO_4
10mM KH_2PO_4
150mM NaCl
0,1% NaN_3

For the indirect or direct immunofluorescence, microscope slides with specimen cavities were used. To prepare these, 5µL 0,1% polylysine was put on each cavity and immediately removed after 5-10'' by suction with a water jet vacuum pump equipped with a pasteur pipette capillary. The microscope slide was dried by exposure to air. Then, the specimen cavities were rinsed with dH_2O and dried again. To immobilize the spheroplasts on the microscopy slide, 10µL of the spheroplast resuspension were pipeted on one specimen cavity. After 10'', the liquid was removed and the slide was briefly dried leaving it ready for antibody incubation.

10µL of the 1° antibody dilution in BSA-PBS was put on one specimen cavity. The slide was incubated with the 1° antibody in a wet chamber in the dark at RT for 1h. Afterwards, three washing steps with BSA-PBS followed. 10µL BSA-PBS were used per cavity and when the washing solution was removed, new solution was immediately added to prevent the drying of the cavities. For direct immunofluorescence, the slide was ready for microspcopic inspection because the 1° antibody is already fluorescently labelled. For indirect immunofluorescence incubation with a 2° antibody followed and was carried out the same way as the incubation with the 1° antibody. Eventually, the specimen cavities were washed with BSA-PBS four times. The BSA-PBS was removed, one drop of ProLong Gold (Invitrogen) was put on each specimen cavity and the microscopy slide was covered by a cover slip. After 24h the slide was sealed with nail polish and ready for microscopy.

5.5.2 Fluorescent labelling of parts of the the organellar pellet

5.5.2.1 Limited proteolysis

1µL 100mM $CaCl_2$ and 1,25µL Thermolysin (2mg/ml) were added to 25µL of the OP

resuspension. The mixture was incubated on ice for 2', 10' or 20'. The proteolysis was stopped by the addition of 1µL 0,5M EDTA.

5.5.2.2 Labelling the organellar pellet

The OP was incubated with 0,5% BSA (0,5µL 10% BSA in dH_2O to 10µL OP) for 10' at 4°C to block unspecific interactions with the antibodies. Afterwards, the fluorescently labelled antibody was added to the OP resuspension so that the desired end dilution of the antibody was achieved. After incubation in the dark at 4°C for 20', the OP was inspected by fluorescence microscopy.

5.5.3 Embedding in agarose

0,5% agarose solution was heated until its completely dissolution. 5µL were pipeted onto a microscopy slide, the cells of interest were streaked from the plate into this solution and a cover slip was added very quickly because otherwise the agarose becomes solid. The sample was immediately ready for microscopy.

5.6 GROWTH PROCEDURES FOR YEAST *S.C.* CELLS

5.6.1 Growth on solid media (plates)

The plates were prepared according to the following recipes. The hygromycin B, nourseothricin (CloNAT), G-418, threonine or tryptophan stock solutions, respectively, could not be added until the autoclaved mixture had been cooled to approximately 40°C. Generally, the plates were poured using ~20mL medium per plate except for oleic acid plates for halo assays which were poured with 11mL per plate.

YPD:

2% Peptone
1% YE
2% Glucose
3% AgarAgar

YPD + Hygromycin:

2% Peptone
1% YE
2% Glucose
3% AgarAgar
300mg/l Hygromycin B

YPD + CloNAT:

2% Peptone
1% YE
2% Glucose
3% AgarAgar
100mg/l CloNAT

YPD + G-418:

2% Peptone
1% YE
2% Glucose
3% AgarAgar
200mg/l G 418 Sulphate

SC – Ura:

0,67% YNB w/o aa
2% or 0,5% Glucose
1% 100x aa-stock solution w/o uracil
3% AgarAgar

SC + oleic acid:

0,67% YNB w/o aa
0,1% YE
0,125% oleic acid
0,5% Tween 80
30mM KH_2PO_4/K_2HPO_4 pH 6,0
1% 100x aa-stock solution
3% AgarAgar

Plates with *S.c.* yeast cells were always incubated at 30°C. If a yeast strain was only streaked onto a plate for the purpose of storage or propagation of a frozen stock strain, the plate was removed from 30°C after 2d and can be stored at 4°C after sealing it with Parafilm. When yeast cells were plated after transformation, the plates were incubated for

about 3-5d until sufficiently big colonies appeared. These colonies were re-streaked onto plates containing the same medium. For the formation of halos on turbid plates, the oleic acid plates were incubated for more than 5d until proper halo formation was visible.

5.6.2 Growth in liquid culture

Yeast cells were grown at 30°C in liquid medium. The volume of the culture flasks was chosen 4-5 times bigger than the volume of the culture and the flasks were shaken at 190-200rpm to ensure sufficient supply of oxygen. The media were prepared as described below. In SC (synthetic complete) and Rytka medium, selection for auxotrophy markers was possible by simply using a 100x aa-stock solution lacking the amino acids and/or nucleic acid bases necessary for selection. The amino acid stock solutions of threonine and tryptophane had to be added after autoclaving.

5.6.2.1 Glucose grown cells (repressed peroxisomes)

SC medium:
0,67% YNB w/o aa 2% Glucose 1% 100x aa-stock solution

An o/n culture in SC 2% glucose was diluted to an OD_{600} of 0,2 into the appropriate volume of the same medium. The yeast cells were allowed to grow until an OD_{600} of 2 was reached. After another dilution into the same medium to OD_{600} = 0,03 cells were grown o/n and expected to reach an OD_{600} of 2 in the morning.

5.6.2.2 EtOH grown cells for peroxisome isolation (derepressed peroxisomes)

SC medium:	YPE:
0,67% YNB w/o aa 2% or 0,5% Glucose 1% 100x aa-stock solution	2% Peptone 1% YE 2% Ethanol

From 3mL overnight culture grown at 30°C in the appropriate synthetic complete medium with 2% glucose, 50mL SC medium with 2% glucose were inoculated to an OD_{600} of 0,03.

This culture was again shaken o/n at 30°C. On the next day, 250mL of SC 0,5% glucose were inoculated to an OD_{600} of 0,2 and grown until an OD_{600} of 2 was reached. Cells from this culture were used to inoculate two flasks with 500mL YPE media each in a way that an OD_{600} of 2 was expected in the morning. (The estimated doubling time of *S.c.* in YPE is about 4,5h. One generation was taken account of for the lag phase.)

5.6.2.3 Oleic acid grown cells (induced peroxisomes)

Rytka medium:

SC medium:	Rytka medium:
0,67% YNB w/o aa 0,3% Glucose 1% 100x aa-stock solution	0,67% YNB w/o aa 0,1% Glucose 0,1% YE 1% 100x aa-stock solution adjust to pH 6,0 with KOH 0,05% Tween 40 0,1% Oleic acid

An o/n culture in synthetic SC medium with 0,3% glucose was diluted into the same medium to an OD_{600} of 0,2 and grown at 30°C until an OD_{600} = 2 was reached. Starting with this culture, the Rytka medium was inoculated to OD_{600} = 0,2 and incubated o/n at 30°C.

Oleic acid induction medium [81]:

SC medium:	induction medium:	OA stock solution:
0,67% YNB w/o aa 2% or 0,5% Glucose 1% 100x aa-stock solution	0,3% YE 0,5% Pepton 30mM K_2HPO_4/KH_2PO_4 pH 6,0	10% Oleic acid 1% Tween 80 177mM NaOH boil 1-2h

Yeast cells were grown o/n in SC medium with 2% glucose. The cell suspension was diluted into the same SC medium containing only 0,5% glucose to an OD_{600} of 0,2 and grown until an OD_{600} of 2 was reached. The final induction medium prepared by adding 2% of the reboiled oleic acid stock solution to the induction medium was inoculated to OD_{600} = 1 and cells were incubated o/n to reach an OD_{600} of 2 in the morning because the cells can only undergo one duplication in this medium.

5.6.2.4 Galactose induced cells (induction of GAL-driven PEX genes)

SC medium:	YPD (4%):	YPG:	YPR:
0,67% YNB w/o aa 2% Glucose 1% 100x aa-stock solution	2% Peptone 1% YE 4% Glucose	2% Peptone 1% YE 2% Galactose	2% Peptone 1% YE 4% Raffinose

Yeast cells grown in 3mL SC medium with 2% glucose over night were used to inoculate 20mL YPR culture to an OD_{600} of 0,3 and grown a few hours until an OD_{600} of 0,7-0,8 was reached. Then, the cells were pelleted by centrifugation at 1000 x g for 4' and resuspended in 20ml YPG to start the induction by the *GAL* promoter. The galactose induction was either carried out for at least 4h or was stopped after 30' by pelleting the cells of 10mL culture and resuspending the pellet in 10mL YPD with 4% glucose. Peroxisome biogenesis was followed by fluorescence microscopy employing various fluorescent marker proteins. At different time points, 100µL aliquots were taken from the YPR culture and from the galactose-induced cultures as well as from the YPD cultures after the short galactose induction pulse. Immediately after removal, the cells were pelleted (4', 1000 x g) and washed with dH_2O. Then, cells were fixed for at least 5' by resuspending the cell pellet in 100µL 0,1M K_2HPO_4/KH_2PO_4 pH 6,5 with 3,7% formaldehyde. Afterwards, the cells were pelleted again, resuspended in 0,1M K_2HPO_4/KH_2PO_4 pH 6,5 and stored in the dark until fluorescence microscopy could be carried out.

5.7 PROCEDURE FOR PEROXISOME ISOLATION

The procedures for peroxisome isolation including spheroplasting, homogenization, generation of an OP and density gradient centrifugation were performed according to an adapted procedure from [65].

5.7.1 Spheroplasting

SP buffer:	Tris/Sulfate with DTT:	Lysis buffer:
1,2M Sorbitol 20mM K_2HPO_4/KH_2PO_4 pH 7,4	0,1M Tris/Sulfate pH 9,4 0,15% DTT (add shortly before usage!)	3% Lauroylsarcosine 0,5M Tris/HCl pH 9,0 40µM EDTA

The OD_{600} of the yeast culture was determined and the culture was inspected for contamination. The cells were pelleted by centrifugation at 2700 x g for 3' in GS3 tubes. The pellet was resuspended in dH_2O and transferred to a weighted SS34 tube, pelleted by centrifugation and the wet weight of the cell pellet was determined. After resuspension of the cell pellet in 1mL/0,5g cells Tris/Sulfate with DTT, the mixture was incubated for 15' in a water bath at 30°C with slight agitation. Afterwards, the cells were pelleted by centrifugation at 3000 x g for 4' and the cell pellet was washed once in SP buffer. The pellet was resuspended in 1mL/0,15g cells SP buffer, and 5mg/g cells Zymolyase 20T (Seikagaku Biobusiness) was added, and the suspension was further incubated at 30°C in the water bath with constant agitation. Spheroplast formation was followed microscopically (see below) every few minutes but was never carried out for more than 30'. To follow spheroplast formation, 5µL of the suspension were mixed with 45µL lysis buffer. After 1-2', the cells were inspected with a phase contrast microscope. Intact cells are surrounded by a bright circle resulting from the difference in refractive index between the cells and the buffer and can therefore be distinguished from spheroplasts which have lysed under these conditions. When >80% of cells had been converted into spheroplasts, the spheroplast formation was stopped by centrifugation at 1500 x g for 5' and the spheroplasts were carefully washed twice in cold SP buffer yielding the spheroplast pellet. From this step forward, every step should be carried out at 4°C (using cold buffers and cooling the tubes in ice).

5.7.2 Homogenization and generation of the PNS (post nuclear supernatant)

PSB:
5mM MES 1mM KCl 0,5mM EDTA 160mM Sucrose adjust to pH 6,0 with NaOH 12% PEG 1450

The spheroplast pellet was resuspended in cold PSB (1,5mL/g cells) with PMSF (1mM) and Complete protease inhibitor mix (EDTA free; Roche) added shortly before usage. The resuspended spheroplasts were broken and homogenized by 20 strokes with a cooled Potter homogenizer, the pistil turning at 1200rpm. The homogenate was spun in a centrifuge at 1500 x g for 5' at 4°C. The pellet was discarded and the supernatant was again cleared by centrifugation at 3000 x g for 5'. The resulting supernatant was the PNS. Starting with the PNS, one can either generate the OP (organellar pellet) or the peroxisomal fraction by density gradient centrifugation.

5.7.3 Generation of the OP (organellar pellet)

The PNS was spun in a centrifuge at 27 000 x g for 15'. The resulting pellet was considered to be the organellar pellet and the supernatant the POS (post organellar supernatant). The OP was resuspended in PSB and OP and POS were stored at -80°C.

5.7.4 Generation of the peroxisomal fraction by density gradient centrifugation

5.7.4.1 Preparation of the Nycodenz solutions

To separate peroxisomes from other organelles, especially mitochondria, a Nycodenz (Axis-Shield) density gradient centrifugation was carried out. Nycodenz was used because it is not osmotically active in contrast to sucrose for instance. To prepare the different Nycodenz solutions (normally 50%, 32%, 20%$_{w/v}$), a defined amount of Nycodenz was weighed and a defined volume of PSB was added. The tube should not be filled with PSB to the final volume because of a notable increase in volume during the dissolution of the

Nycodenz. The mixture was shaken o/n at 30°C to obtain complete dissolution. When the Nycodenz had completely dissolved, the correct density of Nycodenz was adjusted by stepwise adding PSB and measuring the refractive index of the solution. The refractive indices of the utilized Nycodenz solutions are listed below:

Nycodenz solution:	refractive index:
50% $_{w/v}$	1,4280
40% $_{w/v}$	1,4146
35% $_{w/v}$	1,4070
33,5% $_{w/v}$	1,4045
32% $_{w/v}$	1,40275
30% $_{w/v}$	1,4000
25% $_{w/v}$	1,3930
20% $_{w/v}$	1,3875

5.7.4.2 Nycodenz density gradient centrifugation

The PNS was adjusted to 10% Nycodenz by dropwise adding and gently mixing 50% Nycodenz solution. Afterwards, the density adjusted PNS was loaded onto an already prepared Nycodenz gradient. The gradient was prepared in an Ultra-Clear Centrifuge tube (Beckman, # 344060) containing a maximum volume of 13mL. The centrifuge tube should be filled with 12mL at minimum. In general, the gradient was prepared as follows with minor changes in the volume of the Nycodenz solutions if the volume of the PNS varied. 2mL 50% Nycodenz solution covered the bottom of the tube, then a layer of 5mL 32% Nycodenz solution was laid on top, which was covered by 2mL of 20% Nycodenz solution. 2-3mL of PNS were loaded onto the gradient. Ultracentrifugation was carried out in the SW40Ti rotor at 111 000 x g at maximum for 2,5h at 4°C.

After centrifugation, small turbid layers at the interface of the 50% and the 32% Nycodenz solution (the peroxisomal fraction) and between the 32% and the20% Nycodenz solution (the mitochondrial fraction) were visible. On top of the 20% Nycodenz solution cell debris was deposited. To collect the fractions of the gradient, a hole was punched in the Ultra Clear centrifuge tube just below the interface between the 50% and the 32% Nycodenz solution with a 0,70mm needle. The gradient started to drop and fractions were collected. The volume of the fractions was 1,5mL except for the peroxisomal and the mitochondrial

one. In these two cases, only the turbid layer was collected – so the volume of the fraction varied. The fractions were stored at -80°C. The peroxisomal fraction was used to generate the peroxisomal pellet PxP.

5.7.5 Generation of the PxP (peroxisomal pellet)

The peroxisomal fraction from the Nycondenz gradient was diluted 1:3,5 by drop wise adding cold PSB with PMSF and Complete Protease Inhibitor Mix (EDTA free; Roche) so that the final concentration of Nycodenz was ~10%. This solution was filled into an Ultra-Clear Centrifuge tube (Beckman, # 344057) containing a maximum volume of 5mL. If the volume of the diluted peroxisomal fraction was smaller than 5mL, the peroxisomal fraction was overlaid with PSB. To pellet the peroxisomes, an ultracentrifugation in the SW65 rotor at 30 000 x g for 10' was carried out. The centrifugation yielded a very small, often not clearly visible pellet. The supernatant was discarded and the peroxisomal pellet resuspended in 200µL PSB with PMSF and Complete Protease Inhibitor Mix. The resuspension of the PxP was stored at -80°C.

5.7.6 Sorting by FAOS (fluorescence activated organellar sorting)

The BD FACSAria flow cytometer was used to sort fluorescently labelled peroxisomes out of the PNS, the OP resuspension or the PxP resuspension. The sorting process was performed by the BioOptics Department of the IMP.

The BD FACSAria flow cytometer is equipped with a 488nm laser and can therefore excite labels with green fluorescence. To measure the emitted fluorescence, two channels were used: phycoerythrin (585/42nm filter) and GFP-FITC (530/30nm filter). So, the PNS, OP or PxP of CB80 wild type cells with the pCB367 (mCherry-SKL) plasmid served as negative control because the red fluorescent label can not be excited. First, the negative control sample was tested and according to the distribution of the events in the diagrams forward scatter area versus side scatter area (FSC-A/SSC-A), forward scatter width versus forward scatter area (FSC-W/FSC-A) and phycoerythrin versus GFP-FITC fluorescence intensity (PE/GFP-FITC) "gates" were set. The first diagram displays the relative differences of the size (FSC) and of the internal complexity (SSC) of the particles. Almost all events were gated in this dot plot representation. The events represented in the FSC-W/FSC-A diagram were gated in a way that events producing signals with a very high

width are discriminated due to potential association or overlapping. In the fluorescence intensity diagram, the gate for the “positive” events was set in a way that all the events from the strain expressing mCherry-SKL (resulting only from autofluorescence) are excluded. The “negative” events were defined by a gate in the area of autofluorescence. To exclude ambiguous events a gap between these two gates was spared. Eventually, the sample of interest was inserted into the machine and was then either simply monitored for events with higher fluorescence intensity (“positive events”) or indeed sorted according to the set gates.

6 REFERENCES

[1] de Duve C, Baudhuin P, *Peroxisomes (microbodies and related particles).* Physiol Rev, 1966. **46(2)**: 323-357

[2] Titorenko VI, Rachubinsky RA, *The Life Cycle of the Peroxisome.* Nat Rev Mol Cell Biol, 2001. **2**(**5)**: 357-68

[3] Tabak HF, van der Zand A, Braakman I, *Peroxisomes: minted by the ER.* Curr Opinion Cell Biol, 2008. **20(4)**: 393-400

[4] van der Zand A, Braakman I, Geuze HJ, Tabak HF, *The return of the peroxisome.* J Cell Science, 2006. **119(6)**: 989-994

[5] Wanders RJA, Waterham HR, *Peroxisomal disorders: The single peroxisomal enzyme deficiencies.* Biochim Biophys Acta, 2006. **1763(12)**: 1707-1720

[6] van der Klei IJ, Veenhuis M, *Yeast and filamentous fungi as model organisms in microbody research.* Biochim Biophys Acta, 2006. **1763(12)**: 1364-1373

[7] Saleem RA, Knoblach B, Mast FD, Smith JJ, Boyle J, Dobson CM, Long-O'Donnel R, Rachubinski RA, Aitchison JD, *Genome-wide analysis of signaling networks regulating fatty acid-induced gene expression and organelle biogenesis.* J Cell Biol, 2008. **181(2)**: 281-292

[8] Erdmann R, Veenhuis M, Mertens D, Kunau WH, *Isolation of peroxisome-deficient mutants of Saccharomyces cerevisiae*, Proc. Natl Acad Sci USA, 1989. **86(14)**: 5419-5423

[9] Veenhuis M, van der Klei IJ, Titorenko V, Harder W, *Hansenula polymorpha: an attractive model organism for molecular studies of peroxisome biogenesis and function*. FEMS Microbiol Lett, 1992. **79(1-3)**: 393-403

[10] Nuttley WM, Brade AM, Eitzen GA, Veenhuis M, Aitchison JD, Szilard RK, Glover JR, Rachubinski RA, *PAY4, a gene required for peroxisome assembly in the yeast Yarrowia lipolytica, encodes a novel member of a family of putative ATPases*. J Biol Chem, 1994. **269(1)**: 556-566

[11] Gould SJ, McCollum D, Spong AP, Heyman JA, Subramani S, *Development of the yeast Pichia pastoris as a model organism for a genetic and molecular analysis of peroxisome assembly*. Yeast, 1992. **8(8)**: 613-628

[12] Tabak HF, Hoepfner D, van der Zand A, Geuze HJ, Braakman I, Huynen MA, *Formation of Peroxisomes: Present and Past.* Biochim Biophys Acta, 2006. **1763(12)**: 1647-1654

[13] Lazarow PB, Fujiki Y, *Biogenesis of Peroxisomes*. Annu Rev Cell Biol, 1985. **1**: 489-530

[14] Gould SG, Keller GA, Subramani S, *Identification of a peroxisomal targeting signal at the carboxy terminus of firefly luciferase.* J Cell Biol, 1987. **105(6 Pt 2)**: 2923-2931

[15] Swinkels BW, Gould SJ, Bodnar AG, Rachubinski RA, Subramani S, *A novel, cleavable peroxisomal targeting signal at the amino-terminus of the rat 3-ketoacyl-CoA thiolase.* EMBO J, 1991. **10(11)**: 3255-3262

[16] Novikoff PM, Novikoff AB, *Peroxisomes in absorptive cells of mammalian small intestine.* J Cell Biol, 1972. **53(2)**: 532-560

[17] Ganzalez E, *Glycoproteins in the matrix of glyoxysomes in endosperm of Castor bean seedlings.* Plant Physiol, 1986. **80(4)**: 950-955

[18] Höhfeld J, Veenhuis M, Kunau WH, *PAS3, a Saccharomyces cerevisiae gene encoding a peroxisomal integral membrane protein essential for peroxisome biogenesis.* J Cell Biol, 1991. **114(6)**: 1167-1178

[19] Hoepfner D, Schildknegt D, Braakman I, Philippsen P, Tabak HF, *Contribution of the Endoplasmic Reticulum to Peroxisome Formation.* Cell, 2005. **122(1)**: 85-95

[20] Tam YY, Fagarasanu A, Fagarasanu M, Rachubinski RA, *Pex3p Initiates the Formation of a Preperoxisomal Compartment from a Subdomain of the Endoplasmic Reticulum in Saccharomyces cerevisiae.* J Biol Chem, 2005. **280(41)**: 34933-34939

[21] Gabaldón T, Snel B, van Zimmeren F, Hemrika W, Tabak H, Huynen MA, *Origin and Evolution of the peroxisomal proteome.* Biology Direct, 2006. **1**: 8

[22] Geuze HJ, Murk JL, Stroobants AK, Griffith JM, Kleijmeer MJ, Koster AJ, Verkleij AJ, Distel B, Tabak HF, *Involvement of the endoplasmic reticulum in peroxisome formation.* Mol. Biol Cell, 2003. **14(7)**: 2900–2907

[23] Schekman R, *Peroxisomes: another branch of the secretory pathway?* Cell, 2005. **122(1)**: 1-2

[24] Motley AM, Hettema EH, *Yeast peroxisomes multiply by growth and division*. J Cell Biol, 2007. **178(3)**: 399-410

[25] Praefcke GJ, McMahon HT, *The dynamin superfamily: universal membrane tubulation and fission molecules*. Nat Rev Mol Cell Biol, 2004. **5(2)**: 133-147

[26] Li X, Gould SJ, *The dynamin-like GTPase DLP1 is essential for peroxisome division and is recruited to peroxisomes in part by PEX11*. J Biol Chem, 2003. **278(19)**: 17012-17020

[27] Vizeacoumar FJ, Vreden WN, Fagarasanu M, Eitzen GA, Aitchison JD, Rachubinski RA, *The dynamin-like protein Vps1p of the yeast Saccharomyces cerevisiae associates with peroxisomes in a Pex19p-dependent manner*. J Biol Chem, 2006. **281(18)**: 12817-12823

[28] Nagotu S, Saraya R, Otzen M, Veenhuis M, van der Klei IJ, *Peroxisome proliferation in Hansenula polymorpha requires Dnm1p which mediates fission but not de novo formation*. Biochim Biophys Acta, 2008. **1783(5)**: 760-769

[29] Kim PK, Mullen RT, Schumann U, Lippincott-Schwartz J, *The origin and maintenance of mammalian peroxisomes involves a de novo PEX16-dependent pathway from the ER*. J Cell Biol, 2006. **173(4)**: 521-532

[30] Rottensteiner H, Kramer A, Lorenzen S, Stein K, Landgraf C, Volkmer-Engert R, Erdmann R, *Peroxisomal membrane proteins contain common Pex19p-binding sites that are an integral part of their targeting signals.* Mol Biol Cell, 2004. **15(7)**: 3406-3417

[31] Saleem RA, Smith JJ, Aitchison JD, *Proteomics of the Peroxisome.* Biochim Biophys Acta, 2006. **1763(12)**: 1541-1551

[32] Neuberger G, Maurer-Stroh S, Eisenhaber B, Hartig A, Eisenhaber F, *Prediction of peroxisomal targeting signal 1 containing proteins from amino acid sequence*. J Mol Biol, 2003. **328(3)**: 581-592

[33] Hettema EH, van Roermund CW, Distel B, van den Berg M, Vilela C, Rodrigues-Pousada C, Wanders RJ, Tabak HF, *The ABC transporter proteins Pat1 and Pat2 are required for import of long-chain fatty acids into peroxisomes of Saccharomyces cerevisiae.* EMBO J, 1996. **15(15)**: 3813-3822

[34] Faergeman NJ, Di Russo CC, Elberger A, Knudsen J, Black PN, *Disruption of the Saccharomyces cerevisiae Homologue to the Murine Fatty Acid Transport Protein Impairs Uptake and Growth on Long-chain Fatty Acids.* J Biol Chem, 1997. **272(13)**: 8531-8538

[35] Palmieri L, Rottensteiner H, Girzalsky W, Scarcia P, Palmieri F, Erdmann R, *Idendification and functional reconstitution of the yeast peroxisomal adenine nucleotide transporter.* EMBO J, 2001. **20(18)**: 5049-5059

[36] Neuberger G, Maurer-Stroh S, Eisenhaber B, Hartig A, Eisenhaber F, *Motif refinement of the peroxisomal targeting signal 1 and evaluation of taxon-specific differences*. J Mol Biol, 2003. **328(3)**: 567-579

[37] Kumar A, Agarwal S, Heyman JA, Matson S, Heidtman M, Piccirillo S, Umansky L, Drawid A, Jansen R, Liu Y, Cheung KH, Miller P, Gerstein M, Roeder GS, Snyder M, *Subcellular localization of the yeast proteome.* Genes Dev, 2002. **16(6)**: 707-719

[38] Huh WK, Falvo JV, Gerke LC, Carroll AS, Howson RW, Weissman JS, O'Shea EK, *Global analysis of protein localization in budding yeast.* Nature, 2003. **425(6959)**:686-691

[39] www.yeastgenome.org

[40] Uetz P, Giot L, Cagney G, Mansfield TA, Judson RS, Knight JR, Lockshon D, Narayan V, Srinivasan M, Pochart P, Qureshi-Emili A, Li Y, Godwin B, Conover D, Kalbfleisch T, Vijayadamodar G, Yang M, Johnston M, Fields S, Rothberg JM, *A comprehensive analysis of protein-protein interactions in Saccharomyces cerevisiae*. Nature, 2000. **403(6770)**: 623-627

[41] Ito T, Chiba T, Ozawa R, Yoshida M, Hattori M, Sakaki Y, *A comprehensive two-hybrid analysis to explore the yeast protein interactome*. Proc Natl Acad Sci USA, 2001. **98(8)**: 4569-4574

[42] Johnsson N, Varshavsky A, *Split ubiquitin as a sensor of protein interactions in vivo*. Proc Natl Acad Sci USA, 1994. **91(22)**: 10340-10344

[43] Miller JP, Lo RS, Ben-Hur A, Desmarais C, Stagljar I, Noble WS, Fields S, *Large-scale identification of yeast integral membrane protein interactions*. Proc Natl Acad Sci USA, 2005. **102(34)**: 12123-12128

[44] Goll J, Uetz P, *The elusive yeast interactome*. Genome Biol, 2006. **7(6)**: 223

[45] Gavin AC, Aloy P, Grandi P, Krause R, Boesche M, Marzioch M, Rau C, Jensen LJ, Bastuck S, Dümpelfeld B, Edelmann A, Heurtier MA, Hoffman V, Hoefert C, Klein K, Hudak M, Michon AM, Schelder M, Schirle M, Remor M, Rudi T, Hooper S, Bauer A, Bouwmeester T, Casari G, Drewes G, Neubauer G, Rick JM, Kuster B, Bork P, Russell RB, Superti-Furga G, *Proteome survey reveals modularity of the yeast cell machinery*. Nature, 2006. **440(7084)**: 631-636

[46] Krogan NJ, Cagney G, Yu H, Zhong G, Guo X, Ignatchenko A, Li J, Pu S, Datta N, Tikuisis AP, Punna T, Peregrín-Alvarez JM, Shales M, Zhang X, Davey M, Robinson MD, Paccanaro A, Bray JE, Sheung A, Beattie B, Richards DP, Canadien V, Lalev A, Mena F, Wong P, Starostine A, Canete MM, Vlasblom J, Wu S, Orsi C, Collins SR, Chandran S, Haw R, Rilstone JJ, Gandi K, Thompson NJ, Musso G, St Onge P, Ghanny S, Lam MH, Butland G, Altaf-Ul AM, Kanaya S, Shilatifard A, O'Shea E, Weissman JS, Ingles CJ, Hughes TR, Parkinson J, Gerstein M, Wodak SJ, Emili A, Greenblatt JF, *Global landscape of protein complexes in the yeast Saccharomyces cerevisiae*. Nature, 2006. **440(7084)**: 637-643

[47] Fields S, *High-throughput two-hybrid analysis. The promise and the peril*. FEBS J, 2005. **272(21)**: 5391-5399

[48] Brunet S, Thibault P, Gagnon E, Kearney P, Bergeron JJ, Desjardins M, *Organelle proteomics: looking at less to see more.* Trends Cell Biol, 2003. **13(12)**: 629-638

[49] Karas M, Hillenkamp F, *Laser desorption ionization of proteins with molecular masses exceeding 10,000 daltons.* Anal Chem, 1988. **60(20)**: 2299-2301

[50] Fenn JB, Mann M, Meng CK, Wong SF, Whitehouse CM, *Electrospray ionization for mass spectrometry of large biomolecules.* Science, 1989. **246(4926)**: 64-71

[51] Gygi SP, Corthals GL, Zhang Y, Rochon Y, Aebersold R, *Evaluation of two-dimensional gel electrophoresis-based proteome analysis technology.* Proc Natl Acad Sci USA, 2000. **97(17)**: 9390-9395

[52] Wessel D, Flügge UI, *A method for the quantitative recovery of protein in dilute solution in the presence of detergents and lipids.* Anal Biochem, 1984. **138(1)**: 141-143

[53] Wolters DA, Washburn MP, Yates JR 3rd, *An automated multidimensional protein identification technology for shotgun proteomics.* Anal Chem, 2001. **73(23)**: 5683-5690

[54] Link AJ, Eng J, Schieltz DM, Carmack E, Mize GJ, Morris DR, Garvik BM, Yates JR 3rd, *Direct analysis of protein complexes using mass spectrometry*. Nat Biotechnol, 1999. **17(7)**: 676-682

[55] Aebersold R, Mann M, *Mass spectrometry-based proteomics.* Nature, 2003. **422(6928)**: 198-207

[56] Herzenberg LA, Parks D, Sahaf B, Perez O, Roederer M, Herzenberg LA, *The history and future of the fluorescence activated cell sorter and flow cytometry: a view from Stanford.* Clin Chem, 2002, **48(10)**: 1819-1827

[57] BD FACS Aria User's Guide

[58] Tung JW, Heydari K, Tirouvanziam R, Sahaf B, Parks DR, Herzenberg LA, Herzenberg LA, *Modern flow cytometry: a practical approach.* Clin Lab Med, 2007. **27(3)**: 453-468

[59] Murphy RF, Jorgensen ED, Cantor CR, *Kinetics of Histone Endocytosisin Chinese Hamster Ovary Cells.* J Biol Chem, 1982. **257(4)**: 1695-1701

[60] Allen JK, Dennison DK, Schmitz KS, Morrisett JD, *Direct observation of the distribution of fluorescent probes in phosphatidylcholine/cholesterol vesicles using flow microfluorometry.* Anal Biochem, 1984. **140(2)**: 409-416

[61] Gorvel JP, Mishal Z, *Flow cytometry, a very useful technique for the characterization of intestinal membrane vesicles.* Biol Cell, 1986. **58(2)**: 157-167

[62] Böck G, Steinlein P, Huber LA, *Cell biologists sort things out: Analysis and purification of intracellular organelles by flow cytometry.* Trends Cell Biol, 1997. **7(12)**: 499-503

[63] Bananis E, Nath S, Gordon K, Satir P, Stockert RJ, Murray JW, Wolkoff AW, *Microtubule-dependent movement of late endocytic vesicles in vitro: requirements for Dynein and Kinesin.* Mol Biol Cell, 2004. **15(8)**: 3688-3697

[64] Cao Z, Li C, Higginbotham JN, Franklin JL, Tabb DL, Graves-Deal R, Hill S, Cheek K, Jerome WG, Lapierre LA, Goldenring JR, Ham AJL, Coffey RJ, *Use of Fluorescence-activated Vesicle Sorting for Isolation of Naked2-associated, Basolaterally Targeted Exocytic Vesicles for Proteomic Analysis.* Mol Cell Prot, 2008. **7(9)**: 1651-1667

[65] Grosschopf K, PhD thesis, 2008

[66] Marelli M, Smith JJ, Jung S, Yi E, Nesvizhskii AI, Christmas RH, Saleem RA, Tam YY, Fagarasanu A, Goodlett DR, Aebersold R, Rachubinski RA, Aitchison JD, *Quantitative mass spectrometry reveals a role for the GTPase Rho1p in actin organization on the peroxisome membrane.* J Cell Biol, 2004. **167(6)**: 1099-1112

[67] Gauthier DJ, Lazure C, *Complementary methods to assist subcellular fractionation in organellar proteomics.* Expert Rev Proteomics, 2008. **5(4)**: 603-617

[68] Wuestehube LJ, Schekman RW, *Reconstitution of transport from endoplasmic reticulum to Golgi complex using endoplasmic reticulum-enriched membrane fraction from yeast*. Methods Enzymol, 1992. **219**: 124-36

[69] Kunze M, Pracharoenwattana I, Smith SM, Hartig A, *A central role for the peroxisomal membrane in glyoxylate cycle function.* Biochim Biophys Acta, 2006. **1763(12)**: 1441-1452

[70] Kunze M, Kragler F, Binder M, Hartig A, Gurvitz A, *Targeting of malate synthase 1 to the peroxisomes of Saccharomyces cerevisiae cells depends on growth on oleic acid medium.* Eur J Biochem, 2002. **269(3)**: 915-922

[71] Cristea IM, Williams R, Chait BT, Rout MP, *Fluorescent proteins as proteomic probes.* Mol Cell Proteomics, 2005. **4(12)**: 1933-1941

[72] Ito H, Fukuda Y, Murata K, Kimura A, *Transformation of intact yeast cells treated with alkali cations*. J Bacteriol, 1983. **153(1)**: 163-168

[73] Schiestl RH, Gietz RD, *High efficiency transformation of intact yeast cells using single stranded nucleic acids as a carrier*. Curr Genet, 1989. **16(5-6)**: 339-346

[74] Brocard C, Lametschwandtner G, Koudelka R, Hartig A, *Pex14p is a member of the protein linkage map of Pex5p*. EMBO J, 1997. **16(18)**: 5491-5500

[75] Bradford MM, *A rapid and sensitive method for the quantitation of microgram quantities of protein utilizing the principle of protein-dye binding*. Anal Biochem, 1976. **72**: 248-254

[76] Blackshear PJ, *Systems for polyacrylamide gel electrophoresis*. Methods Enzymol, 1984. **104**: 237-255

[77] Current Protocols in Molecular Biology, 2000. **2**: 10.8.4.

[78] Neuhoff V, Stamm R, Pardowitz I, Arold N, Ehrhardt W, Taube D, *Essential problems in quantification of proteins following colloidal staining with coomassie brilliant blue dyes in polyacrylamide gels, and their solution*. Electrophoresis, 1990. **11(2)**: 101-117

[79] Shevchenko A, Wilm M, Vorm O, Mann M, *Mass spectrometric sequencing of proteins silver-stained polyacrylamide gels*. Anal Chem, 1996. **68(5)**: 850-858

[80] Pringle JR, Preston RA, Adams AE, Stearns T, Drubin DG, Haarer BK, Jones EW, *Fluorescence microscopy methods for yeast*. Methods Cell Biol, 1989. **31**: 357-435

[81] Thieringer R, Shio H, Han YS, Cohen G, Lazarow PB, *Peroxisomes in Saccharomyces cerevisiae: immunofluorescence analysis and import of catalase A into isolated peroxisomes*. Mol Cell Biol, 1991. **11(1)**: 510-522

APPENDIX

ABBREVIATIONS

’	minutes
’’	seconds
°C	degree celcius
2DE	two dimensional gel electrophoresis
A	area
aa	amino acid
ADP/ATP	adenine nucleotide di/triposphate
APS	ammonium persulfate
BB	boiled beads buffer
bp	base pairs
BSA	bovine serum albumin
CoA	coenzyme A
CTHA	calmodulin-TEV site-hemagglutinin tag
DNA	desoxyribonucleic acid
DOC	desoxycholate
DTT	dithiothretol
EDTA	ethylenediaminetetraacetic acid
EGFP	enhanced green fluorescent protein
ER	endoplasmic reticulum
ERAD	endoplasmic reticulum assisted decay
ESI	electrospray ionisation
EtOH	ethanol
FACS	fluorescence activated cell sorter or sorting
FAOS	fluorescence activated organelle sorting
FAVS	fluorescence activated vesicle sorting
FSC	forward scatter width
Gal	galactose
GFP	green fluorescent protein
h	hours
HA	hemagglutinin tag
HS-DNA	herings sperm DNA
Kan	kanamycin
kDa	kilo Dalton
LC	liquid chromatography
MALDI	matrix assisted laser desorption ionisation
MS	mass spectrometry
nat	nourseothricin
o/d	over day
o/n	over night
OD_{600}	optical density at 600nm
OP	organellar pellet
ORF	open reading frame
PAGE	polyacrylamide gel electrophoresis

PBS	phosphate buffered saline
PCR	polymerase chain reaction
PE	phycoerythrin
PEG	polyethylene glyocol
PMP	peroxisomal membrane protein
PMSF	phenylmethylsulphonyl fluoride
PNS	post nuclear supernatant
PSB	PEG sorbitol buffer
PTS	peroxisomal targeting signal
PxP	peroxisomal pellet
Raff	raffinose
RT	room temperature
S.c.	Saccharomyces cerevisiae
SC	synthetic complete medium
SDS	sodium dodecyl sulphate
SGD	Saccharomyces genome database
SSC	side scatter width
Taq	thermus aquaticus
TCA	trichloro acetic acid
TEMED	tetramethylethylenediamine
ura	uracile
W	width
w/o	without
YPD	yeast peptone dextrose medium
YPE	yeast peptone ethanol medium
YPG	yeast peptone galactose medium
YPR	yeast peptone raffinose medium
YTH	yeast two hybrid

abbreviations for amino acids

alanine	Ala (A)
arginine	Arg (R)
asparagine	Asn (N)
aspartic acid	Asp (D)
cysteine	Cys (C)
glutamic acid	Glu (E)
glutamine	Gln (Q)
glycine	Gly (G)
histidine	His (H)
isoleucine	Ile (I)
leucine	Leu (L)
lysine	Lys (K)
methionine	Met (M)
phenylalanine	Phe (F)
proline	Pro (P)
serine	Ser (S)
threonine	Thr (T)
tryptophan	Trp (W)
tyrosine	Tyr (Y)
valine	Val (V)

ABSTRACT

Peroxisomes are small, single membrane bound organelles present in all eukaryotic cells. Depending on the cell type and the environment peroxisomes harbour various metabolic pathways amongst others the ß-oxidation of fatty acids, the glyoxylate cycle and the metabolism of hydrogen peroxide. To meet these wide-ranging requirements, peroxisomes must possess a large set of proteins. Although various metabolic pathways and new proteins of different functions have been assigned to peroxisomes since their first isolation in the 1960s, peroxisomal proteomic studies currently remain a field of intensive research. In this study employing yeast as model organism, we aimed at the establishment of a new isolation procedure for peroxisomes – and in the long run for peroxisomal precursors – combining classical subcellular fractionation by density gradient centrifugation with FAOS or FAVS respectively (Fluorescence Activated Organellar / Vesicle Sorting). These purified fractions should be subjected to LC coupled tandem MS to determine the protein content of peroxisomes from yeast grown under different conditions supplementing existing data and to gather new information about the dynamic changes of the protein composition of peroxisomal precursors during peroxisome biogenesis. We were able to establish sufficiently intense labelled mature peroxisomes to perform FAOS and the MS analysis of the sorted fractions revealed several candidates for new peroxisomal proteins which remain to be confirmed by independent methods. Concerning the peroxisomal precursors, the ER regions representing the putative starting points of peroxisome biogenesis could be labelled fluorescently allowing for future tests aiming at the implementation of FAVS as purification step prior to the MS analysis.

ZUSAMMENFASSUNG

Peroxisomen sind kleine, von einer Einzelmembran umgebene Organellen, die in allen eukaryotischen Zellen vorkommen. Je nach Zelltyp und Umgebung beherbergen sie diverse Stoffwechselwege, unter anderem die ß-Oxidation von Fettsäuren, den Glyoxylatzyklus und den Stoffwechsel von Wasserstoffperoxid und anderen „reactive oxygen species“. Um diesen breitgefächerten Anforderungen gerecht zu werden müssen Peroxisomen ein breites Spektrum an Proteinen besitzen. Obwohl den Peroxisomen, seit ihrer ersten Isolierung in den 60er Jahren, viele Stoffwechselwege und neue Proteine mit unterschiedlicher Funktion zugeordnet werden konnten, bleibt das Studium des peroxisomalen Proteoms ein interessantes Arbeitsfeld. Diese Studie im Modellorganismus Hefe hatte zum Ziel eine neue Isolationsmethode für Peroxisomen – und langfristig gesehen auch für peroxisomale Vorstufen – einzuführen, die die klassische subzelluläre Fraktionierung durch Dichtegradientenzentrifugation mit FAOS bzw. FAVS (Fluorescence Activated Organelle / Vesicle Sorting) verbindet. Diese gereinigten Fraktionen sollten einer LC gekoppelten Tandem MS Analyse unterzogen werden um einerseits den Proteininhalt von Peroxisomen aus Hefezellen, die unter unterschiedlichen Bedingungen gewachsen sind, zu bestimmen und damit existierende Daten zu ergänzen und um andererseits neue Informationen über die dynamische Änderung der Proteinzusammensetzung der peroxisomalen Vorstufen während der Peroxisomen-Biogenese zu erlangen. Wir konnten reife Peroxisomen ausreichend intensiv mit fluoreszierenden Proteinen markieren um FAOS durchzuführen. Die MS Analyse der sortierten Fraktionen lieferte mehrere Kandidaten für neue peroxisomale Proteine, welche noch durch unabhähgige Methoden bestätigt werden müssen. Die peroxisomalen Vorstufen betreffend konnten die vermeintlichen Startpunkte der Peroxisomen Biogenese im ER mit fluoreszierenden Proteinen markiert werden, was weitere Tests ermöglicht, die sich mit der Einführung von FAVS als Reinigungsschritt vor der MS Analyse beschäftigen.

DANKSAGUNG

An dieser Stelle möchte ich mich bei allen bedanken, die mir die Diplomarbeit ermöglicht bzw. mich in dieser – für mich sehr wichtigen – Zeit begleitet haben.

Mein Dank gilt allen voran natürlich Andreas Hartig, der mir einerseits ermöglichte in seinem Labor meine Diplomarbeit zu schreiben und andererseits jederzeit ein offenes Ohr für meine Probleme und Anliegen hatte und mir somit einen Leitfaden durch die Diplomarbeit gab. Weiters möchte ich mich für die herzliche Aufnahme in Andreas Hartigs und Cécile Brocards Labors bedanken. Meine Kollegen – Christine David, Thomas Heil, Anja Huber, Johannes Koch, Anita Kruzik, Sophie Melchior und Jürgen Steiner – haben mir sowohl mit ihrer lehrenden Tätigkeit als auch mit dem freundschaftlichen Kontakt meine Diplomarbeitszeit so angenehm gestaltet, dass dieses Jahr wie im Flug verging.

Nun möchte ich mich noch bei den Menschen bedanken, die mir am Nächsten sind. Ein liebevolles Dankeschön an meine Eltern, die mir das Studium ermöglicht haben und mich während meiner ganzen Studienzeit und natürlich auch während der Zeit meiner Diplomarbeit unterstützt haben. Mein größter Dank geht an meinen Freund, Manfred Graf, der diese Zeit mit mir sehr intensiv erlebt hat und mir immer wenn es nötig war seelischen Beistand leistete.
Sie alle haben mit mir meine Hochs und Tiefs während dieser Zeit durchlebt und waren immer für mich da – vielen Dank für eure Liebe und Unterstützung!

CURRICULUM VITAE

PERSÖNLICHE DATEN

Name:	Isbella Magyar
Geburtsdatum:	29.04.1985
Geburtsort:	Mödling

SCHULBILDUNG

1991-1995	Volksschule Hinterbrühl
1995-2003	Bundesgymnasium und Bundesrealgymnasium Keimgasse, Mödling
11.06.2003	Reifeprüfung mit Auszeichnung

STUDIUM

2003-2004	Ernährungswissenschaften, 1.Semester
2004-2006	Chemie, 1. Studienabschnitt
01.08.2006	1. Diplomprüfung mit Auszeichnung
2006-2008	Chemie, 2. Studienabschnitt
2008-2009	Chemie, Diplomarbeit